

Supplementary Methods

A	Online resources
B	Motivation for PIQ
C	Implementation of PIQ
D	Computational analysis and metrics
E	Mouse embryonic stem cell line generation, culture, and differentiation
F	Tol2 GFP reporter transposon construct generation, transfection, and flow cytometry
G	Antibodies and immunofluorescence
H	ChIP-qPCR
I	Table of Oligonucleotides
J	DNase-seq
K	DNase-qPCR
L	References

Supplementary Figures

Supplementary Figure 1	Detection and evolutionary clustering of TF-specific profiles
Supplementary Figure 2	PIQ displays higher AUC and PPV than and comparable site coverage to other DNase-Seq algorithms
Supplementary Figure 3	Efficient differentiation of mES cells to endodermal and mesodermal lineages
Supplementary Figure 4	Pioneer TFs are consistent across cell type and do no exclusively populate promoters
Supplementary Figure 5	Some pioneer TFs open chromatin asymmetrically
Supplementary Figure 6	Pioneer reporter assay faithfully measures motif-induced RAR binding and activation potential
Supplementary Figure 7	TF prediction is enhanced by motif-dependence and DNA methylation information
Supplementary Figure 8	PIQ allows for binding prediction for pioneers with weak footprints.

Supplementary Figure 9	Profile level significance test to avoid sequence bias
-------------------------------	---

Supplementary Tables

Supplementary Table 1	DNase-Seq predictions compared with matched ChIP-Seq binding sites calls
Supplementary Table 2	Pioneer TF computational index values
Supplementary Table 3	Directional pioneer TF classification
Supplementary Table 4	Motif and chromatin dependence values
Supplementary Table 5	Table of Oligonucleotides

Supplementary Methods

A. Online resources

The following items are available at <http://piq.csail.mit.edu/> (temporary reviewer login/password “piqreview/tr31193a”): PIQ implementation for EC2 server, documentation, DNase-Seq data for mES lineage tree, and PIQ binding calls for mES lineage tree and human H1 hESC and K562.

B. Motivation for PIQ

Below we explain the biological motivation and constraints underlying Protein-DNA Interaction Quantitation (PIQ), a tool for global transcription factor (TF) binding site detection.

DNase I is known to cleave DNA preferentially in regions of accessible, or hypersensitive, chromatin¹. DNase I cleavage is sterically hindered by DNA-bound proteins such as TFs, leading to the creation of “DNase footprints” in which the bound TF diminishes DNase cleavage at its motif and “DNase profiles” in which the TF affects DNA shape and nucleosome occupancy in the hundreds of base pairs surrounding its binding sites^{2,10,15,17}. Translation of DNase hypersensitivity analysis to the genomic scale³ has revealed that a large majority of TFs show footprints and profiles when directly bound to DNA⁴. Thus, it should be possible to map TF-DNA interactions for a large majority of TFs at a large majority of their bound sites through DNase activity.

In practice, DNase hypersensitivity analysis is a statistical battle of signal and noise. DNase I will cleave non-hypersensitive DNA if given enough time, so the DNase-Seq protocol strives to enrich the signal-to-noise ratio by restricting DNase concentration and cleavage time such that a minority of hypersensitive DNA will be cleaved. Collection of only small (in our case 175-400 bp) DNA fragments after DNase treatment selects for regions in which DNase can cut twice (at both ends), enriching for hypersensitive regions, although background reads resulting from indiscriminate DNase cutting and DNA shearing are also seen. The stochasticity inherent in DNase hypersensitivity analysis informs the need for a computational approach that smooths noise.

After DNase-Seq data collection, the reads must be deconvolved to identify individual TF binding sites. This problem has been approached in two conceptually distinct ways, either by detecting footprints and subsequently matching them to underlying motifs⁴⁻⁷ or by beginning with potentially bound motifs and subsequently determining whether each site has a footprint or profile⁸. We choose the latter approach because of the non-uniform nature of TF footprints and the complexity of TF interactions. Each TF leaves a signature profile that reflects the biophysics of protein-DNA bonding^{4,5,7}, and thus motif-centered profile searching can incorporate this information to improve footprint detection. Additionally, TF binding sites are nearly always clustered into enhancers and promoters, creating complex hypersensitivity patterns reflecting the combination of profiles in that vicinity. Motif-centered profile searching facilitates disambiguation of these complex profile clusters through deconvolution of motif-specific profile information.

We have used motifs from three databases: JASPAR, UniPROBE, and TRANSFAC⁹⁻¹¹. These databases use disparate techniques to assemble motifs, and the motifs vary in specificity, sensitivity, and biological accuracy. In particular, UniPROBE uses the systematic PBM assay to characterize motifs, leading to a more comprehensive picture of TF binding preference than the often empirical JASPAR and TRANSFAC, which are sometimes based on a small sampling of *in vivo* binding sites. Additionally, all three databases present motifs in the position weight matrix (PWM) format in which TF binding is represented as position-independent at each base, which is known not to be accurate for some TFs^{12,13}. Even combining the three databases, the motif set obtained is still likely an incomplete set of DNA-binding factors.

Nonetheless, we have collected 1331 motifs from JASPAR, UniPROBE, and TRANSFAC that span TFs from vertebrate and invertebrate species. While some cross-species motifs likely do not have homologs in mouse, starting with a broad list allows detection of profiles from TFs whose binding

properties in mouse have yet to be characterized. Genomic binding of all 1331 motifs is measured by PIQ as described in the following section. As a post-processing step, motifs that do not show measurable genomic binding as assessed by profile strength are discarded. Similarly, motifs with highly similar motifs and binding patterns are clustered. We perform these steps as post-processing because motif usage changes depending on cell type, so PIQ can determine the motif usage profile for each cell type *de novo*. For our mESC lineage, we analyze binding of 733 informative, non-redundant motifs.

Lastly, how do we interpret the existence of a profile at a given motif in the genome? Recent studies have indicated that TFs constantly bind and unbind to DNA and are bound at a particular site only a fraction of the time^{14,15}. Additionally, many TFs with overlapping motifs are co-expressed, and evidence is mounting that motifs can be shared among multiple TFs in the same cell¹⁶. TFs from the same family can also exhibit temporal dependencies during development such that binding at an earlier timepoint primes the site for binding of a related TF at a later timepoint^{17,18}. Thus, a profile simply represents a statistical probability that the underlying motif is bound at a given time by a member of a TF family that yields the signature profile observed. This reality motivates an advantage to time-series DNase-Seq analysis. As many motifs are shared across differentiation state, even in cases when individual bound TFs change, profile information can be shared across time to improve profile detection.

C. Implementation of PIQ

Next, we explain the logic underlying the implementation of PIQ. Our goal for PIQ was to develop a novel method for detecting transcription factor binding events from DNase-Seq data. Taking into account the biological considerations outlined above, we have tailored the statistical model and inference framework to meet several design goals:

- 1. Resistance to low coverage and noisy data:** Share strength across neighboring bases by modeling reads as arising from a Gaussian Process.
- 2. Integrate multiple experiments, whether replicates or time-series data:** Learn the cross-experiment structure as a Gaussian graphical model using L_1 regularization.
- 3. High spatial accuracy:** Use motifs to inform base-pair level positions rather than *de novo* footprinting.

4. Robust worst case behavior: Use priors that guarantee monotonicity with respect to motif score and read coverage.

5. Scalability to thousands of motifs genome-wide: Fast approximate inference strategies and use of Amazon EC2.

The five design goals correspond to the major subcomponents of the algorithm and will be covered below.

C.0 Indexing and notation.

Throughout we use μ for log-rates, Σ for covariances. Indexes $i, j \in \{1..N\}$ refer to bases on the genome, $k \in \{1 .. K\}$ refer to experiments, $l \in \{1 .. L\}$ to transcription factors and $m_l \in \{1 .. M_l\}$ refer to the motif matches for a factor l . W refers to the number of bases each profile affects around a motif match.

C.1 Generative model for reads

We construct the generative model of reads in the single-experiment, single-strand, no factor binding case as a two-step process. First we generate the underlying per-base accessibility of the genome to DNase as a Gaussian Process, which is a distribution over functions of a particular level of smoothness⁵¹. The Gaussian Process is parametrized by μ_0 , average log-read rate per base represented as a vector of length N with identical entries, σ_0 the marginal deviation in log-read rates, and $k_{|i-j|}$, the correlation between neighboring bases.

$$\begin{aligned}\mu_i &\sim \text{Multivariate Normal}(\mu_0, \Sigma) \\ \Sigma_{(i,j)} &= \text{Covariance}(\mu_i, \mu_j) = \sigma_0 k_{|i-j|}\end{aligned}$$

Given the per-base rates, μ_i we define the read per base x_i as being distributed Poisson with log-rate equal to μ_i

$$x_i \sim \text{Poisson}(\exp(\mu_i))$$

Intuitively, μ_0, σ model the overdispersion of read counts relative to a Poisson, while $k_{|i-j|}$ defines the degree and type of smoothness we have across the genome, allowing us to share information across adjacent bases. In the multi-experiment case, we estimate the parameters $(\mu_0, \sigma, k_{|i-j|})$ for each experiment.

We used the inference technique outlined in C.6 to estimate the long-distance correlation between bases and used this to set the upper bound for the window size (400bp) used in both the kernel size k and the transcription factor profile size M .

C.2 Cross-experiment and cross-strand model

Cross-experiment and cross-strand effects for DNase affinity are treated identically. Let $\mu_{i,k}$ be the read rate at base i in experiment or strand $k \in \{1 \dots K\}$ then we model the distribution over different experiments as a multivariate Gaussian parametrized by a cross-experiment correlation matrix Σ subject to a L_1 penalty prior with parameter λ ,

$$\begin{aligned}\mu_{i,1} \dots \mu_{i,K} &\sim \text{Multivariate Normal}(\mu_0, \Sigma) \\ \log(P(\Sigma)) &\propto -\lambda |\Sigma^{-1}|\end{aligned}$$

Parameterizing the cross-experiment correlation by a matrix Σ is natural, since the single experiment rates μ_i are already Gaussian. The L_1 penalty induces sparsity over the precision matrix (Σ^{-1}) which has the effect of preventing loosely related experiments from sharing information⁵². In our experimental design, this penalty is particularly important, since the differentiation protocol results in a highly structured cross-experiment correlation structure.

C.3 Binding model

We will first cover the single-experiment, single-factor case since the generalization to multi-experiment and multifactor are straightforward.

PIQ represents a transcription factor as a motif (shared cross-experiment) and a DNase profile parameter β representing a TF's effect W base pairs around a motif match, not shared across either experiment or factor. A particular binding site is represented as a pair of variables, indicating the binding site location and whether the site is bound, (y_m, I_m) .

Given a motif for some factor, we call a base a binding site candidate if its score passes some threshold (in all analysis, we used any position occurring with less than 1e-5 frequency with respect to background sequence). For the binding site candidate indexed by m , let y_m be the base-pair representing the

midpoint of such a motif match. Then we define the binding-adjusted read rates for the two strands at a base i ($\hat{\mu}_i^+, \hat{\mu}_i^-$) in terms of the binding indicator I_m which is one if a factor is bound, the strand specific read rate (μ_i^+, μ_i^-) defined in section C.2, and DNase-profile parameters (β^+, β^-) .

$$\hat{\mu}_i^+ = \mu_i^+ + \begin{cases} \beta_{i-j,l}^+ & : |y_m - j| \leq W \text{ and } I_m = 1 \\ 0 & \text{otherwise} \end{cases}$$

In the multi-experiment case, each experiment and factor receives its own profile (β^+, β^-) making the above equation in terms of $\beta_{(i-j,l,k)}^+$ and in the multi-factor case we simply sum over all matching β

C.4 Prior model

Our prior model over binding indicators I_j for a single experiment and single factor encodes the requirement that binding events should occur more frequently as motif score and overall hypersensitivity increases.

Let f and g be arbitrary monotone functions, and let s_j and c_j be the motif score for candidate j and the total number of DNase counts within M base pairs respectively, then we can define a prior based upon monotone regression⁵³ as,

$$\log(P(I_j = 1)) = f(s_j) + g(c_j)$$

The functions f and g are estimated to maximize marginal likelihood and are factor and experiment specific.

C.5 Inference and scaling

Data: A list of binding site candidates, a matrix of DNase read counts.

Result: Probability of binding for each binding site

```

begin fit background parameters
  | for 1 ... K experiments do
  |   | fit ( $\mu, \sigma, k_{i-j}$ )
  |   | estimate  $\sigma_k$ , the vector of length K encoding the per-base correlation with all other
  |   | experiments
  | end
  | fit ( $\Sigma^{-1}$ ), the regularized precision matrix using the set of K correlation vectors
  | { $\sigma_k : k \in \{1 \dots K\}$ }
end

begin initialize binding parameters
  | set the priors f and g to zero.
  | for 1 ... K experiments and 1 ... L factors do
  |   | calculate  $(\beta_{i,l,k}^+, \beta_{i,l,k}^-)$  assuming the top 10,000 motifs are bound.
  | end
  | set all binding sites  $I_j = 0$ 
end

while change in parameters  $I_j < \text{threshold}$  do
  | Estimate  $E[\mu_i | I_j], E[\mu_i^2 | I_j]$  via expectation propagation
  | Calculate  $E[I_j]$  conditional on the current  $\mu_i, f, g$  estimates. Update  $f, g$  according to
  | maximum likelihood.
end
```

C.5.1 Estimating the background parameters μ, σ_k

Most of the computational strength for our model comes from accurate inference of the kernel k . We begin by identifying the marginal variance, or the diagonal entries of the covariance matrix.

Given some counts C_i , the marginal probability of C_i given marginals μ_0, σ_0^2 is

$$P(C_i | \mu_0, \sigma_0^2) = \int_{-\infty}^{\infty} \text{Pois}(C_i; \exp(\lambda_i)) N(\lambda_i; \mu_0, \sigma_0^2) d\lambda_i$$

We approximate this with Gauss-Hermite integration⁵⁴, which uses N_{quad} weights w_i and test points n_i , to approximate arbitrary integrals of the form

$$\int_{-\infty}^{\infty} e^{-x^2} f(x) dx \approx \sum_{i=1}^{N_{\text{quad}}} w_i f(n_i)$$

Therefore we approximate the above integral as

$$P(C_i | \mu_0, \sigma_0^2) = \sum_{j=1}^{N_{\text{quad}}} \frac{w_j}{\pi} \text{Pois}\left(C_i; \exp\left(\mu_0 + n_j \sqrt{2\sigma_i^2}\right)\right)$$

If we let C_{max} be the maximum observed count per base (in our experiments we truncated to 50), then the overall marginal likelihood for the whole dataset is defined in terms of the sufficient statistics $|\{k: C_k = i\}|$ or the number of bases with count i .

$$\log(P(C|\mu_0, \sigma_0^2)) = \sum_{i=1}^{C_{max}} |\{k : C_k = i\}| \log \left(\sum_{j=1}^{N_{quad}} \frac{w_j}{\pi} \text{Pois} \left(i; \exp \left(\mu_0 + n_j \sqrt{2\sigma_j^2} \right) \right) \right)$$

We identify the maximum μ_0, σ_0^2 by successive binary search for each strand in each experiment. The optimization time is dominated by calculation of the sufficient statistics $|\{k: C_k = i\}|$

After identifying the marginal distribution, we find for the correlation between entries between each entry in the covariance matrix. In the single-day case we have the same marginal mean and variance, giving the marginal likelihood for a single datapoint

$$P(C_i, C_j | \mu_0, \sigma_0^2, \rho) = \iint_{(\lambda_i, \lambda_j) \in \mathbb{R}^2} \text{Pois}(C_i; \exp(\lambda_i)) \text{Pois}(C_j; \exp(\lambda_j)) N \left([\lambda_i, \lambda_j]; \mu_0, \sigma_0^2 \begin{bmatrix} 1 & \rho \\ \rho & 1 \end{bmatrix} \right) d\lambda_i d\lambda_j$$

Similarly to before, we can use the sufficient statistics of C and Gauss Hermite quadrature to efficiently calculate the overall marginal likelihood. When calculating the correlation for a particular offset δ , let $T_{i,j}$ be the number of pairs of bases with i counts on one base and j counts on the base δ away.

$$h_a = \sqrt{1 + \rho n_a \sigma_0^2}$$

$$g_b = \sqrt{1 - \rho n_b \sigma_0^2}$$

$$P(T | \mu_0, \sigma_0^2, \rho) = \sum_{i=1}^{C_{max}} \sum_{j=1}^{C_{max}} T_{i,j} \log \left(\sum_{a=1}^{N_{quad}} \sum_{b=1}^{N_{quad}} w_a w_b \text{Pois}(i; \exp(h_a + g_b + \mu_0)) \text{Pois}(j; \exp(h_a - g_b + \mu_0)) \right)$$

Using binary search, we can identify the optimal ρ for each entry in the kernel matrix rapidly. Finding the full kernel matrix for a 4-experiment 400 bp window problem takes less than an hour on a standard quad core i7 laptop

To scale to a larger number of experiments, we parallelize over pairs of bases (i,j) which are completely separable optimization problems.

C.5.II Cross experiment and strand rate estimates.

We use existing graphical lasso solvers in R on the estimated inverse correlations σ_{k_1, k_2}^+ above to obtain the cross-experiment parameters Σ^{-1} . The regularizer λ is fixed *a priori*.

This two-step procedure of first estimating σ_{k_1, k_2}^+ via marginal likelihood maximization and then estimating Σ^{-1} is not identical to optimizing a regularized estimate of σ_{k_1, k_2}^+ but in controlled tests with fewer than 3 experiments we find that sparsity pattern inferred by Σ^{-1} exactly matches that of the full regularized solution.

C.5.III Latent rate (μ) estimate.

Given the fixed background parameters $(\mu_0, \sigma_0, k_{|i-j|}, \Sigma^{-1})$ and current estimates of the binding identity I_j , we estimate the latent rate using the expectation propagation technique. Algorithmically, expectation propagation takes the parameters $(\mu_0, \sigma_0, k_{|i-j|}, \Sigma^{-1})$, data (c_i) and returns the posterior mean $E[\mu_i | c_i]$ and variance $\text{Var}[\mu_i | c_i]$ by fitting a Gaussian approximation to the posterior.

Expectation propagation (EP)⁵⁵ takes a complex distribution q (in this case the posterior distribution of μ_i given reads c_i) and approximates it as a product of 'terms' $q \approx \prod t_i$. In our case we will represent q as the product of contributions from the prior (t_{pri}), observed counts (t_c) and intra-experiment terms (t_{exp}).

For simplicity, let μ be a matrix of size $(N \times K)$ representing a region of N bases over K experiments, and Σ be a $(K \times K)$ matrix over experiments, and $\bar{\Sigma}$ be the $(N \times N)$ covariance matrix implied by $k_{|i-j|}$ and σ_k . Then the full posterior over μ and our approximation takes the form,

$$q(\mu | c) \propto t_{pri}(\mu | \bar{\Sigma}, \mu_0) t_c(c_i | \mu) t_{exp}(\mu_k | \mu_{-k})$$

Inference over μ in this no-binding setting is straightforward and follows from standard EP theory for exponential families⁵⁶. In the binding setting, we simply define the binding adjusted prior $\widehat{\mu}_0$ analogously to before in section 3,

$$\hat{\mu}_0^+ = \mu_0^+ + \begin{cases} E[I_j]\beta_{i-j}^+ & : |i-j| \leq M \\ 0 & : \text{otherwise} \end{cases}$$

We exploit some problem-specific structures to modify standard EP updates to reduce the runtime from $O(N^2)$ to $O(N \log(N))$.

Since $\bar{\Sigma}$ is over a single time-point, and $k_{|i-j|}$ within a single time point is a stationary kernel⁵⁷, we know that $\bar{\Sigma}$ has a Toeplitz structure, and that for a sufficiently large matrix $\bar{\Sigma}$, any row of $\bar{\Sigma}^{-1}$ defines a stationary kernel $k_{|i-j|}^{-1}$.

This special structure over $\bar{\Sigma}$ makes it so that any matrix multiplication of the form $\bar{\Sigma}^{-1}x$ can be calculated using the fast Fourier transform in time $O(N \log(N))$. Since all EP update steps in a Gaussian are matrix multiplications over $\bar{\Sigma}^{-1}$ ⁵⁶, we exploit this equivalence to obtain sub-quadratic runtimes while still modeling base to base interactions.

C.5.IV Binding site estimates.

For I_j we estimate the distribution over binding events by estimating the logistic odds of binding,

$$L_j = \text{logit}(P(I_j = 1)) = E[\log(P(I_j = 1))] - E[\log(P(I_j = 0))]$$

Given the posterior mean and variance of per base rates, $E[\mu_i]$, $\text{Var}[\mu_i]$, binding identity for a single binding site is inferred exactly via the likelihood ratio

$$\begin{aligned} P(c_i|I_j, \mu_i) &= \int_{-\infty}^{\infty} \text{Pois}(c_i|\exp(x + I_j\beta_{i-j}))N(x|E[\mu_i], \text{Var}[\mu_i]) \\ P(I_j|c_i, \mu_i) &= \frac{\prod_i P(c_i|I_j = 1, \mu_i)}{\prod_i P(c_i|I_j = 0, \mu_i)} \end{aligned}$$

For multiple binding sites with overlapping β , we account for the correlations between I_j by taking conditional probabilities where we order binding sites ($j_1 \dots j_m$) according to their prior and single-site estimates $E[I_j|c_i, \mu_i]$. Which is a greedy approximation to the true joint probabilities p_j . We found that this greedy approximation is sufficient to control the effects of similar and overlapping motifs.

Finally, given prior functions f and g taking on values f_j and g_j at a particular binding site j , we let the overall posterior be

$$L_j = f_j + g_j + \text{logit}(p_j)$$

C.5.V Prior functions f, g

Given binding estimates L_j and matched motif scores and DNase counts s_j and c_j , we define f and g to be the least-squares monotone regression,

$$\begin{aligned} \min_f (f_i - L_j)^2 & \text{ subject to} \\ \forall (i, j) s.t. \quad s_i < s_j \quad f_i & < f_j \end{aligned}$$

Similarly for g and c .

The optimization problem above is solved directly via a standard monotone regression function in R.

C.6. Constructing binary binding site calls.

PIQ primarily operates as a ranking algorithm and scores every possible PWM candidate as output. However, in order to match outputs with ChIP and DNase peak callers, we use a straightforward t-test based cutoff to call sites as binary bound/unbound.

We use binding-rate as the primary metric (probability of binding times local chromatin accessibility) and fit a normal to the unbound portion using the median and interquartile range. Compared to nonparametric testing via the bootstrap or permutation testing, we find this method more robustly handles cases with degenerate PWMs and profiles.

We cut off calls at 0.01 p-value and detect on average ten thousand binding sites per factor.

D. Computational analysis and metrics

D.1 Pioneer TF scoring metrics

Throughout this section we index binding sites by j , genomic coordinates by I , transcription factor identity by m and experiments by k . We also define c_i^k to be the counts at base i in experiment k , p_j^k to be the PIQ estimated binding probability at site j , x_j to be the coordinate of binding site j , and S_m to be the set of binding sites for transcription factor m .

The pioneer index p_m is defined as the expected change in reads at bound motifs with respect to baseline, where binding is observed in the immediately preceding time point from the read counts. For convenience let experiment $k+1$ be the experiment following experiment k in the lineage.

$$p_m = \frac{1}{399 k} \sum_{i=-199}^{199} \sum_k \log \left(\frac{\sum_{j \in S_m} c_{x_j+i}^{k+1} p_j^k}{\sum_{j \in S_m} c_{x_j+i}^{k+1} (1 - p_j^k)} \right)$$

The chromatin opening index b_m is defined as the expected change in reads at bound motifs with respect to baseline.

$$b_m = \frac{1}{399 k} \sum_{i=-199}^{199} \sum_k \log \left(\frac{\sum_{j \in S_m} c_{x_j+i}^k p_j^k}{\sum_{j \in S_m} c_{x_j+i}^k (1 - p_j^k)} \right)$$

The social index s_m is defined similarly to the chromatin opening index, but with expected binding instead of expected number of reads. Let $y_i^k = \sum_{\{j: x_j=i\}} p_j$, then,

$$s_m = \frac{1}{399 k} \sum_{i=-199}^{199} \sum_k \log \left(\frac{\sum_{j \in S_m} (y_{x_j+i}^k - p_j^k) p_j^k}{\sum_{j \in S_m} (y_{x_j+i}^k - p_j^k) (1 - p_j^k)} \right)$$

The motif dependence of a factor m is defined as the Pearson correlation between the logistic binding probability and the PWM score at site j , defined as z_j , $\text{cor}(\text{logit}(p_j^k), z_j)$

The chromatin dependence is defined similarly as the Pearson correlation between logistic binding and the log number of DNase reads within a 399 bp window, $\text{cor}(\text{logit}(p_j^k), \log(\sum_{i=-199}^{199} c_{x_j+i}^k))$.

The asymmetry index is designed to capture the imbalance between chromatin opening between the left and right sides of a motif. We define this as the expected change between left and right sides in the squared chromatin opening index.

$$a_m = b_m^2 \left| \sum_{i=1}^{199} \sum_k \log \left(\frac{\sum_{j \in S_m} c_{x_j+i}^k p_j^k}{\sum_{j \in S_m} c_{x_j+i}^k (1 - p_j^k)} \right) - \sum_{i=-199}^{-1} \sum_k \log \left(\frac{\sum_{j \in S_m} c_{x_j+i}^k p_j^k}{\sum_{j \in S_m} c_{x_j+i}^k (1 - p_j^k)} \right) \right|$$

D.2 Comparison of PIQ predictions against ChIP-seq

For binding site candidate matching, we used 1313 mouse and mammalian PWMs provided by JASPAR, as well as 18 PWMs generated by prior mouse ChIP-seqs^{58, 59} (unpublished observations). These 18 PWMS were not used for either the mouse or 303 K562 ChIP-seq comparisons⁶⁰. A candidate site is a particular PWM match with p value less than $1e^{-4}$ with respect to a uniform baseline sequence.

Throughout, we define the binding site coordinate to be the midpoint of the PWM. A candidate PWM is defined to be covered by a particular ChIP-seq experiment if it is within 10 base pairs of a ChIP-seq binding event. In order for a ChIP-seq event to have a candidate PWM nearby, it must both be hypersensitive and have PWM score greater than -4 . Within the K562 dataset, candidate PWMs were matched for 12–64% of ChIP-seq events.

For ChIP-seqs with unambiguous mappings in JASPAR, we use the mapping directly, otherwise we use the JASPAR motif with highest concordance to ChIP-seq, as defined as the motif whose PWM score has highest AUC.

D.3 DNase Profile method comparison

For the digital genomic footprint (DGF), we used published data on K562, took our set of binding site candidates, and called those overlapped by a DGF as bound, and the rest unbound. For CENTIPEDE, we ran the package provided by authors over the same 199bp window on our candidate sites, and ran the method using the PWM score as an auxiliary prior track as well as with no prior and used the run resulting in a higher AUC.

D.4 Clustering and thresholding factors

For clustering, we took the set of candidate PWM sites on chromosome one, and calculated the number candidate sites less than 10bp apart between two factors. If N is the total number of overlapping sites and N_1 and N_2 are the number sites for each factor, we define the correlation between factors to be $\rho = \frac{N}{\sqrt{N_1 N_2}}$. And the distance between factors to be $1 - \rho$. We use single linkage clustering with cutoff of 0.1 to generate clusters.

To threshold, we took the DNase profiles for each motif and counted the number of bases exceeding a noise threshold, defined as the median absolute deviation over all profiles. A factor is defined as having significant signal if at least half its bases within the profile exceed the noise threshold.

D.5 Calculation of ChIP concordance metrics

We compared DNase-Seq based factor binding to ChIP-seq by taking each candidate binding site (PWM score above threshold) and annotating it as bound if it was within 10bp of a ChIP-seq event range as called by ENCODE k562 ChIP-seq.

We used three different metrics to compare DNase-Seq based factor binding calls to ENCODE ChIP-seq data: AUC (area under the curve), defined as the probability that an algorithm will rank a ChIP-bound event over an unbound event; PPV, defined as the fraction of the top 500 DNase-Seq based binding site estimates that were bound in ChIP-Seq; and Coverage, defined as the fraction of ChIP-Seq binding events that were called as bound using DNase-Seq.

D.6 Removal of potential promoter-associated PIQ binding events

To ensure that identified chromatin effects are not promoter-associated, transcriptionally active areas of the genome were not considered by PIQ for any data presented. These are defined by the union of all annotated transcripts in the UCSC Browser Gene tracks: UCSC Genes, RefSeq Genes, Other RefSeq, MGC Genes, ORFeome Clones, Vega Genes, Ensembl Genes, AceView Genes, and Genscan Genes, expanded upstream and downstream by 1kb. In total this excludes 760Mbp of the genome.

Further, to account for unannotated promoters, a more thorough test was applied to pioneer factor PIQ predictions by excluding regions exhibiting mES GRO-seq enrichment⁶¹, RNA-seq enrichment⁶², or high H3K4me3/H3K4me1 ratios⁶³ commonly associated with promoters (Supplementary Figure 3D). GRO-seq and RNA-seq segments were called from aligned read data using MACS2⁶⁴ with default parameters and the option “–nolambda,” and expanded upstream and downstream 1kb. Regions with a high H3K4me3/H3K4me1 ratio were determined by their log read Z-score ratio over a 1kb window; windows with a ratio over 3 were expanded by 1kb and excluded. This excludes an additional 687Mbp beyond annotations above. Metapeak plots (Supplementary Figure 3E) were generated by accumulating relative read positions across all binding sites, separately scaling the maximum height of each data type (DNase-seq=1, H3K4me4/H3K4me1=0.6, and GRO-seq/RNA-seq=0.4), and smoothing using a Savitzky-Golay filter.

D.7 Correlation between DNase-seq and DNA CpG methylation

To investigate how DNA CpG methylation data may be used to enhance TF binding site predictions we compare mES DNase-seq read data against mES whole genome bisulfite sequencing (WGBS) data⁶⁵. WGBS reads were aligned and CpG sites called using Bismark⁶⁶, providing bp-level CpG rates. From this an anti-correlation is seen between methylated binding site motifs and DNase-seq reads (Supplementary Figure 5C) – PIQ predicted binding sites are similarly associated with an increase in DNase-seq reads within $\pm 399\text{bp}$ as they are to a reduction in the amount of CpG methylation within $\pm 10\text{bp}$ of the center of the motif.

D.8 Visualization of DNase-profiles via multidimensional scaling.

We visualized the set of DNase-seq profiles (Supplementary Figure 1A) via multidimensional scaling. Distance between motifs were determined via symmetrized KL divergence at maximal alignment for any two motifs, assuming any overhanging parts were matched to a uniform distribution.

These distances were then metricized by using cophenetic distances and embedded into two dimensions using multidimensional scaling.

Coloring and annotation was done using JASPAR annotations for factor DNA binding domains.

E. Mouse embryonic stem cell line generation, culture, and differentiation

Mouse embryonic stem cell culture and endoderm differentiation was modified slightly from previously published protocols³⁵. Undifferentiated 129P2/OlaHsd mouse ES cells were maintained on gelatin-coated plates with mouse embryonic fibroblast (MEF) feeders in mES media composed of Knockout DMEM (Life Technologies) supplemented with 15% defined fetal bovine serum (FBS) (HyClone), 0.1mM nonessential amino acids (Life Technologies), Glutamax (Life Technologies), 0.55mM 2-mercaptoethanol (Sigma), and 1X ESGRO LIF (Millipore). Cells were regularly tested for mycoplasma and normal karyotype.

Prior to differentiation, ES cells were passaged onto gelatin-coated plates for 25 minutes to deplete MEFs. MEF-depleted ES cells were then seeded at $1 * 10^4 \text{ cells/cm}^2$ onto gelatin-coated dishes in mES media. After 12-24 hours, media was changed to Advanced DMEM (Life Technologies) supplemented with N-2 (Life Technologies), B27 Supplement without vitamin A (Life Technologies), and

Glutamax. After 44-48 hours, media was changed to Advanced DMEM with 2% FBS, Glutamax, 5 nM GSK-3 inhibitor XV and 50 ng/mL E. coli-derived Activin A (Peprotech) for 24 hours to produce mesendoderm. For endoderm differentiation, cells were then fed with Advanced DMEM with 2% FBS, Glutamax, 50 ng/mL Activin A and 1 μM Dorsomorphin (Sigma) for 48 hours. For intestinal endoderm differentiation, cells at the endoderm stage were fed for 24 hours with Advanced DMEM with B-27 supplement without vitamin A, Glutamax, and 100 nM GSK-3 inhibitor XV. For pre-pancreatic endoderm differentiation, cells at the endoderm stage were fed for 24 hours with Advanced DMEM with B-27 supplement without vitamin A, Glutamax, 500 nM retinoic acid (Calbiochem), 50 nM A-83-01 (Calbiochem), and 8 ng/mL Bmp4 (Stemgent). For mesodermal differentiation, cells at the mesendoderm stage were treated for 48 hours with 10 ng/mL Bmp4.

ES cells with doxycycline-inducible alleles for Sox2, Foxa1, Hnf1 β , Cdx2, Gata6, Zfp161, and Klf7 in the HPRT locus were created as described ³⁶ and maintained and differentiated as above. For dominant negative lines, DNA-binding domains of NFYA and Nrf1 were used to create doxycycline-inducible HPRT lines as above.

Dominant negative lines were grown for >7 days in mES media supplemented with 5 nM GSK-3 inhibitor XV and 500 nM UO126 to enhance pluripotency³⁷ and 2 μg/mL Doxycycline. Cells were harvested at this stage for DNase-qPCR. For ChIP-qPCR, cells were treated for 6 hours with mES media with 1 μM retinoic acid.

F. Tol2 GFP reporter transposon construct generation, transfection, and flow cytometry

PCR-amplified constructs containing pioneer and non-pioneer motif regions and RXR:RAR binding sites were generated from primers listed below and cloned into Pael and Ascl sites of p2TAL200R175-minHsp-GFP-BIR (Sherwood et al, manuscript under review). To generate the reporter construct with 2 kb spacer DNA added between the enhancer and promoter, 2 kb of genomic DNA from a consistently DNase-insensitive genomic region (primers included in oligonucleotide section) was cloned into the Pael site of p2TAL200R175-minHsp-GFP-BIR.

Tol2-containing reporter plasmids and transposase-containing pCAGGS-mT2TP (Sherwood et al, manuscript under review) were transfected into the mES lines noted in the text using Xfect for mES cells

transfection reagent (Clontech). Blasticidin selection was performed for >7 days in mES media with 5 nM GSK-3 inhibitor XV and 500 nM UO126 added to enhance pluripotency³⁷.

For flow cytometric GFP detection, cells were trypsinized and seeded at 3×10^4 cells/cm² onto 96-well plates. Cells were treated with mES media alone or supplemented with 1 µM retinoic acid and/or 2 µg/mL Doxycycline or differentiated into mesendoderm prior to treatment. After 24 hours, cells were trypsinized, quenched, and fluorescence of 5-20*10³ cells was measured using a BD Accuri C6 flow cytometer and accompanying software (BD Biosciences). Flow cytometry is known to be highly reproducible and preliminary experiments showed that flow cytometric measurement could robustly distinguish known positive and negative control reporter cell lines with high consistency. Thus, we chose to perform four biological replicates of each flow cytometric experiment to ensure adequate statistical power and to control for experimental variability, which was minimal and relatively similar in all sample groups. Significance was calculated using a one-tailed Welch's t-test at P<0.01 as pioneer TFs might be expected to have distinct variance to non-pioneers.

G. Antibodies and immunofluorescence

For cell immunofluorescence analysis, tissue culture plates were fixed for 20 minutes in 4% paraformaldehyde (Electron Microscopy Sciences) and washed in PBS with 0.1% Triton X-100 (Sigma). Tissues were blocked by 20 minute incubation at 4 degrees in PBS with 20% donkey serum (Jackson Immunoresearch) and 0.1% Triton X-100. Primary and secondary antibody staining were performed overnight at 4 degrees in PBS with 5% donkey serum and 0.1% Triton X-100, and after primary and secondary antibody staining, washing was performed with PBS with 0.1% Triton X-100. After staining, plates were washed and incubated with 1 µg/mL Hoechst 33342 (Life Technologies). Imaging was performed using a DMI 6000b inverted fluorescence microscope (Leica), and image analysis with the Leica AF6000 software package.

The following primary antibodies were used: goat anti-Foxa2 M-20, rabbit anti-RAR M-454, rabbit anti-cMyc N-262 (Santa Cruz Biotechnology), rabbit anti-Foxa2 (Millipore); goat anti-Sox17, mouse anti-Sox2, (R+D Systems); mouse anti-Hnf1β (BD Biosciences). AlexaFluor488 and AlexaFluor594 conjugates (Jackson Immunoresearch) were used for secondary detection. Antibodies were validated for assays in which they were used by the companies.

H. ChIP-qPCR

ChIP was performed according to the “Mammalian ChIP-on-chip” protocol (Agilent). 1-5*10⁷ cells were used for each experiment. qPCR primers are listed in the table of oligonucleotides. ChIP-qPCR is known to be highly reproducible with a sufficient dynamic range to reproducibly distinguish the changes in binding strength we expected in this experimental setup (~2-fold). Thus, three biological replicates of each ChIP-qPCR experiment were performed to control for experimental variability, which was minimal and relatively similar in all sample groups. Significance was calculated using a one-tailed Student’s t-test at P<0.01.

I. Table of Oligonucleotides

Oligonucleotides used in this work are presented in Supplementary Table 3.

J. DNase-Seq

DNase-Seq was performed using adaptations of previous protocols³⁸. 1-3 biological replicate DNase-Seq experiments were performed at six stages of mouse ES cell differentiation: mouse ES cells, mesendoderm, endoderm, lateral plate mesoderm, pre-pancreatic endoderm, and intestinal endoderm (see section E for details on culture conditions to derive each cell type) with high replicate consistency. A detailed protocol ensues:

Mouse ES cells or differentiated cells of various stages (30-90 million cells) were harvested from 15 cm tissue culture plates, pelleted at 800g for 5 minutes at 4°C and the supernatant aspirated. Cells were washed twice with 2.5 ml/plate of ice-cold PBS and pelleted (800g, 5 minutes, 4°C). The supernatant was aspirated and cells were resuspended 2.5 mL/plate Buffer A containing 15 mM Tris HCl (pH 8), 15 mM NaCl, 60 mM KCl, 1 mM EDTA (Ambion, pH 8), 0.5 mM EGTA (pH 8) and 0.5 mM Spermidine (Sigma-Aldrich). An equal volume of 2X Igepal in Buffer A (earlier samples with a 0.05% Igepal final concentration, later samples with a 0.00165% Igepal final concentration) was added to the resuspended cells and the nuclei were pelleted (800g, 5 minutes, 4°C). The supernatant was aspirated

promptly and the cells resuspended in 2.5 mL/plate Buffer A. An aliquot of the resuspended nuclei was taken and counted on a hematocytometer with 1:10 Trypan Blue. Nuclei were pelleted (800g, 5 minutes, 4°C) and either digested immediately as below, or stored in 20 mM Tris HCl (pH 8), 75 mM NaCl, 0.5 mM EDTA (Ambion) 50% glycerol, 0.85 mM DTT, and 0.125 mM PMSF, flash frozen in liquid nitrogen and stored at -80°C for a later digestion.

If frozen, nuclei were washed twice with 2.5 mL/plate Buffer A, pelleted (800g, 5 minutes, 4°C) and the supernatant discarded before proceeding to digestion. Digestion volumes are given for 10^7 nuclei. Volumes should be scaled as per cell number. Digestion buffer (850 μ l per 10^7 nuclei) was prepared by diluting 10X stock of CaCl₂ and NaCl in Buffer A (above) for a final concentration of 6 mM CaCl₂ and 75 mM NaCl. Stop buffer (950 μ l per 10^7 nuclei) was prepared with final concentrations as follows: 50 mM Tris HCl (pH 8), 100 mM Na Cl, 0.1 % SDS, 100 mM EDTA (Ambion, pH 8), 10 μ g/ml RNase A (Invitrogen), 1 mM Spermidine (Sigma-Aldrich) and 0.5 M Spermine (Sigma-Aldrich). Both digestion and stop buffers were warmed at 37°C. DNasel enzyme was combined with warmed digestion buffer for a final volume of 100 μ l per 10^7 nuclei. If multiple concentrations of DNasel were tested, nuclei were separated equally amongst each concentration. Prior to digestion, a small aliquot was reserved as an undigested control for quantitative PCR analysis. The DNasel/ digestion buffer mix was warmed in a 37°C water bath for 2 minutes, and the nuclei were gently resuspended in digestion buffer. The warmed DNasel/ digestion buffer mix was promptly added to the nuclei and digested for 2 minutes at 37°C. Pre-warmed stop buffer was added and the tube inverted multiple times to stop the digestion. Digested samples were transferred to a 55°C incubator for 15 minutes. Proteinase K (Ambion, 20 mg/mL) was added to each sample for a final concentration of 2 μ g/mL and samples were incubated overnight at 55°C.

DNA fragments were purified by adding an equal volume of phenol:chloroform:isoamyl alcohol to each sample and mixing. The suspension was transferred to a phase-lock tube and centrifuged for 5 minutes at 12-16,000g. The aqueous phase was isolated and combined with 0.1 volumes 3M sodium acetate, 2 volumes absolute ethanol and 1:600 Glycoblue. This mixture was incubated at -20°C for 5-6 hours or at -80°C for 30-45 minutes. DNA was pelleted by centrifugation at 12-16000g for 10-20 minutes and the supernatant aspirated. The DNA pellet was washed with 70% ethanol and re-pelleted by centrifugation at 4000 rpm for 5 minutes. The supernatant was carefully aspirated and the DNA pellet air-dried for 5-10 minutes before resuspending in TE buffer.

To enrich for hypersensitive regions, size selection was performed on the purified fragments by either 2% agarose gel band purification or the Invitrogen E-Gel® Agarose System. Fragments were collected in the 175-400 bp region so as to avoid empirically-determined complications by the ~150 bp nucleosomal signal. Size selection enrichment was tested by quantitative PCR using primers (three positive control primers and three negative control primers) for constitutively DNase hypersensitive regions and insensitive regions as positive and negative controls respectively, on both the samples as well as the reserved undigested controls. Size selection enrichment was calculated as follows:

$$\text{Enrichment} = 2^{((Ct_{(\text{negative control primer})}-Ct_{(\text{positive control primers})})_{\text{digested, size selected fragments}} - (Ct_{(\text{negative control primer})}-Ct_{(\text{positive control primers})})_{\text{undigested control}})}$$

Size selected DNA fragments underwent Illumina sequencing library preparation and quality control assessment, according to the procedures at MIT's BioMicro Center. Samples were sequenced by Illumina Hi-Seq.

K. DNase-qPCR

DNase-qPCR samples were prepared from the doxycycline-induced dominant-negative cell lines and control cell lines in the absence of doxycycline as per the DNase-seq protocol above. Experimental primers were designed for pioneer transcription factor binding sites and used in conjunction with the positive and negative hypersensitivity control primers described above in quantitative PCR analyses. Hypersensitivity at experimental primers sites was calculated for the dominant negative lines and control lines as follows:

$$2^{((\text{Average } Ct_{(\text{negative control primers})}-Ct_{(\text{experimental primer})}) - (\text{Average } Ct_{(\text{negative control primers})}-\text{Average } Ct_{(\text{positive control primers})}))}$$

DNase-qPCR is known to be highly reproducible with a sufficient dynamic range to reproducibly distinguish the changes in binding strength we expected in this experimental setup (~2-fold). Four biological replicates of each DNase-qPCR experiment were performed to control for experimental variability, which was minimal and relatively similar in all sample groups. Significance was calculated using a one-tailed Student's t-test at P<0.01.

L. References

1. Takahashi, K. & Yamanaka, S. Induction of pluripotent stem cells from mouse embryonic and adult fibroblast cultures by defined factors. *Cell* **126**, 663-676 (2006).
2. Hanna, J.H., Saha, K. & Jaenisch, R. Pluripotency and cellular reprogramming: facts, hypotheses, unresolved issues. *Cell* **143**, 508-525 (2010).
3. Mullen, A.C. et al. Master transcription factors determine cell-type-specific responses to TGF-beta signaling. *Cell* **147**, 565-576 (2011).
4. Trompouki, E. et al. Lineage regulators direct BMP and Wnt pathways to cell-specific programs during differentiation and regeneration. *Cell* **147**, 577-589 (2011).
5. Young, R.A. Control of the embryonic stem cell state. *Cell* **144**, 940-954 (2011).
6. Davidson, E.H. Emerging properties of animal gene regulatory networks. *Nature* **468**, 911-920 (2010).
7. Johnson, D.S., Mortazavi, A., Myers, R.M. & Wold, B. Genome-wide mapping of in vivo protein-DNA interactions. *Science* **316**, 1497-1502 (2007).
8. Guo, Y. et al. Discovering homotypic binding events at high spatial resolution. *Bioinformatics* **26**, 3028-3034 (2010).
9. Guo, Y., Mahony, S. & Gifford, D.K. High resolution genome wide binding event finding and motif discovery reveals transcription factor spatial binding constraints. *PLoS Comput Biol* **8**, e1002638 (2012).
10. Boyle, A.P. et al. High-resolution mapping and characterization of open chromatin across the genome. *Cell* **132**, 311-322 (2008).
11. Weintraub, H. & Groudine, M. Chromosomal subunits in active genes have an altered conformation. *Science* **193**, 848-856 (1976).
12. Wu, C. The 5' ends of Drosophila heat shock genes in chromatin are hypersensitive to DNase I. *Nature* **286**, 854-860 (1980).
13. Boyle, A.P. et al. High-resolution genome-wide in vivo footprinting of diverse transcription factors in human cells. *Genome Research* **21**, 456-464 (2011).
14. Pique-Regi, R. et al. Accurate inference of transcription factor binding from DNA sequence and chromatin accessibility data. *Genome Res* **21**, 447-455 (2011).
15. Neph, S. et al. An expansive human regulatory lexicon encoded in transcription factor footprints. *Nature* **489**, 83-90 (2012).
16. Thurman, R.E. et al. The accessible chromatin landscape of the human genome. *Nature* **489**, 75-82 (2012).
17. Hesselberth, J.R. et al. Global mapping of protein-DNA interactions in vivo by digital genomic footprinting. *Nat Methods* **6**, 283-289 (2009).
18. Boyle, A.P. et al. High-resolution genome-wide in vivo footprinting of diverse transcription factors in human cells. *Genome Res* **21**, 456-464 (2011).
19. Chen, X., Hoffman, M.M., Bilmes, J.A., Hesselberth, J.R. & Noble, W.S. A dynamic Bayesian network for identifying protein-binding footprints from single molecule-based sequencing data. *Bioinformatics* **26**, i334-342 (2010).
20. Minka, T. Expectation Propagation for Approximate Bayesian Inference. *UAI '01: Proceedings of the 17th Conference in Uncertainty in Artificial Intelligence*, 362-369 (2001).
21. Chen, X. et al. Integration of External Signaling Pathways with the Core Transcriptional Network in Embryonic Stem Cells. *Cell* **133**, 1106-1117 (2008).
22. Joseph, R. et al. Integrative model of genomic factors for determining binding site selection by estrogen receptor-alpha. *Mol Syst Biol* **6**, 456 (2010).

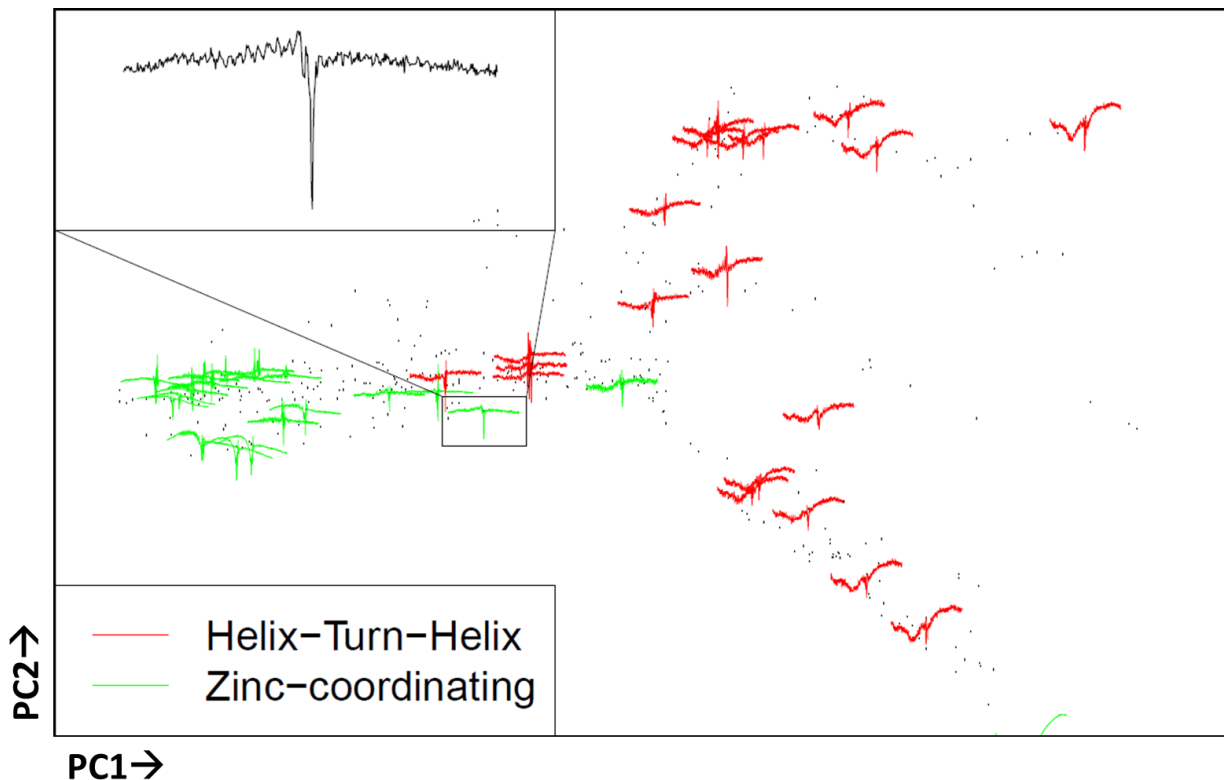
23. Kaplan, T. et al. Quantitative models of the mechanisms that control genome-wide patterns of transcription factor binding during early Drosophila development. *PLoS Genet* **7**, e1001290 (2011).
24. Zaret, K.S. & Carroll, J.S. Pioneer transcription factors: establishing competence for gene expression. *Genes Dev* **25**, 2227-2241 (2011).
25. Gualdi, R. et al. Hepatic specification of the gut endoderm in vitro: cell signaling and transcriptional control. *Genes Dev* **10**, 1670-1682 (1996).
26. Soufi, A., Donahue, G. & Zaret, K.S. Facilitators and impediments of the pluripotency reprogramming factors' initial engagement with the genome. *Cell* **151**, 994-1004 (2012).
27. Sherwood, R.I., Maehr, R., Mazzoni, E.O. & Melton, D.A. Wnt signaling specifies and patterns intestinal endoderm. *Mech Dev* (2011).
28. Cirillo, L.A. et al. Opening of compacted chromatin by early developmental transcription factors HNF3 (FoxA) and GATA-4. *Mol Cell* **9**, 279-289 (2002).
29. Nardini, M. et al. Sequence-specific transcription factor NF-Y displays histone-like DNA binding and H2B-like ubiquitination. *Cell* **152**, 132-143 (2013).
30. Budry, L. et al. The selector gene Pax7 dictates alternate pituitary cell fates through its pioneer action on chromatin remodeling. *Genes Dev* **26**, 2299-2310 (2012).
31. Eeckhoute, J., Carroll, J.S., Geistlinger, T.R., Torres-Arzayus, M.I. & Brown, M. A cell-type-specific transcriptional network required for estrogen regulation of cyclin D1 and cell cycle progression in breast cancer. *Genes Dev* **20**, 2513-2526 (2006).
32. Hori, S. c-Rel: a pioneer in directing regulatory T-cell lineage commitment? *Eur J Immunol* **40**, 664-667 (2010).
33. Treiber, T. et al. Early B cell factor 1 regulates B cell gene networks by activation, repression, and transcription-independent poising of chromatin. *Immunity* **32**, 714-725 (2010).
34. John, S. et al. Chromatin accessibility pre-determines glucocorticoid receptor binding patterns. *Nat Genet* **43**, 264-268 (2011).
35. Kawakami, K. & Noda, T. Transposition of the Tol2 element, an Ac-like element from the Japanese medaka fish Oryzias latipes, in mouse embryonic stem cells. *Genetics* **166**, 895-899 (2004).
36. Kundaje, A. et al. Ubiquitous heterogeneity and asymmetry of the chromatin environment at regulatory elements. *Genome Res* **22**, 1735-1747 (2012).
37. Eddy, J. et al. G4 motifs correlate with promoter-proximal transcriptional pausing in human genes. *Nucleic Acids Res* **39**, 4975-4983 (2011).
38. Sekiya, T., Muthurajan, U.M., Luger, K., Tulin, A.V. & Zaret, K.S. Nucleosome-binding affinity as a primary determinant of the nuclear mobility of the pioneer transcription factor FoxA. *Genes Dev* **23**, 804-809 (2009).
39. Dunham, I. et al. An integrated encyclopedia of DNA elements in the human genome. *Nature* **489**, 57-74 (2012).
40. Bhattacharya, A. et al. The B subunit of the CCAAT box binding transcription factor complex (CBF/NF-Y) is essential for early mouse development and cell proliferation. *Cancer Res* **63**, 8167-8172 (2003).
41. Huo, L. & Scarpulla, R.C. Mitochondrial DNA instability and peri-implantation lethality associated with targeted disruption of nuclear respiratory factor 1 in mice. *Mol Cell Biol* **21**, 644-654 (2001).
42. Koohy, H., Down, T.A. & Hubbard, T.J. Chromatin accessibility data sets show bias due to sequence specificity of the DNase I enzyme. *PLoS One* **8**, e69853 (2013).
43. He, H.H. et al. Refined DNase-seq protocol and data analysis reveals intrinsic bias in transcription factor footprint identification. *Nat Methods* (2013).

44. Sekiya, T. & Zaret, K.S. Repression by Groucho/TLE/Grg proteins: genomic site recruitment generates compacted chromatin in vitro and impairs activator binding in vivo. *Mol Cell* **28**, 291-303 (2007).
45. Watts, J.A. et al. Study of FoxA pioneer factor at silent genes reveals Rfx-repressed enhancer at Cdx2 and a potential indicator of esophageal adenocarcinoma development. *PLoS Genet* **7**, e1002277 (2011).
46. Xu, J. et al. Transcriptional competence and the active marking of tissue-specific enhancers by defined transcription factors in embryonic and induced pluripotent stem cells. *Genes Dev* **23**, 2824-2838 (2009).
47. Li, Z., Schug, J., Tuteja, G., White, P. & Kaestner, K.H. The nucleosome map of the mammalian liver. *Nat Struct Mol Biol* **18**, 742-746 (2011).
48. Iacovino, M. et al. A conserved role for Hox paralog group 4 in regulation of hematopoietic progenitors. *Stem Cells Dev* **18**, 783-792 (2009).
49. Ying, Q.L. et al. The ground state of embryonic stem cell self-renewal. *Nature* **453**, 519-523 (2008).
50. Song, L. & Crawford, G.E. DNase-seq: a high-resolution technique for mapping active gene regulatory elements across the genome from mammalian cells. *Cold Spring Harb Protoc* **2010**, pdb prot5384 (2010).
51. Rasmussen, C.E. & Williams, C.K.I. Gaussian Processes for Machine Learning. (The MIT Press, 2005).
52. Friedman, J., Hastie, T. & Tibshirani, R. Sparse inverse covariance estimation with the graphical lasso. *Biostatistics* **9**, 432-441 (2008).
53. Barlow, R.E. & etc Statistical Inference Under Order Restrictions: Theory and Application of Isotonic Regression. (John Wiley & Sons Ltd, 1972).
54. Liu, Q. & Pierce, D.A. A note on Gauss—Hermite quadrature. *Biometrika* **81**, 624-629 (1994).
55. Minka, T.P. 362-369 (2001).
56. Seeger, M. (Technical report, University of California at Berkeley, 2005. See www. kyb. tuebingen. mpg. de/bs/people/seeger, 2005).
57. Schölkopf, B. & Smola, A. Learning with Kernels: Support Vector Machines, Regularization, Optimization, and Beyond (Adaptive Computation and Machine Learning). (The MIT Press, 2001).
58. Chen, X. et al. Integration of external signaling pathways with the core transcriptional network in embryonic stem cells. *Cell* **133**, 1106-1117 (2008).
59. Marson, A. et al. Connecting microRNA genes to the core transcriptional regulatory circuitry of embryonic stem cells. *Cell* **134**, 521-533 (2008).
60. Dunham, I. et al. An integrated encyclopedia of DNA elements in the human genome. *Nature* **489**, 57-74 (2012).
61. Min, I.M. et al. Regulating RNA polymerase pausing and transcription elongation in embryonic stem cells. *Genes Dev* **25**, 742-754 (2011).
62. Guttman, M. et al. Ab initio reconstruction of cell type-specific transcriptomes in mouse reveals the conserved multi-exonic structure of lincRNAs. *Nat Biotechnol* **28**, 503-510 (2010).
63. Creyghton, M.P. et al. Histone H3K27ac separates active from poised enhancers and predicts developmental state. *Proc Natl Acad Sci U S A* **107**, 21931-21936 (2010).
64. Zhang, Y. et al. Model-based analysis of ChIP-Seq (MACS). *Genome Biol* **9**, R137 (2008).
65. Stadler, M.B. et al. DNA-binding factors shape the mouse methylome at distal regulatory regions. *Nature* **480**, 490-495 (2011).
66. Krueger, F. & Andrews, S.R. Bismark: a flexible aligner and methylation caller for Bisulfite-Seq applications. *Bioinformatics* **27**, 1571-1572 (2011).

Supplementary Figures

Supplementary Figure 1: Detection and evolutionary clustering of TF-specific profiles

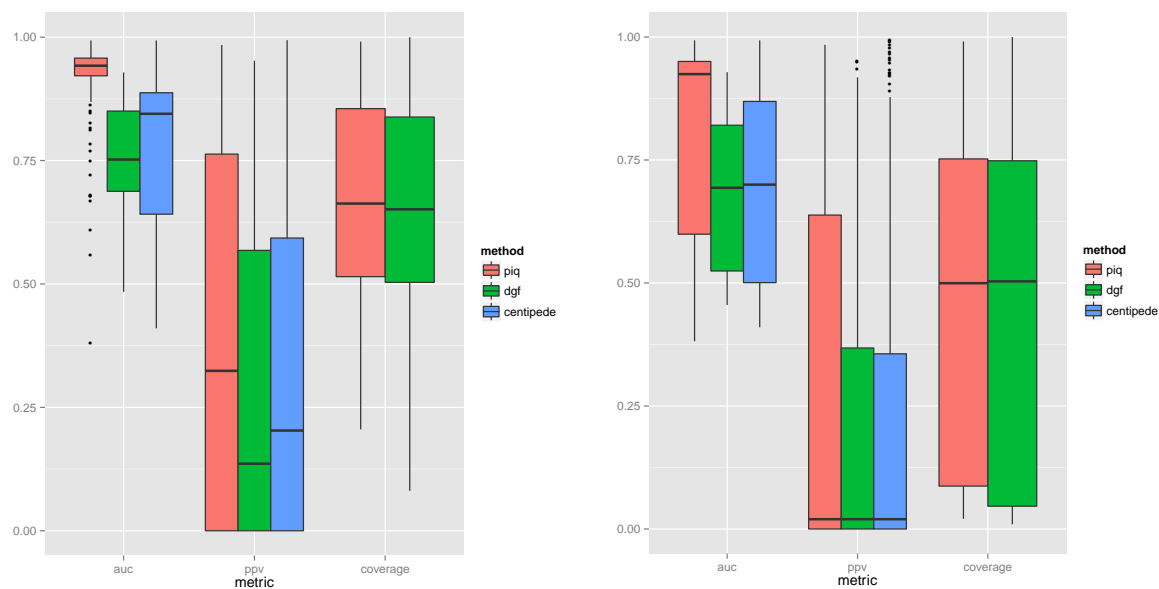
Plot displaying average DNase hypersensitive +/- 200 bp from genomic motif matches for TFs in the Helix-Turn-Helix family (red profiles) or Zinc-Coordinating family (green profiles). Profiles for all TFs were subjected to Principle Component Analysis (PCA) and plotted by their PC1 (X-axis) and PC2 (Y-axis) values. TFs not in either of the above families are represented as dots.



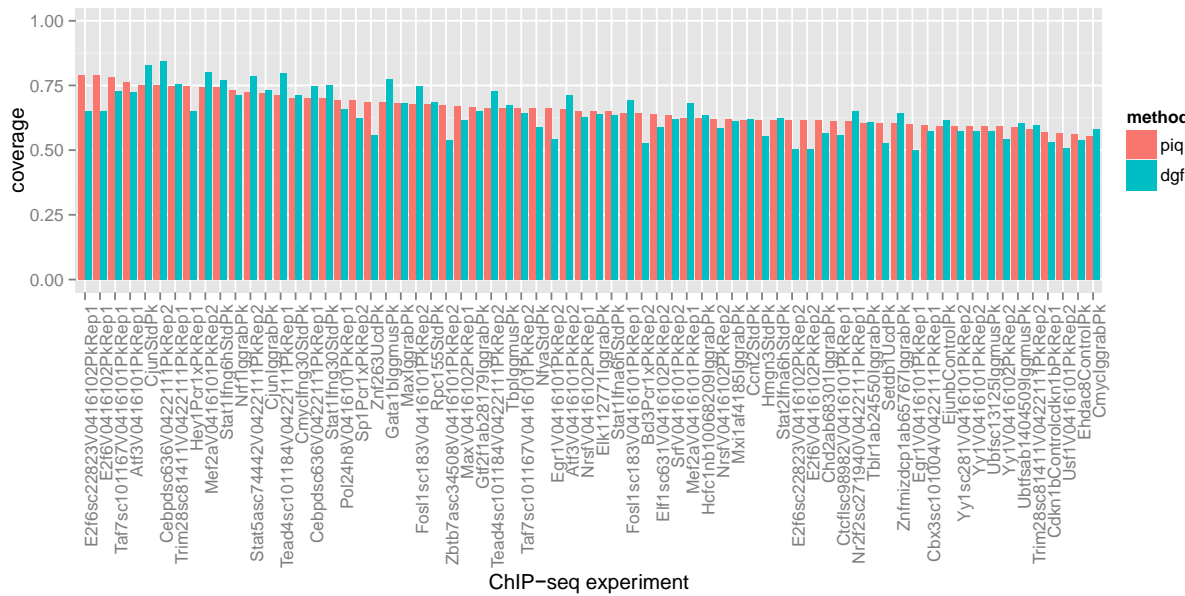
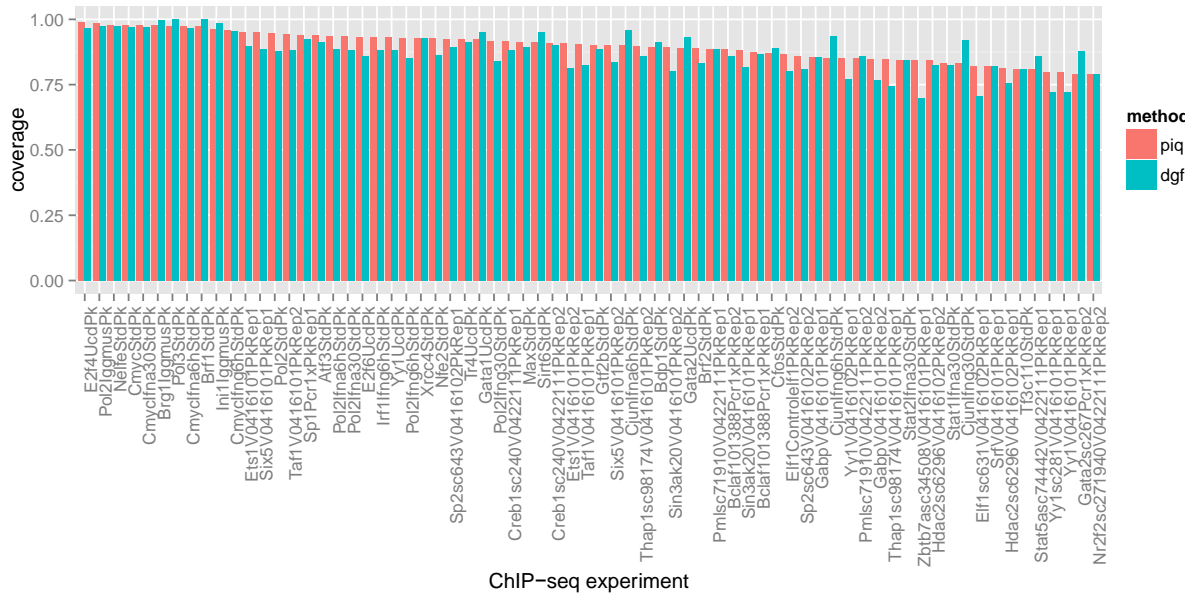
Supplementary Figure 2: PIQ displays higher AUC and PPV than and comparable site coverage to other DNase-Seq algorithms

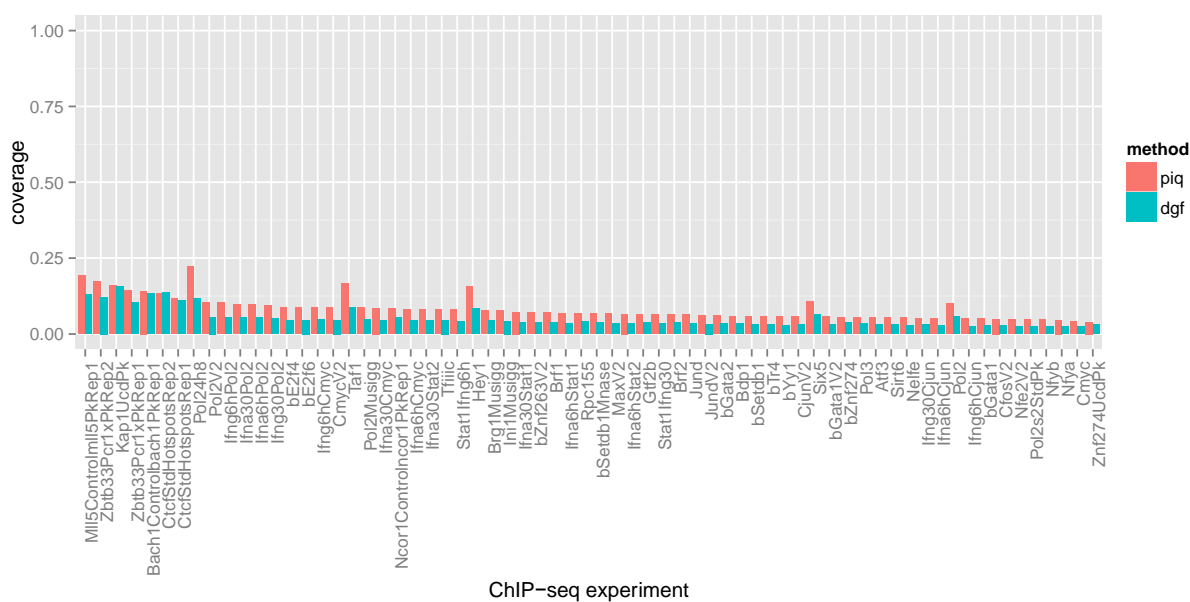
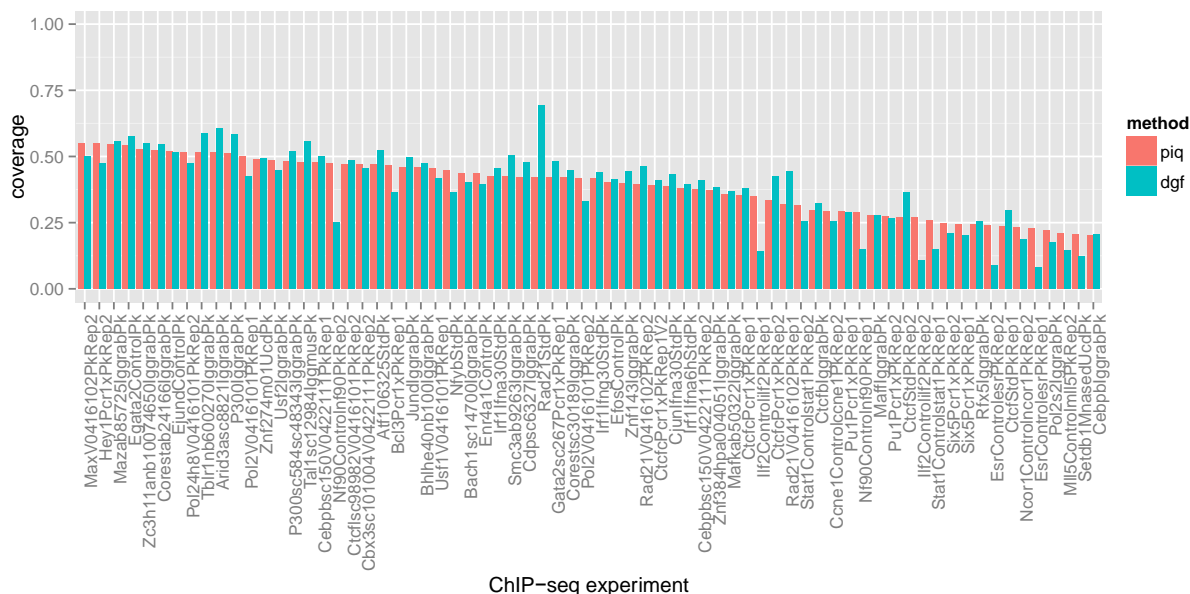
(A) Summary bar charts indicating the median and quartiles for AUC, PPV, and Coverage over the set of 200/303 ChIP-seq experiments with more than 50% of sites matching a PWM (left) and over all 303 ChIP-Seq experiments (right) for PIQ (red), DGF (green), and CENTIPEDE (blue). CENTIPEDE does not make binding call cutoffs and so Coverage cannot be determined. (B) The number of total ChIP-Seq binding site calls which are predicted by PIQ (red) and DGF (blue) are displayed as a fractional coverage. Higher PIQ and DGF coverage scores correlate with more robust ChIP-Seq experiments.

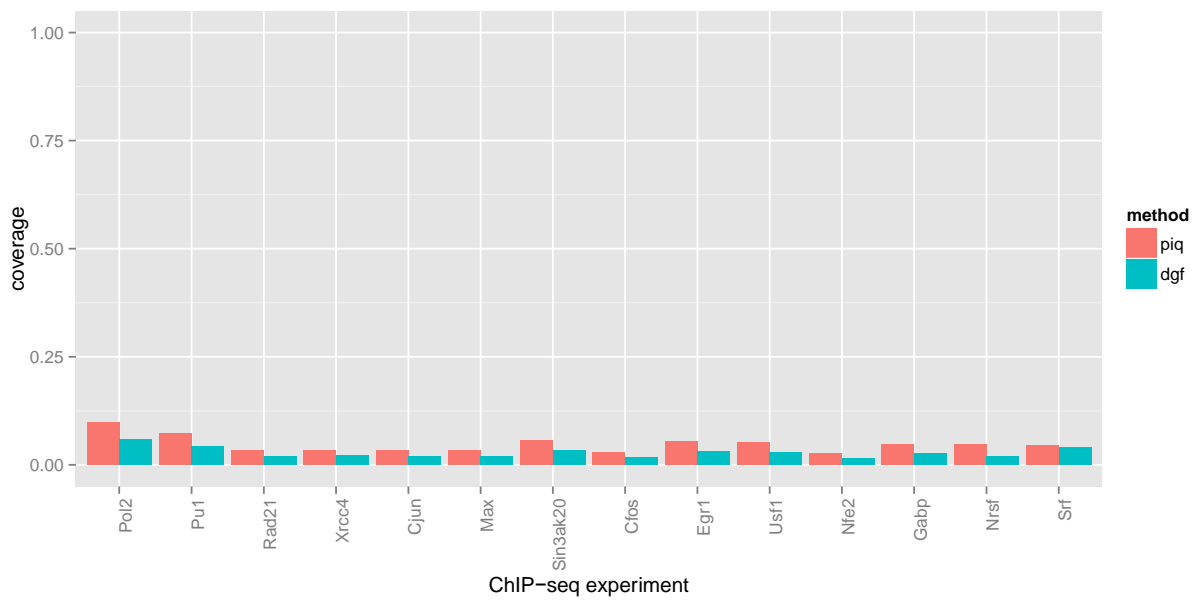
A



B

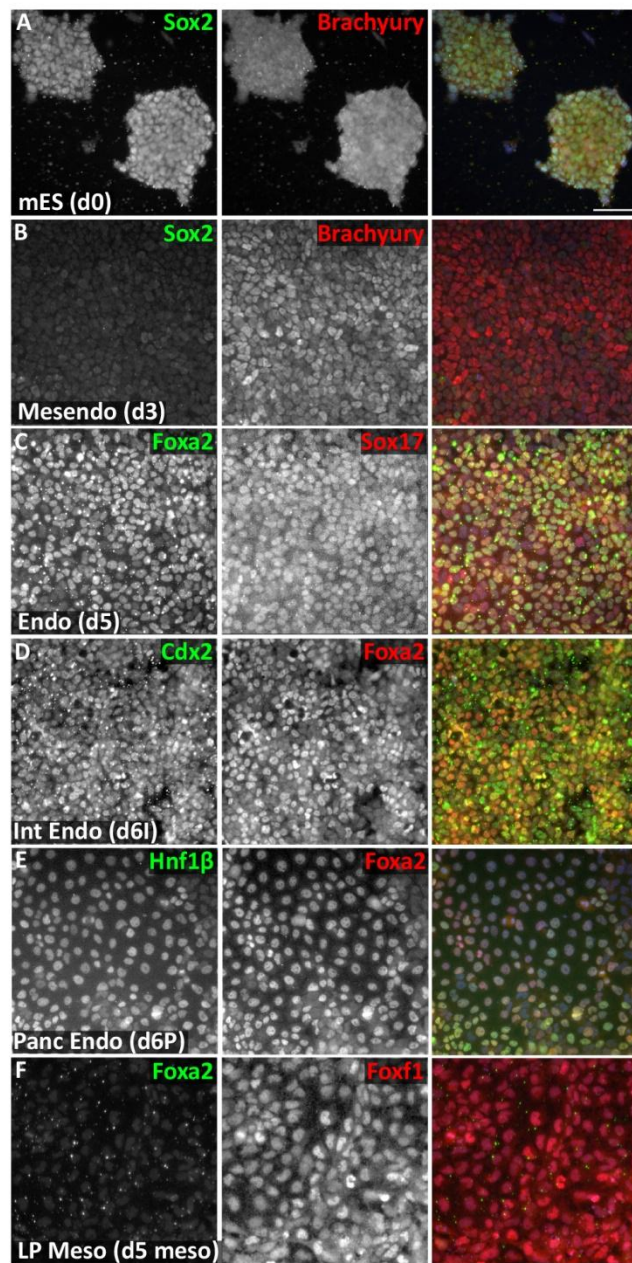






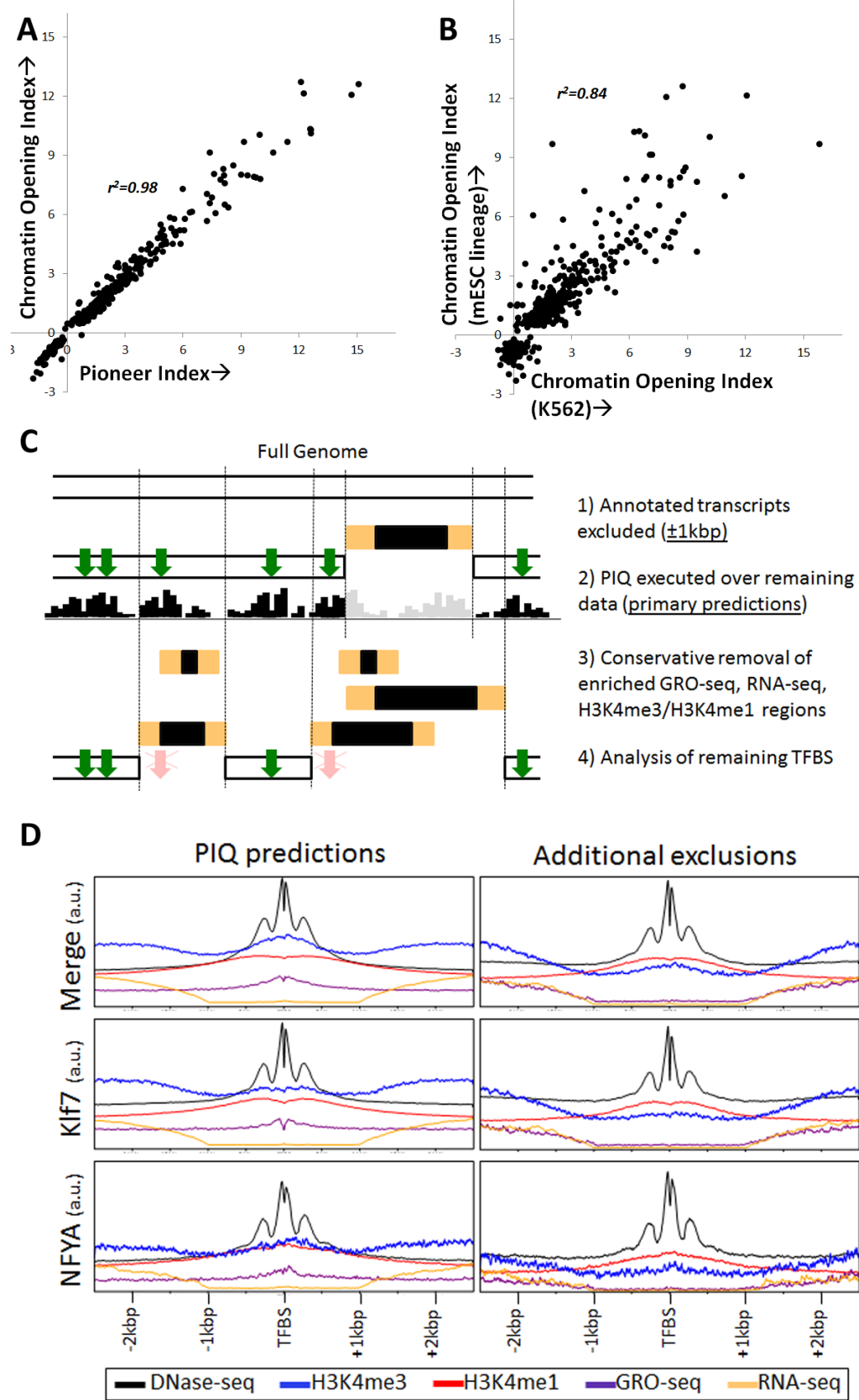
Supplementary Figure 3: Efficient differentiation of mES cells to endodermal and mesodermal lineages

(A-F) Representative immunofluorescence images of mES cells at the six stages of differentiation used for DNase-Seq analysis. Cells are stained with TFs indicative of particular developmental states: Sox2 for mES cells (A), Brachyury for mesendoderm (B), Foxa2 and Sox17 for endoderm (C), Cdx2 for intestinal endoderm (D), Hnf1 β for pre-pancreatic endoderm (E), Foxf1 for lateral plate mesoderm (F).



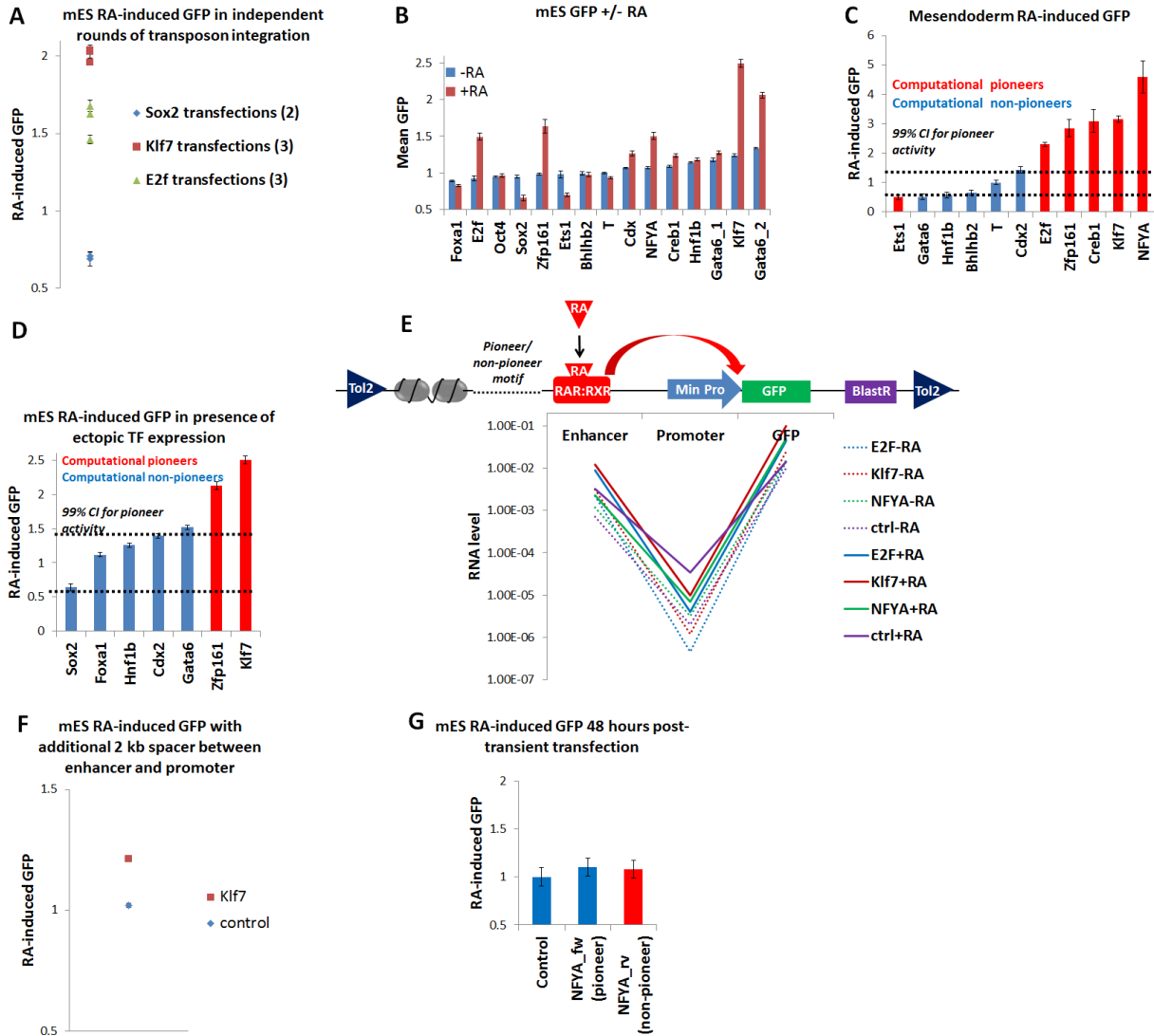
Supplementary Figure 4: Pioneer TFs are consistent across cell type and do no exclusively populate promoters

(A) Plot comparing chromatin opening index vs pioneer index for all 733 motifs in mouse lineage. The r^2 value for a linear trendline is displayed. (B) Plot comparing chromatin opening index in the mESC lineage (Y-axis) with the chromatin opening index in K562 cells (X-axis) for all 733 motifs in mouse lineage. The r^2 value for a linear trendline is displayed. (C) Schematic indicating removal of potential promoter-associated regions to confirm non-promoter pioneer TF activity. Full procedure excludes 56-87% of mES binding events from 9 computationally predicted pioneers (Figure 2E), resulting in approximately 2k-126k events per TF. (D) DNase-seq TF binding profiles remain similar before and after promoter removal, indicated by mES metapeaks over the 9 predicted pioneers binding sites (“Merge”) and individual examples Klf7 and NFYA.



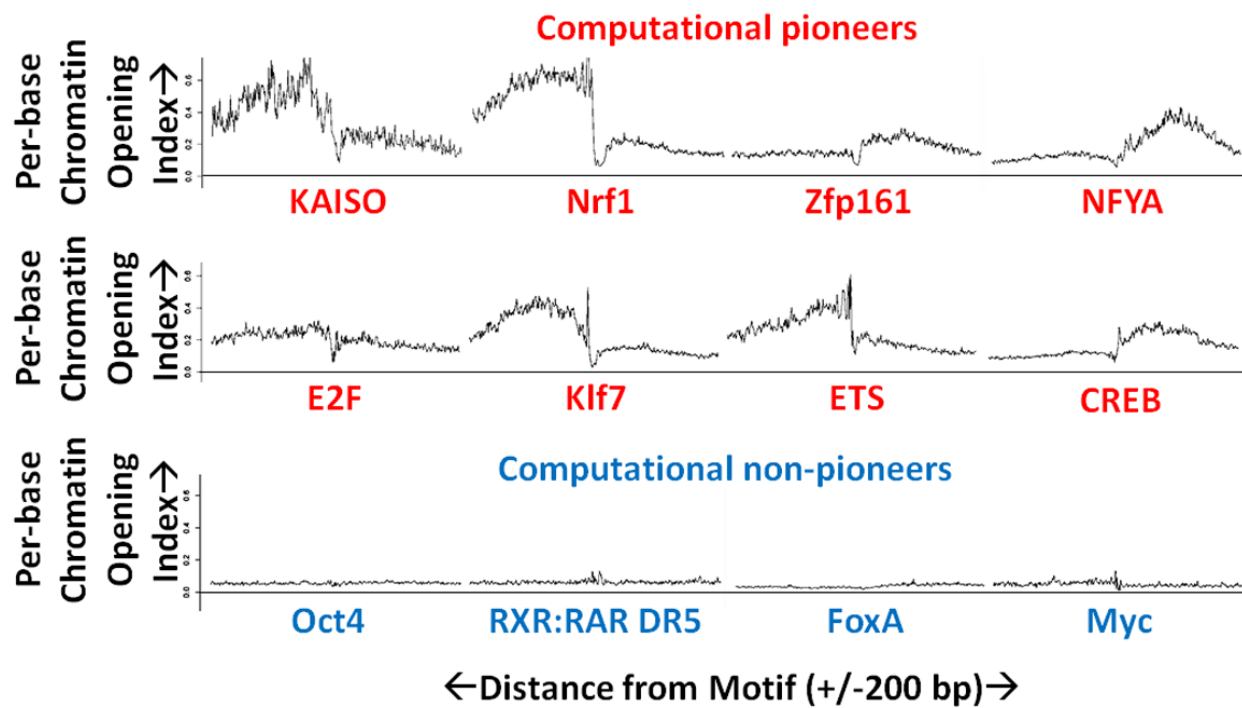
Supplementary Figure 5: Pioneer reporter assay faithfully measures motif-induced RAR binding and activation potential

(A) Plot showing average flow cytometric RA-induced GFP for distinct rounds of transfection for three reporter constructs, each displaying a tight range of fluorescence characteristic of that line. (B) Average GFP fluorescence values for reporter lines in the absence (blue) and presence (red) of RA, normalized to control line fluorescence and plotted according to fluorescence in the absence of RA. There is not a strong correlation between fluorescence in the absence and presence of RA, suggesting that pioneers do not simply induce reporter fluorescence *per se*. (C-D) Plots showing average flow cytometric RA-induced GFP for computational pioneer (red) and non-pioneer (blue) reporter lines after RA induction at the mesendoderm stage (C) and mES stage in the presence of Doxycycline-induced ectopic TF expression (D), displaying significantly increased RA-induced GFP in pioneer reporter lines. (E) RT-qPCR analysis of three pioneer reporter lines (E2F, Klf7, and NFYA) and the control reporter line. RT was performed using random hexamer primers and qPCR performed using primers in the GFP transcript (GFP), in the minimal promoter (Promoter) and in the constant RXR:RAR binding site region of the reporter enhancer (Enhancer). RNA levels at each region in the absence (dotted) and presence (solid) of RA normalized to β -actin and Gapdh are shown. Transcript production in the GFP gene body and enhancer are correlated with fluorescence activity but promoter transcription is uniformly low and uncorrelated with fluorescence, indicating that transcripts do not span the minimal promoter. (F) Plot showing average flow cytometric RA-induced GFP for computational pioneer Klf7 (red) and non-pioneer control (blue) reporter lines in which a 2 kb spacer region was inserted between the enhancer and minimal promoter. The Klf7 line displays significantly increased RA-induced GFP, suggesting position-independent pioneer activity, a hallmark of enhancers. (G) Plot showing normalized average flow cytometric RA-induced GFP for non-pioneer control and NFYA reverse (blue) and pioneer NFYA forward (red) reporter lines 48 hours following transient plasmid transfection. All lines show similar RA-induced GFP suggesting that genomic integration is required for pioneer activity.



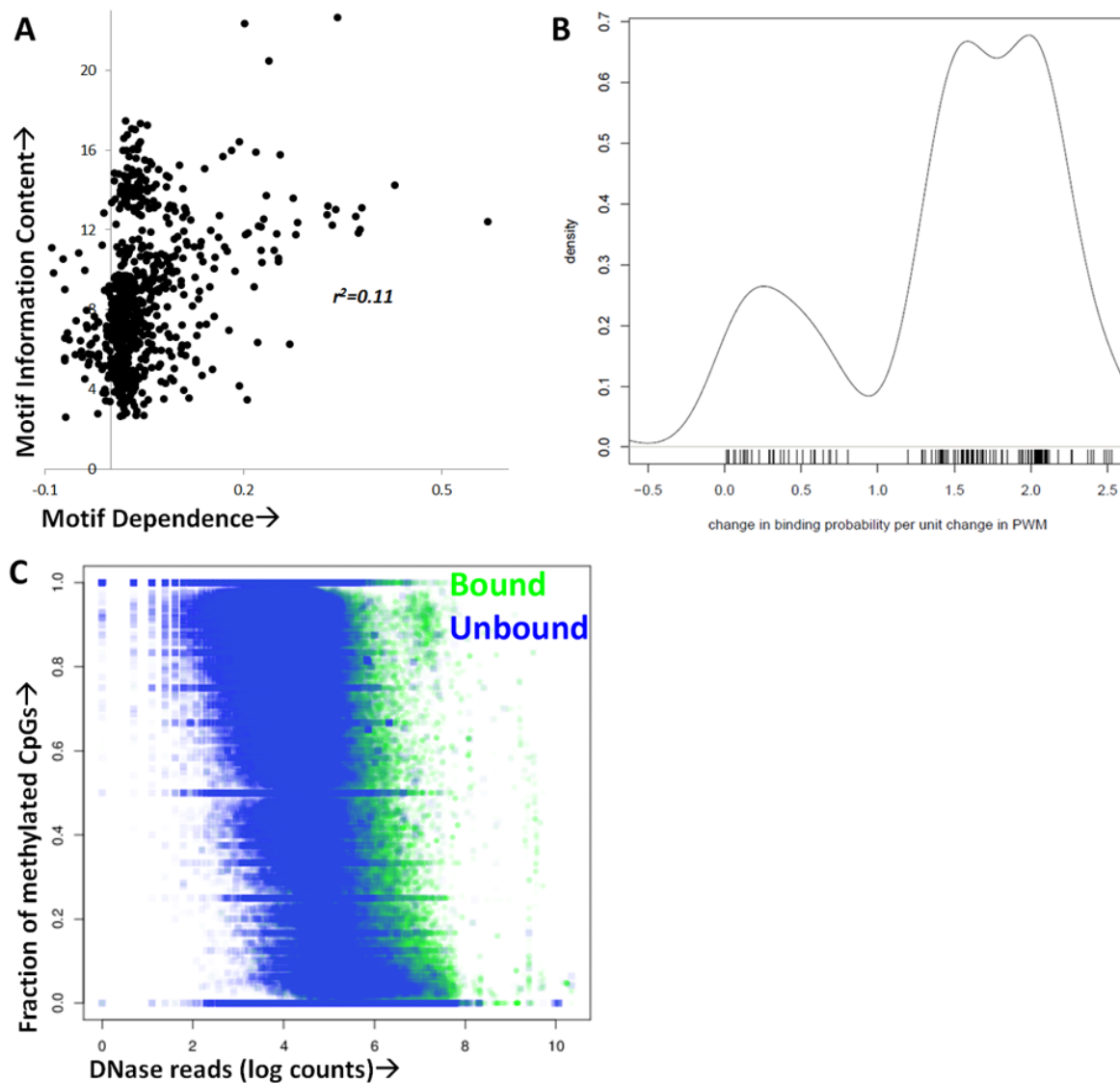
Supplementary Figure 6: Some pioneer TFs open chromatin asymmetrically

Expected per-base chromatin opening in natural log units +/- 200 bp from computational pioneer (red) and non-pioneer (blue) motifs. Note the directional chromatin opening of some pioneer TFs.



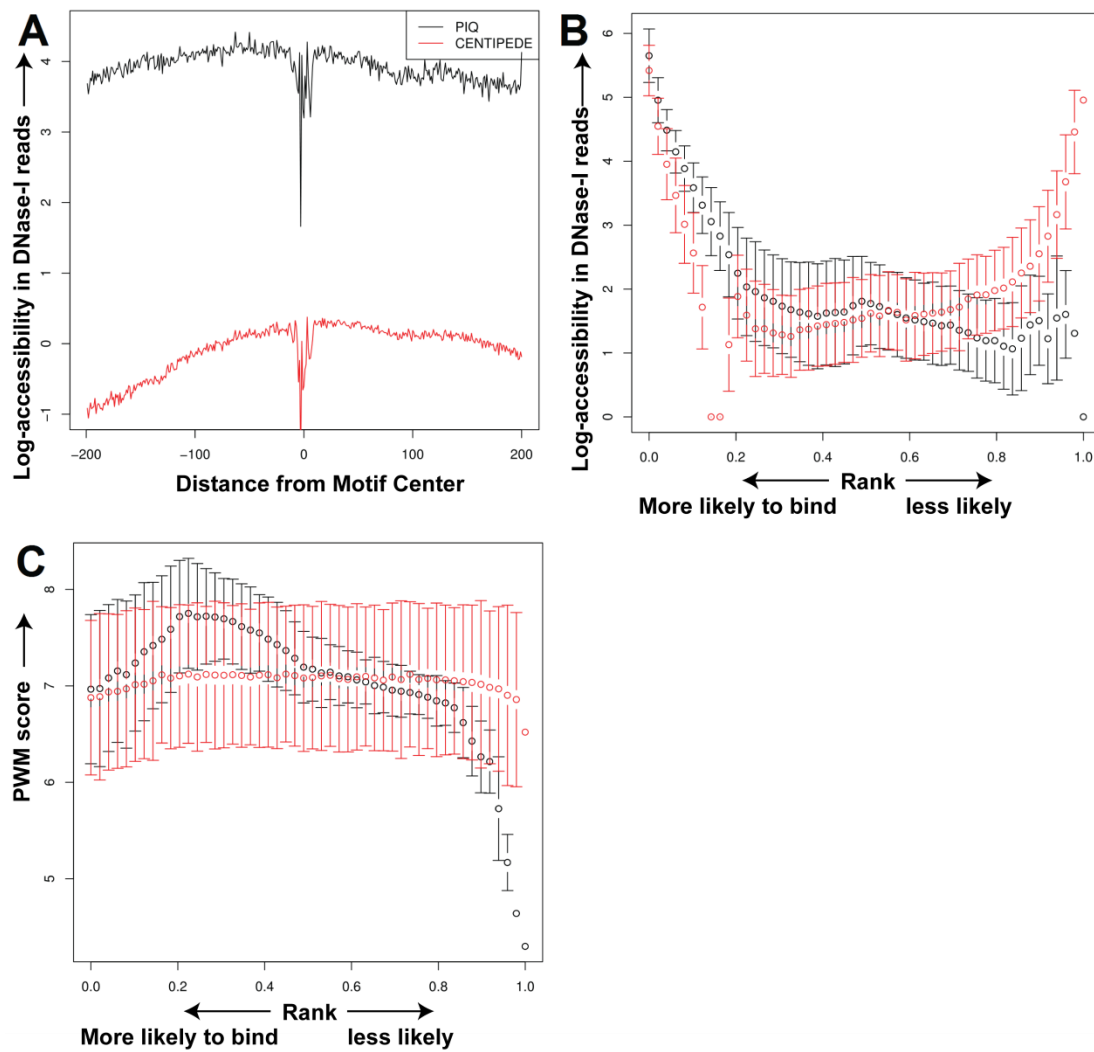
Supplementary Figure 7: TF prediction is enhanced by motif-dependence and DNA methylation information

(A) Plot comparing motif-dependence (X-axis) with motif information content (Y-axis) for all 733 motifs in mouse lineage. The r^2 value for a linear trendline is shown. (B) Histogram showing change in binned binding probability per unit change in log PWM score at a binding candidate (X-axis) for each K562 ChIP-Seq experiments. Note how experiments cluster into motif-dependent and motif-independent clusters. (C) Plot comparing log DNase reads (X-axis) with fraction methylated CpGs +/- 10 bp of a motif for all bound (green) and unbound (blue) PIQ calls in mESC. Note the anti-correlation between DNase reads and methylation.



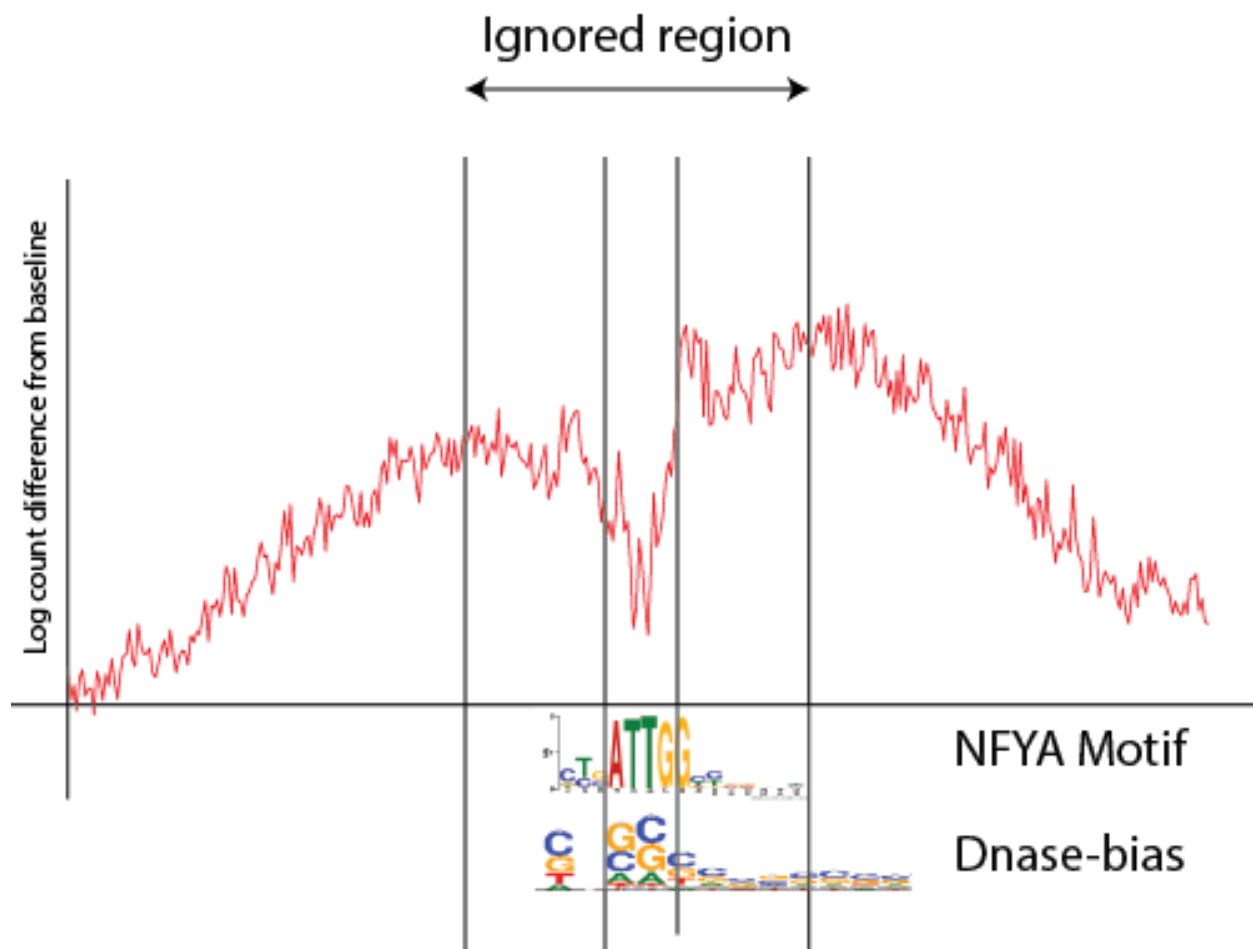
Supplementary Figure 8: PIQ allows for binding prediction for pioneers with weak footprints.

(A) Plot comparing estimated DNase I profiles for Gata6_2 on PIQ (black) and CENTIPEDE (red). Both capture the same footprint pattern, but PIQ captures that Gata6 has higher average accessibility compared to the genome while CENTIPEDE encodes only shape. (B) Comparison of accessibility (y axis) with rankings generated by each algorithm for likelihood of binding (x axis). PIQ shows monotone relationship between accessibility and binding, while CENTIPEDE's U shaped behavior shows that its more stringent reliance on shape makes it reject candidates with high accessibility if it does not precisely match the estimated shape (C) PIQ enriches for PWM (y axis) as a function of binding rank (x axis) compared to CENTIPEDE, showing that PIQ does not simply select more accessible sites, but selects sites that have accessibility, high PWM scores, and correct shape.



Supplementary Figure 9: Profile level significance test to avoid sequence bias

Plot depicting the aggregate DNase profile PIQ generates for NFYA in log count difference from baseline (Y-axis) in the 400 bp region centered on above-threshold NFYA motifs (X-axis). The DNase footprint region in which DNase-seq sequence bias has been reported (inner lines) and the DNase profile used by PIQ to estimate factor binding (outer lines) are shown, demonstrating that PIQ utilizes a substantially larger region to estimate binding than the area potentially affected by DNase sequence bias. NFYA motif logo and reported DNase enzyme bias logo are overlaid under the plot. PIQ performs a profile-level significance test for whether or not an estimated TF profile is significant outside its motif match region, and all identified pioneer TFs are highly significant. Pioneer metrics such as the chromatin opening index are measured only after removal of the motif match region and its flanking elements as a test statistic for sequence bias. Using a null distribution based upon median and IQR fitted normal, we find that our pioneers are statistically significant with p-values ranging from 1.5e-9 (KAISO) to 3.8e-3 (Gata6).



Supplementary Tables

Supplementary Table 1: DNase-Seq predictions compared with matched ChIP-Seq binding sites calls

For each published K562 ChIP-Seq experiment, binding site counts and predictive accuracy statistics are shown for each algorithm. The fraction of total binding site regions which match the appropriate motif above a certain threshold is also given, with these sites used to determine AUC numbers. PPV numbers are calculated comparing the top 500 predictions of each method against matched ChIP-Seq experiments, while coverage (Cov) indicates how many of the total ChIP-Seq annotations are predicted to be bound to any potential factor motif (since ChIP-Seq peaks can result from co-factor binding, and methods such as DGF are factor agnostic). We note that CENTIPEDE natively produces rankings with no default cutoff with which to make a binary call, therefore the coverage can vary from zero to full ChIP-Seq binding site coverage at the cost of PPV. For relative performance comparisons, AUC should be used to gauge the PPV-coverage tradeoff.

ChIP-Seq Experiment	Total annotated binding sites	Percent sites in DHS region	Percent sites with PWM match	PIQ			DGF			CENTIPEDE	
				AU C	PPV	Cov	AU C	PPV	Cov	AU C	PPV
Brf1StdPk	73	100%	100%	98%	0%	97 %	78%	0%	100 %	98%	0%
Brf2StdPk	18	94%	100%	93%	0%	89 %	69%	0%	83%	91%	0%
Pol3StdPk	80	100%	100%	97%	0%	98 %	78%	0%	100 %	98%	0%
Pol2IggmusPk	4,792	100%	100%	92%	0%	99 %	62%	0%	97%	88%	0%
Brg1IggmusPk	637	100%	100%	96%	0%	98 %	71%	0%	100 %	95%	0%
E2f4UcdPk	6,020	100%	100%	96%	0%	99 %	72%	0%	96%	84%	0%
Ini1IggmusPk	451	100%	100%	95%	0%	96 %	68%	0%	98%	92%	0%
CmycStdPk	3,323	100%	100%	95%	0%	98 %	72%	0%	97%	90%	0%
Cmyclfna6hStdPk	3,384	100%	99%	96%	0%	97 %	68%	0%	97%	93%	0%
Cmyclfna30StdPk	1,913	100%	99%	96%	0%	98 %	68%	0%	97%	94%	0%
NelfeStdPk	297	100%	99%	95%	0%	98 %	75%	0%	97%	76%	0%
Taf1V0416101PkRep2	13,570	99%	99%	96%	65 %	94 %	92%	58 %	88%	88%	77 %
Pol2lfna6hStdPk	8,092	98%	99%	93%	0%	94 %	70%	0%	89%	45%	0%
Cmyclfng6hStdPk	6,646	99%	99%	94%	0%	96 %	66%	0%	95%	87%	0%

Pol2Ifna30StdPk	7,672	98%	99%	92%	0%	94 %	69%	0%	88%	45%	0%
Taf1V0416101PkRep1	16,968	99%	99%	96%	%	77 %	91 %	72%	47 %	83%	82% %
Pol2StdPk	11,568	98%	99%	93%	0%	95 %	86%	0%	88%	47%	0%
Ets1V0416101PkRep2	13,721	98%	99%	97%	%	76 %	91 %	91%	70 %	81%	89% 85 %
Ets1V0416101PkRep1	8,074	98%	98%	98%	%	87 %	95 %	90%	85 %	90%	88% 95 %
Pol2Ifng6hStdPk	10,582	97%	98%	93%	0%	93 %	85%	0%	85%	47%	0%
Pol2Ifng30StdPk	11,085	97%	98%	93%	0%	92 %	85%	0%	84%	48%	0%
Sin3ak20V0416101PkRep2	12,944	98%	98%	95%	%	56 %	89 %	90%	47 %	80%	87% 65 %
E2f6UcdPk	11,863	98%	98%	94%	0%	93 %	88%	0%	86%	83%	0%
Gata1UcdPk	1,703	98%	98%	98%	0%	92 %	86%	0%	95%	94%	0%
Yy1UcdPk	3,141	97%	98%	97%	0%	93 %	76%	0%	88%	83%	0%
CjunIfna6hStdPk	1,707	100%	98%	98%	0%	90 %	75%	0%	96%	97%	0%
Bdp1StdPk	339	99%	97%	96%	0%	89 %	72%	0%	91%	94%	0%
Bclaf101388Pcr1xPkRep2	2,364	97%	97%	93%	%	16 %	89 %	65%	4%	86%	90% 16 %
Atf3StdPk	633	96%	97%	96%	0%	94 %	86%	0%	91%	86%	0%
Pmlsc71910V0422111PkRep1	11,535	98%	97%	94%	%	73 %	89 %	71%	53 %	89%	45% 15 %
Tr4UcdPk	357	98%	97%	96%	0%	92 %	74%	0%	91%	87%	0%
Gata2UcdPk	5,517	99%	97%	97%	0%	89 %	77%	0%	93%	93%	0%
Sirt6StdPk	446	99%	97%	96%	0%	91 %	72%	0%	95%	96%	0%
Sp2sc643V0416102PkRep1	3,735	97%	97%	98%	%	67 %	93 %	91%	11 %	89%	95% 65 %
Sin3ak20V0416101PkRep1	2,585	97%	97%	95%	6%	88 %	72%	2%	82%	93%	7% 26 %
Sp1Pcr1xPkRep1	1,953	96%	97%	99%	%	28 %	94 %	83%	2%	93%	89% 87 %
Irf1Ifng6hStdPk	12,978	97%	97%	97%	%	75 %	93 %	91%	66 %	88%	88% 17 %
Bclaf101388Pcr1xPkRep1	2,297	97%	97%	92%	%	17 %	87 %	75%	5%	87%	64% 27 %
Thap1sc98174V0416101PkRep2	4,276	97%	97%	97%	%	28 %	90 %	92%	6%	86%	86% 26 %
Nfe2StdPk	1,226	99%	96%	96%	0%	93 %	75%	0%	86%	94%	0%
CjunIfng6hStdPk	2,051	100%	96%	97%	0%	85 %	74%	0%	94%	96%	0%
Thap1sc98174V0416101PkRep1	4,208	92%	96%	95%	%	27 %	85 %	87%	8%	75%	81% 26 %
CjunIfng30StdPk	3,431	100%	96%	97%	0%	83	73%	0%	92%	96%	0%

					%						
Gtf2bStdPk	9,725	97%	96%	97%	45 %	90 %	73%	10 %	89%	96%	45 %
MaxStdPk	1,917	96%	96%	95%	0%	91 %	81%	0%	89%	92%	0%
Six5V0416101PkRep1	788	98%	96%	99%	40 %	95 %	92%	13 %	89%	99%	38 %
Creb1sc240V0422111PkRep1	6,891	97%	96%	95%	66 %	92 %	87%	19 %	88%	79%	65 %
Hdac2sc6296V0416102PkRep2	5,830	96%	96%	95%	33 %	84 %	76%	7%	83%	87%	34 %
Creb1sc240V0422111PkRep2	5,452	97%	96%	95%	40 %	91 %	65%	9%	90%	92%	40 %
Pmlsc71910V0422111PkRep2	20,260	98%	96%	95%	86 %	85 %	87%	61 %	86%	49%	11 %
CfosStdPk	4,388	97%	96%	97%	0%	87 %	78%	0%	89%	90%	0%
Tf3c110StdPk	1,380	95%	96%	93%	0%	81 %	64%	0%	81%	90%	0%
Hdac2sc6296V0416102PkRep1	20,201	97%	95%	95%	26 %	82 %	78%	24 %	75%	86%	24 %
E2f6sc22823V0416102PkRep1	14,408	95%	95%	94%	32 %	79 %	70%	19 %	65%	83%	26 %
E2f6V0416102PkRep1	14,408	95%	95%	94%	32 %	79 %	70%	19 %	65%	83%	26 %
Stat1lfna30StdPk	257	98%	95%	94%	0%	83 %	81%	0%	82%	80%	0%
Yy1V0416102PkRep1	4,484	94%	95%	98%	80 %	85 %	78%	39 %	77%	78%	46 %
Sp2sc643V0416102PkRep2	3,276	92%	95%	96%	34 %	86 %	85%	15 %	81%	85%	30 %
Elf1sc631V0416102PkRep1	21,305	94%	95%	97%	81 %	82 %	90%	75 %	71%	89%	92 %
Zbtb7asc34508V0416101PkRep1	9,501	94%	95%	91%	22 %	84 %	80%	13 %	70%	75%	22 %
Bach1	18	94%	94%	99%	7%	78 %	88%	0%	78%	48%	1%
Stat2lfna30StdPk	426	97%	94%	96%	0%	85 %	74%	0%	84%	94%	0%
GabpV0416101PkRep1	12,558	97%	94%	97%	60 %	85 %	80%	12 %	86%	92%	60 %
Yy1sc281V0416101PkRep1	23,869	94%	94%	96%	81 %	80 %	89%	75 %	72%	86%	93 %
Yy1V0416101PkRep1	23,869	94%	94%	96%	81 %	80 %	89%	75 %	72%	86%	93 %
GabpV0416101PkRep2	15,275	93%	94%	96%	76 %	85 %	90%	69 %	77%	86%	85 %
CjunStdPk	6,474	99%	93%	95%	0%	75 %	67%	0%	83%	93%	0%
Xrcc4StdPk	14	100%	93%	95%	0%	93 %	83%	0%	93%	99%	0%
Six5V0416101PkRep2	4,180	94%	93%	99%	94 %	90 %	85%	92 %	84%	87%	99 %
Bcl3Pcr1xPkRep2	1,347	90%	92%	82%	11 %	64 %	61%	4%	53%	60%	11 %
Elf1Controlelf1PkRep2	630	96%	92%	98%	0%	87 %	88%	0%	80%	41%	0%

SrfV0416101PkRep1	5,452	94%	92%	97%	27 %	82 %	85%	6%	82%	92%	27 %
Stat5asc74442V0422111PkRep1	14,401	94%	92%	97%	34 %	81 %	72%	19 %	86%	91%	31 %
Gata1bIggmusPk	7,493	96%	92%	85%	0%	69 %	58%	0%	77%	80%	0%
Stat1lfng6hStdPk	698	93%	92%	92%	0%	74 %	69%	0%	77%	90%	0%
CjunlgggrabPk	16,282	95%	91%	90%	0%	72 %	78%	0%	73%	48%	0%
Gata2sc267Pcr1xPkRep2	6,188	97%	91%	97%	23 %	79 %	77%	10 %	88%	93%	23 %
Cebpdsc636V0422111PkRep2	9,852	97%	91%	95%	41 %	75 %	66%	14 %	84%	92%	42 %
Fosl1sc183V0416101PkRep2	6,781	96%	91%	96%	19 %	68 %	75%	7 %	75%	93%	19 %
Atf3V0416101PkRep1	11,124	94%	91%	96%	58 %	76 %	87%	55 %	73%	87%	67 %
Stat1lfng30StdPk	889	93%	91%	92%	0%	70 %	68%	0%	75%	86%	0%
Nr2f2sc271940V0422111PkRep2	25,017	90%	91%	94%	77 %	79 %	62%	39 %	79%	90%	77 %
MaxV0416102PkRep1	45,358	93%	90%	96%	80 %	67 %	88%	79 %	62%	85%	93 %
Fosl1sc183V0416101PkRep1	8,957	95%	90%	93%	25 %	64 %	65%	9 %	69%	88%	25 %
Tead4sc101184V0422111PkRep1	26,768	97%	90%	95%	79 %	71 %	66%	35 %	80%	92%	80 %
Taf7sc101167V0416101PkRep1	2,219	92%	90%	94%	9 %	78 %	85%	2 %	73%	42%	1 %
Tead4sc101184V0422111PkRep2	47,394	96%	90%	95%	93 %	66 %	64%	70 %	73%	65%	95 %
Stat5asc74442V0422111PkRep2	8,807	91%	90%	94%	39 %	73 %	71%	16 %	79%	89%	42 %
Zbtb7asc34508V0416101PkRep2	38,191	87%	89%	93%	51 %	67 %	87%	51 %	54%	84%	58 %
Mef2aV0416101PkRep2	2,228	96%	89%	96%	16 %	74 %	76%	2 %	80%	94%	16 %
MaxlgggrabPk	44,064	95%	88%	95%	94 %	68 %	85%	82 %	68%	46%	10 %
Cmyclfng30StdPk	37,045	95%	88%	94%	90 %	70 %	85%	76 %	71%	47%	11 %
Rpc155StdPk	745	90%	87%	90%	0%	68 %	66%	0%	69%	87%	0%
Ctcflsc98982V0416101PkRep1	8,466	90%	87%	91%	8 %	61 %	80%	3 %	56%	80%	8 %
Hey1Pcr1xPkRep1	26,278	84%	87%	95%	66 %	75 %	88%	61 %	65%	84%	78 %
Pol24h8V0416101PkRep1	25,868	83%	87%	93%	90 %	69 %	69%	70 %	66%	44%	20 %
Egr1V0416101PkRep2	28,340	87%	87%	93%	44 %	66 %	87%	39 %	54%	82%	51 %
E2f6sc22823V0416102PkRep2	41,942	85%	86%	94%	57 %	62 %	88%	57 %	50%	84%	67 %
E2f6V0416102PkRep2	41,942	85%	86%	94%	57 %	62 %	88%	57 %	50%	84%	67 %
Atf3V0416101PkRep2	13,689	93%	86%	94%	22	66	71%	18	71%	81%	21

					%	%		%		%	%
Bcl3Pcr1xPkRep1	912	86%	86%	86%	5%	46%	58%	1%	37%	75%	5%
Egata2ControlPk	44,937	90%	86%	38%	0%	54%	58%	0%	58%	77%	0%
EjunbControlPk	43,160	91%	85%	91%	0%	59%	70%	0%	62%	46%	0%
Elf1sc631V0416102PkRep2	37,844	87%	85%	96%	0%	87%	64%	88%	83%	59%	86%
Cebpdsc636V0422111PkRep1	17,546	86%	85%	95%	0%	62%	70%	68%	20%	75%	63%
Stat1Ifna6hStdPk	343	89%	85%	88%	0%	65%	61%	0%	64%	84%	0%
Rad21StdPk	12,760	99%	85%	91%	0%	42%	75%	0%	69%	92%	0%
Mef2aV0416101PkRep1	3,286	93%	85%	92%	0%	17%	63%	68%	5%	68%	89%
Taf7sc101167V0416101PkRep2	2,483	87%	84%	92%	0%	15%	66%	68%	3%	64%	69%
Ehdac8ControlPk	16,691	88%	84%	93%	0%	56%	88%	0%	54%	86%	0%
Trim28sc81411V0422111PkRep1	16,212	85%	84%	95%	0%	37%	75%	66%	20%	76%	34%
Stat2Ifna6hStdPk	609	89%	84%	89%	0%	62%	65%	0%	63%	84%	0%
Yy1V0416102PkRep2	49,921	85%	83%	97%	0%	86%	59%	87%	83%	54%	97%
Znf263UcdPk	1,894	80%	83%	81%	0%	69%	70%	0%	56%	61%	0%
EjundControlPk	77,487	88%	82%	90%	0%	52%	64%	0%	52%	45%	0%
TbplggmusPk	37,179	90%	82%	95%	0%	97%	66%	69%	84%	68%	30%
Egr1V0416101PkRep1	38,486	81%	82%	93%	0%	56%	60%	86%	51%	50%	65%
MaxV0416102PkRep2	65,983	83%	81%	93%	0%	98%	55%	83%	85%	50%	14%
Hfc1nb10068209IggrabPk	42,131	92%	81%	98%	0%	95%	62%	81%	95%	64%	99%
Nr2f2sc271940V0422111PkRep1	27,125	84%	81%	94%	0%	58%	61%	66%	26%	65%	58%
Gtf2f1ab28179IggrabPk	21,881	89%	81%	96%	0%	63%	67%	93%	51%	65%	75%
Nrf1IggrabPk	7,321	84%	81%	97%	0%	35%	73%	85%	15%	71%	37%
Mazab85725IggrabPk	75,322	91%	80%	94%	0%	97%	55%	82%	89%	56%	14%
Chd2ab68301IggrabPk	32,226	86%	80%	96%	0%	82%	62%	90%	77%	57%	92%
Znfmizdcp1ab65767IggrabPk	47,568	92%	80%	96%	0%	94%	60%	71%	82%	64%	26%
Elk112771IggrabPk	19,408	90%	79%	96%	0%	65%	65%	93%	58%	64%	77%
Tblr1ab24550IggrabPk	38,473	90%	79%	96%	0%	75%	61%	91%	70%	61%	86%
SrfV0416101PkRep2	2,027	82%	79%	95%	0%	15%	64%	86%	2%	62%	16%

Hmgn3StdPk	37,689	78%	79%	95%	66 %	62 %	89%	66 %	55%	85%	77 %
Ccnt2StdPk	44,917	85%	79%	94%	91 %	62 %	85%	73 %	62%	48%	12 %
CmyclggrabPk	64,087	90%	79%	95%	96 %	55 %	84%	84 %	58%	47%	14 %
Ctcflsc98982V0416101PkRep2	13,160	86%	79%	92%	32 %	47 %	71%	10 %	48%	87%	23 %
Ilf2Controlilf2PkRep1	399	70%	78%	67%	0%	35 %	49%	0%	14%	50%	0%
Ubtsfsab1404509IggmusPk	48,824	90%	78%	93%	77 %	59 %	67%	27 %	60%	87%	78 %
Sp1Pcr1xPkRep2	5,566	69%	78%	93%	28 %	69 %	71%	4%	63%	91%	27 %
NfyalphaStdPk	7,646	77%	78%	94%	91 %	66 %	79%	20 %	59%	85%	89 %
Nrsfv0416102PkRep1	23,654	79%	77%	93%	87 %	65 %	84%	14 %	63%	51%	12 %
Cbx3sc101004V0422111PkRep1	47,530	77%	77%	93%	97 %	60 %	84%	70 %	58%	46%	11 %
Pol24h8V0416101PkRep2	50,264	71%	76%	91%	90 %	52 %	83%	65 %	48%	45%	11 %
Smc3ab9263IggrabPk	42,739	90%	76%	90%	92 %	42 %	69%	54 %	50%	88%	70 %
Mxi1af4185IggrabPk	29,566	85%	75%	96%	76 %	62 %	91%	66 %	61%	88%	88 %
Usf1V0416101PkRep2	11,186	79%	75%	93%	27 %	57 %	78%	24 %	51%	82%	32 %
Ubfsc13125IggmusPk	34,426	87%	75%	93%	56 %	59 %	64%	14 %	57%	86%	58 %
Rad21V0416102PkRep2	43,622	86%	74%	92%	89 %	40 %	69%	53 %	46%	88%	70 %
Corestab24166IggrabPk	56,212	86%	74%	94%	80 %	52 %	71%	64 %	55%	45%	22 %
P300IggrabPk	76,017	90%	74%	96%	95 %	51 %	68%	76 %	58%	69%	97 %
Yy1sc281V0416101PkRep2	7,517	76%	74%	95%	39 %	59 %	89%	34 %	57%	88%	45 %
Yy1V0416101PkRep2	7,517	76%	74%	95%	39 %	59 %	89%	34 %	57%	88%	45 %
Setdb1UcdPk	2,475	72%	74%	89%	0%	60 %	79%	0%	53%	79%	0%
Nrsfv0416102PkRep2	11,811	77%	74%	95%	75 %	62 %	88%	5%	59%	50%	5%
JundIggrabPk	98,703	87%	74%	95%	98 %	46 %	68%	92 %	50%	44%	39 %
Pol2V0416101PkRep1	48,048	67%	74%	92%	92 %	50 %	84%	72 %	42%	46%	12 %
Arid3asc8821IggrabPk	48,086	90%	73%	94%	77 %	52 %	71%	40 %	61%	71%	78 %
CtcfcPcr1xPkRep1V2	43,504	79%	73%	83%	15 %	39 %	56%	17 %	41%	73%	15 %
Tblr1nb600270IggrabPk	65,145	87%	72%	96%	97 %	52 %	85%	84 %	59%	47%	15 %
Ilf2Controlilf2PkRep2	427	60%	72%	68%	0%	27 %	48%	0%	11%	52%	0%
Nf90Controlnf90PkRep1	454	63%	71%	68%	0%	29	50%	0%	15%	51%	0%

					%						
Zc3h11anb10074650IggrabPk	35,107	85%	71%	95%	67 %	53 %	90%	59 %	55%	87%	79 %
Tal1sc12984IggmusPk	54,781	89%	71%	93%	69 %	48 %	72%	58 %	56%	45%	21 %
Corestsc30189IggrabPk	111,691	82%	71%	94%	97 %	42 %	81%	91 %	45%	45%	22 %
Cebpbpsc150V0422111PkRep1	28,211	76%	71%	88%	46 %	48 %	74%	33 %	50%	64%	41 %
CtcfcPcr1xPkRep2	38,418	82%	71%	88%	88 %	34 %	68%	53 %	43%	86%	64 %
Bhlhe40nb100IggrabPk	78,071	81%	71%	93%	96 %	46 %	83%	78 %	48%	46%	13 %
Cdkn1bControlcdkn1bPkRep1	51	61%	71%	87%	0%	57 %	75%	0%	53%	88%	0%
Trim28sc81411V0422111PkRep2	4,787	75%	70%	96%	18 %	58 %	81%	2%	60%	50%	5%
Hey1Pcr1xPkRep2	28,876	64%	69%	91%	79 %	55 %	83%	58 %	48%	48%	8 %
EfosControlPk	29,132	75%	69%	77%	0%	40 %	67%	0%	41%	84%	0%
CtcfcPcr1xPkRep1	44,272	75%	69%	87%	85 %	36 %	67%	47 %	38%	84%	62 %
Rad21V0416102PkRep1	36,488	87%	68%	94%	89 %	32 %	70%	50 %	44%	88%	64 %
Usf2IggrabPk	9,427	79%	68%	93%	92 %	48 %	72%	15 %	45%	87%	91 %
Usf1V0416101PkRep1	24,058	72%	68%	92%	38 %	45 %	79%	31 %	42%	81%	42 %
Irf1Ifna30StdPk	2,848	72%	67%	91%	18 %	43 %	60%	2%	45%	87%	19 %
Ccne1	9	67%	67%	87%	0%	56 %	75%	0%	67%	88%	0%
Pol2V0416101PkRep2	57,410	56%	66%	90%	93 %	42 %	82%	72 %	33%	47%	11 %
Atf106325StdPk	45,216	77%	66%	94%	67 %	47 %	86%	57 %	52%	85%	79 %
Enr4a1ControlPk	7,882	64%	66%	85%	0%	43 %	63%	0%	40%	73%	0%
Znf143IggrabPk	74,048	78%	66%	97%	94 %	40 %	81%	95 %	44%	82%	98 %
Cebpbpsc150V0422111PkRep2	12,814	75%	64%	89%	25 %	38 %	66%	5%	41%	82%	24 %
Nf90Controlnf90PkRep2	6,987	54%	63%	75%	0%	48 %	62%	0%	25%	60%	0%
Cdpsc6327IggrabPk	51,920	81%	63%	93%	60 %	42 %	69%	34 %	48%	69%	62 %
CtcfStdPkRep2	47,630	81%	63%	93%	0%	27 %	70%	0%	37%	87%	0%
Znf384hpa004051IggrabPk	77,062	71%	62%	91%	75 %	37 %	71%	60 %	38%	47%	29 %
Cbx3sc101004V0422111PkRep2	15,528	62%	61%	90%	25 %	47 %	76%	19 %	46%	78%	24 %
Znf274m01UcdPk	5,857	60%	60%	91%	42 %	49 %	74%	12 %	49%	85%	44 %
Gata2sc267Pcr1xPkRep1	27,875	60%	59%	93%	27 %	42 %	68%	16 %	48%	86%	25 %

Stat1Controlstat1PkRep2	414	48%	58%	79%	0%	32 %	60%	0%	25%	68%	0%
NfybStdPk	17,571	56%	58%	93%	37 %	45 %	83%	33 %	37%	82%	41 %
CtcfbIggrabPk	88,140	70%	58%	91%	63 %	30 %	84%	54 %	32%	83%	74 %
Bach1sc14700IggrabPk	23,999	71%	58%	91%	90 %	44 %	69%	34 %	40%	76%	82 %
Irf1Ifng30StdPk	45,005	68%	56%	95%	90 %	42 %	71%	73 %	44%	45%	25 %
CtcfStdPkRep1	67,985	70%	56%	93%	0%	23 %	68%	0%	29%	84%	0%
Cjunlfna30StdPk	40,635	65%	56%	93%	61 %	39 %	71%	30 %	43%	70%	64 %
P300sc584sc48343IggrabPk	17,899	66%	55%	96%	38 %	48 %	78%	20 %	52%	93%	37 %
Setdb1MnasedUcdPk	1,125	52%	55%	61%	0%	21 %	54%	0%	12%	50%	0%
Pu1Pcr1xPkRep1	50,208	59%	53%	91%	28 %	29 %	82%	18 %	29%	84%	32 %
Mafkab50322IggrabPk	80,333	65%	53%	93%	71 %	36 %	86%	59 %	37%	84%	80 %
EsrControlesrPkRep1	1,000	38%	52%	68%	0%	23 %	49%	0%	8%	60%	0%
Irf1Ifna6hStdPk	41,689	64%	52%	95%	83 %	38 %	73%	67 %	40%	44%	23 %
EsrControlesrPkRep2	746	39%	51%	72%	0%	24 %	50%	0%	9%	58%	0%
Stat1Controlstat1PkRep1	1,569	39%	51%	56%	0%	26 %	52%	0%	15%	58%	0%
Ncor1Controlncor1PkRep2	287	43%	49%	81%	0%	23 %	65%	0%	19%	45%	0%
Mll5Controlmll5PkRep1	256	43%	48%	60%	0%	19 %	51%	0%	13%	48%	0%
Mll5Controlmll5PkRep2	396	42%	45%	61%	0%	21 %	57%	0%	14%	48%	0%
Pu1Pcr1xPkRep2	24,005	45%	45%	91%	18 %	27 %	83%	11 %	27%	84%	19 %
Pol2s2IggrabPk	96,639	40%	44%	84%	85 %	22 %	72%	66 %	18%	52%	86 %
MaffIggrabPk	65,407	52%	42%	90%	91 %	28 %	84%	88 %	28%	47%	47 %
CebpbIggrabPk	110,400	44%	39%	91%	85 %	20 %	81%	63 %	21%	46%	11 %
Ccne1Controlccne1PkRep2	102	34%	36%	77%	0%	29 %	67%	0%	25%	84%	0%
Six5Pcr1xPkRep1	10,137	24%	34%	98%	90 %	24 %	89%	84 %	20%	89%	96 %
Ncor1Controlncor1PkRep1	237	22%	34%	67%	0%	8%	49%	0%	5%	50%	0%
CtcfStdHotspotsRep2	161,211	38%	34%	88%	0%	13 %	67%	0%	14%	75%	0%
Six5Pcr1xPkRep2	11,385	25%	33%	99%	93 %	25 %	87%	90 %	21%	88%	99 %
Rfx5IggrabPk	41,218	42%	33%	94%	87 %	24 %	85%	58 %	25%	48%	10 %
Zbtb33Pcr1xPkRep2	12,114	20%	32%	93%	98 %	17 %	82%	94 %	12%	44%	57 %

Pol24h8	59,530	24%	31%	54%	9%	11 %	51%	6%	6%	53%	5%
Pol24h8	32,204	24%	31%	59%	4%	11 %	56%	4%	6%	52%	3%
Kap1UcdPk	23,949	35%	31%	81%	13 %	16 %	71%	8%	16%	51%	4%
Bach1Controlbach1PkRep1	113	31%	31%	73%	0%	14 %	68%	0%	13%	78%	0%
Pol2V2	21,630	23%	30%	53%	3%	10 %	52%	3%	6%	54%	3%
CtcfStdHotspotsRep1	239,361	33%	30%	88%	0%	12 %	68%	0%	11%	75%	0%
Ifng6hPol2	24,641	23%	29%	53%	2%	10 %	51%	3%	5%	53%	2%
Ifna30Pol2	23,970	23%	29%	54%	2%	10 %	55%	3%	5%	54%	2%
bE2f4	15,278	21%	28%	56%	2%	9%	51%	1%	5%	48%	0%
Ifna30Stat2	6,241	21%	28%	60%	0%	8%	51%	1%	4%	48%	0%
Pol2Musigg	43,954	22%	28%	54%	3%	9%	49%	2%	5%	50%	3%
Ifna6hPol2	26,421	23%	28%	52%	3%	10 %	51%	3%	5%	53%	2%
CmycV2	15,748	21%	28%	58%	0%	9%	51%	2%	5%	51%	1%
bE2f6	21,973	21%	28%	54%	1%	9%	49%	1%	5%	47%	0%
Tfiiic	5,872	20%	28%	58%	0%	8%	51%	0%	5%	45%	0%
Taf1	8,249	20%	28%	62%	0%	9%	48%	1%	5%	48%	0%
Ifng30Pol2	29,176	22%	28%	52%	3%	9%	51%	3%	5%	52%	2%
Ifng6hCmyc	21,348	21%	27%	55%	1%	9%	55%	1%	5%	46%	1%
Ifna30Cmyc	11,504	21%	27%	60%	0%	9%	52%	2%	5%	49%	0%
Ifna6hCmyc	16,343	20%	27%	59%	1%	8%	52%	2%	4%	51%	1%
Ini1Musigg	16,004	21%	27%	53%	0%	8%	52%	0%	4%	48%	1%
Stat1Ifng6h	5,225	21%	27%	59%	0%	8%	49%	0%	4%	50%	0%
Brg1Musigg	14,706	21%	27%	56%	1%	8%	50%	1%	4%	53%	2%
Ifna30Stat1	1,953	21%	27%	63%	0%	7%	50%	0%	4%	55%	0%
Taf1	11,330	19%	26%	52%	0%	8%	48%	1%	4%	42%	1%
Hey1	25,200	20%	26%	58%	3%	8%	53%	4%	4%	51%	3%
Hey1	23,584	19%	26%	57%	2%	8%	53%	4%	4%	50%	2%
bZnf263V2	27,548	19%	25%	56%	1%	7%	51%	2%	4%	47%	0%
Zbtb33Pcr1xPkRep1	10,489	14%	25%	93%	%	96 %	14 %	83%	%	11%	45% %
Ifna6hStat1	2,038	19%	25%	58%	0%	7%	50%	1%	4%	49%	0%
Ifna6hStat2	3,886	19%	24%	59%	0%	7%	51%	0%	3%	52%	0%
Gtf2b	4,627	18%	24%	53%	0%	7%	49%	1%	4%	54%	0%
MaxV2	10,479	18%	24%	55%	0%	7%	52%	0%	4%	52%	0%
Rpc155	2,711	16%	24%	57%	0%	7%	50%	0%	4%	53%	0%
bSetdb1Mnase	6,402	19%	24%	56%	1%	7%	48%	0%	4%	51%	1%
Stat1Ifng30	4,076	19%	24%	58%	0%	6%	52%	1%	4%	50%	0%

bGata2	12,487	18%	24%	58%	0%	6%	50%	0%	3%	51%	1%
Jund	2,324	17%	24%	55%	0%	6%	56%	0%	3%	44%	0%
bGata1V2	5,495	17%	23%	58%	0%	6%	53%	0%	3%	52%	0%
Brf1	330	15%	23%	61%	0%	7%	49%	0%	4%	58%	0%
bYy1	6,463	17%	23%	57%	0%	6%	53%	0%	3%	48%	0%
CjunV2	26,919	17%	23%	54%	1%	6%	49%	1%	3%	50%	1%
Sirt6	6,528	18%	22%	57%	0%	5%	49%	0%	3%	49%	0%
bSetdb1	10,612	17%	22%	55%	0%	6%	53%	0%	3%	53%	0%
JundV2	1,499	16%	22%	57%	0%	6%	52%	0%	3%	59%	0%
bGata1	9,462	17%	22%	57%	0%	5%	48%	0%	3%	51%	0%
Six5	3,183	16%	22%	57%	0%	6%	51%	0%	3%	56%	0%
Znf274UcdPk	255	16%	22%	74%	0%	4%	55%	0%	3%	76%	0%
Ifna6hCjun	8,257	16%	21%	55%	0%	5%	49%	0%	3%	53%	0%
Ifng30Cjun	14,714	17%	21%	55%	2%	5%	52%	1%	3%	50%	1%
Nelfe	1,739	14%	21%	62%	0%	5%	51%	0%	3%	54%	0%
Six5	2,610	14%	21%	56%	0%	5%	51%	0%	3%	55%	0%
Bdp1	1,409	14%	21%	62%	0%	6%	52%	0%	3%	56%	0%
Ifng6hCjun	10,116	16%	21%	57%	0%	5%	50%	0%	3%	51%	0%
CfosV2	18,962	16%	20%	57%	0%	5%	53%	1%	3%	51%	0%
Atf3	1,919	14%	20%	64%	0%	5%	51%	0%	3%	54%	0%
Nfe2V2	5,070	15%	19%	54%	0%	5%	50%	0%	3%	49%	0%
Nfyb	15,610	14%	19%	53%	0%	5%	50%	0%	3%	53%	0%
Nfyd	13,050	14%	18%	56%	0%	5%	50%	0%	3%	51%	0%
Pu1	16,694	14%	18%	54%	0%	4%	49%	1%	2%	52%	0%
bTr4	759	12%	18%	66%	0%	6%	48%	0%	3%	56%	0%
Pol2s2StdPk	70,610	14%	18%	52%	1%	5%	46%	2%	2%	53%	1%
Pol2	76,820	16%	17%	58%	0%	5%	53%	0%	3%	54%	0%
Brf2	220	10%	17%	60%	0%	6%	52%	0%	4%	54%	0%
Pol3	956	10%	17%	53%	0%	6%	50%	0%	3%	53%	0%
Pu1	45,528	13%	17%	57%	1%	4%	50%	1%	2%	51%	0%
bZnf274	557	11%	16%	63%	0%	6%	50%	0%	4%	53%	0%
Cmyc	66,452	14%	16%	55%	0%	4%	51%	0%	2%	49%	0%
Rad21	28,621	12%	16%	54%	1%	3%	51%	1%	2%	49%	1%
Sin3ak20	983	13%	15%	52%	0%	3%	50%	0%	2%	53%	0%
Xrcc4	349	8%	15%	72%	0%	3%	49%	0%	2%	59%	0%
Cjun	99,894	13%	15%	56%	0%	3%	48%	0%	2%	52%	0%
Max	59,545	13%	14%	55%	0%	3%	53%	0%	2%	52%	0%
Cfos	73,374	12%	13%	56%	0%	3%	51%	0%	2%	53%	0%
Sin3ak20	678	12%	13%	56%	0%	3%	53%	0%	1%	56%	0%

Egr1	2,845	12%	13%	57%	0%	3%	53%	0%	1%	56%	0%
Usf1	6,757	12%	13%	55%	0%	3%	52%	0%	2%	57%	0%
Gabp	3,284	11%	12%	53%	0%	2%	47%	0%	1%	51%	0%
Pol2	14,836	12%	12%	57%	0%	3%	52%	0%	1%	53%	0%
Usf1	8,838	12%	12%	55%	0%	3%	53%	0%	1%	49%	0%
Gabp	2,836	11%	12%	53%	0%	2%	53%	0%	1%	52%	0%
Pol2	10,753	12%	12%	53%	0%	2%	51%	0%	2%	49%	0%
Srf	454	10%	11%	56%	0%	2%	51%	0%	2%	47%	0%
Nfe2	25,445	12%	11%	58%	0%	3%	51%	0%	2%	53%	0%
Egr1	424	11%	11%	56%	0%	3%	50%	0%	2%	54%	0%
Nrsf	2,567	10%	11%	53%	0%	2%	50%	0%	1%	48%	0%
Nrsf	2,541	10%	11%	54%	0%	2%	52%	0%	1%	53%	0%
Srf	553	11%	10%	57%	0%	2%	49%	0%	2%	47%	0%
Znf263	209,651	10%	9%	53%	0%	2%	51%	0%	1%	53%	0%

Supplementary Table 2: Pioneer TF computational index values

For each motif used in PIQ, the number of PIQ calls in mESC are shown as well as the values for the computational pioneer TF indices in the mESC lineage (columns 4–6) or in K562 cells (column 7).

Motif	TF name	Number of PIQ calls	Pioneer Index	Chromatin Opening Index	Social Index	K562 Chromatin Opening Index
CN0001.1 LM1		35,649	1.842	1.736	0.101	2.444
CN0002.1 LM2		52,968	1.593	2.419	0.096	2.930
CN0003.1 LM3		6,044	1.141	1.203	0.048	1.553
CN0004.1 LM4		20,932	7.414	9.129	0.111	7.074
CN0005.1 LM5		2,874	-0.534	-0.614	0.021	-0.098
CN0006.1 LM6		64	1.877	1.778	0.021	1.707
CN0007.1 LM7		53,315	2.106	2.817	0.107	3.126
CN0008.1 LM8		5,576	-0.667	-0.735	0.023	-0.015
CN0009.1 LM9		19,651	1.871	1.534	0.078	1.277
CN0010.1 LM10		57,931	1.980	1.964	0.135	2.154
CN0011.1 LM11		3,770	-0.586	-0.739	0.016	0.203
CN0017.1 LM17		5,776	-0.493	-0.609	0.020	0.030
CN0018.1 LM18		7,845	-0.543	-0.569	0.032	-0.087
CN0019.1 LM19		1,573	0.380	0.575	0.068	0.664
CN0021.1 LM21		4,940	-0.566	-0.599	0.030	-0.137
CN0022.1 LM22		11,982	0.890	0.517	0.037	0.875
CN0023.1 LM23		44,408	2.547	3.343	0.092	3.216
CN0025.1 LM25		9,979	-0.732	-0.771	0.022	-0.029
CN0030.1 LM30		2,966	-1.070	-1.141	0.023	0.181
CN0031.1 LM31		15,121	-0.746	-0.812	0.015	0.069
CN0034.1 LM34		12,423	-1.420	-1.550	0.027	0.040
CN0036.1 LM36		2,746	-0.591	-0.693	0.018	0.308
CN0039.1 LM39		20,832	1.690	1.691	0.117	1.724
CN0041.1 LM41		10,544	-0.867	-0.771	0.029	0.030
CN0047.1 LM47		5,657	1.423	1.969	0.102	2.166
CN0048.1 LM48		2,319	-0.785	-0.969	0.026	0.115
CN0051.1 LM51		9,406	-0.548	-0.556	0.027	0.128
CN0052.1 LM52		1,789	-0.879	-0.926	0.016	-0.144
CN0053.1 LM53		13,036	-1.161	-1.208	0.030	-0.071
CN0056.1 LM56		99	-0.389	-0.556	0.017	0.125
CN0059.1 LM59		6,248	-0.368	-0.531	0.016	0.175
CN0061.1 LM61		4,748	-0.528	-0.585	0.016	0.109
CN0065.1 LM65		14,516	-1.102	-1.032	0.029	0.005

CN0067.1 LM67		1,094	-0.822	-0.919	0.017	0.042
CN0076.1 LM76		3,123	-0.556	-0.631	0.024	0.082
CN0077.1 LM77		2,722	-0.473	-0.626	0.020	0.120
CN0080.1 LM80		564	-0.601	-0.689	0.016	0.128
CN0081.1 LM81		1,360	-0.484	-0.560	0.019	0.076
CN0085.1 LM85		1,913	-0.581	-0.682	0.016	0.148
CN0087.1 LM87		1,520	-0.656	-0.753	0.017	0.019
CN0088.1 LM88		1,561	-0.675	-0.715	0.018	0.068
CN0090.1 LM90		3,537	1.183	0.749	0.029	1.326
CN0092.1 LM92		3,681	-0.650	-0.849	0.016	0.099
CN0094.1 LM94		3,951	-0.863	-0.920	0.019	-0.138
CN0096.1 LM96		4,446	-0.808	-0.829	0.018	-0.198
CN0098.1 LM98		5,703	-0.513	-0.546	0.031	-0.069
CN0100.1 LM100		2,685	1.446	1.225	0.052	1.623
CN0102.1 LM102		9,505	-0.497	-0.596	0.015	0.250
CN0108.1 LM108		2,743	-0.891	-0.991	0.019	-0.042
CN0110.1 LM110		2,030	-0.580	-0.762	0.017	0.136
CN0114.1 LM114		1,815	-0.518	-0.592	0.016	0.073
CN0116.1 LM116		3,065	-0.642	-0.728	0.016	0.023
CN0117.1 LM117		715	-0.654	-0.718	0.019	-0.081
CN0118.1 LM118		3,261	-0.700	-0.770	0.025	0.328
CN0122.1 LM122		1,241	-0.730	-0.863	0.016	0.035
CN0123.1 LM123		2,127	-0.372	-0.604	0.017	0.316
CN0125.1 LM125		1,532	-0.575	-0.661	0.018	0.075
CN0130.1 LM130		7,811	2.729	2.825	0.143	2.346
CN0131.1 LM131		747	-0.668	-0.764	0.016	0.069
CN0132.1 LM132		1,205	-0.388	-0.495	0.015	0.014
CN0138.1 LM138		2,931	-0.418	-0.524	0.016	0.114
CN0142.1 LM142		857	-0.435	-0.578	0.016	0.224
CN0143.1 LM143		2,298	-0.444	-0.551	0.016	0.378
CN0146.1 LM146		15,710	0.629	0.954	0.079	2.228
CN0147.1 LM147		3,188	-0.521	-0.641	0.015	0.016
CN0150.1 LM150		1,862	-0.602	-0.676	0.019	0.065
CN0151.1 LM151		1,189	-0.574	-0.667	0.016	-0.066
CN0153.1 LM153		2,224	-0.452	-0.641	0.014	-0.030
CN0158.1 LM158		6,665	-0.745	-0.885	0.018	0.055
CN0160.1 LM160		5,784	-0.710	-0.810	0.017	-0.002
CN0161.1 LM161		3,085	-0.375	-0.554	0.016	0.156
CN0162.1 LM162		5,390	-0.547	-0.655	0.016	0.053
CN0163.1 LM163		8,009	-0.552	-0.705	0.016	0.307
CN0164.1 LM164		6,011	-0.577	-0.690	0.016	0.202

CN0169.1 LM169		3,411	1.013	0.613	0.037	0.920
CN0170.1 LM170		3,327	-0.623	-0.671	0.016	0.150
CN0171.1 LM171		1,999	-0.555	-0.684	0.016	0.060
CN0172.1 LM172		2,373	-0.685	-0.785	0.018	0.138
CN0173.1 LM173		4,932	-0.527	-0.741	0.016	0.212
CN0176.1 LM176		2,641	1.430	0.843	0.070	1.817
CN0178.1 LM178		16,767	-0.765	-0.932	0.015	0.161
CN0180.1 LM180		4,901	-0.844	-0.914	0.016	-0.082
CN0182.1 LM182		6,080	-0.740	-0.866	0.017	0.084
CN0185.1 LM185		4,565	-0.420	-0.637	0.015	0.104
CN0187.1 LM187		2,909	-0.451	-0.557	0.017	0.067
CN0188.1 LM188		4,068	-0.398	-0.606	0.014	0.087
CN0189.1 LM189		6,212	-0.632	-0.646	0.017	0.109
CN0190.1 LM190		2,674	-0.531	-0.643	0.016	0.050
CN0192.1 LM192		2,981	-0.881	-0.939	0.020	-0.063
CN0193.1 LM193		5,961	-0.607	-0.704	0.016	-0.122
CN0194.1 LM194		3,722	0.931	0.912	0.090	1.590
CN0196.1 LM196		4,868	-0.537	-0.625	0.016	-0.002
CN0197.1 LM197		5,183	-0.574	-0.676	0.015	0.194
CN0200.1 LM200		2,784	-0.957	-1.019	0.016	-0.163
CN0201.1 LM201		5,363	-0.668	-0.753	0.017	0.200
CN0203.1 LM203		3,369	-0.494	-0.695	0.016	0.067
CN0204.1 LM204		3,796	-0.455	-0.605	0.018	0.090
CN0205.1 LM205		3,381	-0.755	-0.838	0.016	0.006
CN0206.1 LM206		4,279	-0.479	-0.577	0.016	0.197
CN0209.1 LM209		5,819	-0.402	-0.547	0.015	0.285
CN0210.1 LM210		6,167	-0.875	-1.013	0.016	0.032
CN0215.1 LM215		8,028	-0.428	-0.586	0.017	0.386
CN0216.1 LM216		8,785	-0.485	-0.514	0.016	0.106
CN0217.1 LM217		6,734	-0.972	-1.078	0.017	-0.072
CN0223.1 LM223		2,563	-1.107	-1.211	0.017	-0.243
CN0224.1 LM224		2,943	-0.905	-1.060	0.015	-0.046
CN0226.1 LM226		3,590	-0.577	-0.664	0.016	0.029
CN0227.1 LM227		2,836	-0.422	-0.548	0.016	0.162
CN0228.1 LM228		2,230	-0.377	-0.545	0.018	0.216
CN0229.1 LM229		1,672	-0.451	-0.579	0.015	0.115
CN0230.1 LM230		5,445	-0.772	-0.832	0.016	-0.032
CN0232.1 LM232		7,333	-0.373	-0.525	0.017	0.255
CN0233.1 LM233		7,232	-0.454	-0.545	0.017	0.203
ES_Nr5a2_3_0_c3657		35,984	0.660	0.784	0.214	0.738
ES_Suz12_3_0_c598		2,893	3.864	3.746	0.052	2.477

ES_Tbx3_R1D3_3_0_c387		22,874	1.025	0.754	0.333	0.703
MA0003.1 TFAP2A	TFAP2A	388,679	7.287	5.659	1.212	4.276
MA0004.1 Arnt	Arnt	21,303	1.646	1.437	0.835	1.823
MA0006.1 Arnt::Ahr	Arnt::Ahr	230,940	1.806	1.523	0.614	1.955
MA0008.1 HAT5	HAT5	116	-0.845	-0.934	0.023	-0.095
MA0010.1 br_Z1	br	4,053	-0.811	-0.864	0.016	-0.124
MA0011.1 br_Z2	br	6	-0.909	-0.998	0.018	-0.094
MA0012.1 br_Z3	br	1,515	-0.540	-0.577	0.017	0.068
MA0014.1 Pax5	Pax5	123,797	2.700	2.122	0.984	2.911
MA0015.1 Cf2_II	Cf2	2,235	-1.172	-1.235	0.034	-0.527
MA0016.1 usp	usp	49,983	1.839	1.340	0.503	1.576
MA0018.1 CREB1	CREB1	11,552	3.687	3.477	0.457	5.085
MA0018.2 CREB1	CREB1	114,212	4.360	4.430	0.629	5.671
MA0021.1 Dof3	Dof3	266,206	2.214	2.055	0.952	2.456
MA0022.1 dl_1	dl	61,075	0.914	0.741	0.378	1.152
MA0024.1 E2F1	E2F1	3,964	3.647	3.409	0.610	4.657
MA0025.1 NFIL3	NFIL3	12,090	-0.683	-0.793	0.016	0.028
MA0026.1 Eip74EF	Eip74EF	146,314	4.183	4.211	0.890	6.814
MA0028.1 ELK1	ELK1	248,061	3.736	3.716	0.854	7.381
MA0029.1 Evi1	Evi1	19,413	-0.528	-0.609	0.016	0.754
MA0030.1 FOXF2	FOXF2	5,346	-0.480	-0.597	0.017	0.255
MA0033.1 FOXL1	FOXL1	0	-1.011	-1.084	0.030	-0.358
MA0034.1 Gamyb	Gamyb	169,045	2.870	2.511	0.707	2.908
MA0035.1 Gata1	Gata1	23,941	0.936	0.694	0.800	0.645
MA0039.2 Klf4	Klf4	141,323	1.984	2.153	0.899	5.303
MA0040.1 Foxq1	Foxq1	5,811	-0.954	-1.032	0.017	-0.145
MA0042.1 FOXI1	FOXI1	866	-1.525	-2.010	0.016	-0.207
MA0044.1 HMG-1	HMG-1	3,499	-1.087	-1.621	0.015	0.299
MA00445.1 D	D	10,878	-0.057	0.177	0.193	0.242
MA0045.1 HMG-I/Y	HMG-I/Y	29,678	-0.496	-0.465	0.077	-0.394
MA0046.1 HNF1A	HNF1A	11,769	-0.675	-0.789	0.020	-0.007
MA0047.1 Foxa2	Foxa2	7,255	-0.940	-0.999	0.019	-0.196
MA0048.1 NHLH1	NHLH1	53,425	4.335	3.439	0.816	2.634
MA0052.1 MEF2A	MEF2A	15,393	-0.686	-0.919	0.018	0.215
MA0055.1 Myf	Myf	37,857	1.750	1.249	0.660	1.652
MA0056.1 MZF1_1-4	MZF1	172,816	1.132	0.858	0.967	1.040
MA0057.1 MZF1_5-13	MZF1	176,785	1.507	1.452	1.034	2.018
MA0058.1 MAX	MAX	52,729	1.343	1.296	0.544	2.234
MA0059.1 MYC::MAX	MYC::MAX	43,963	0.983	0.703	0.200	1.887
MA0060.1 NFYA	NFYA	66,434	4.877	5.472	0.461	6.400
MA0061.1 NF-kappaB	NF-kappaB	55,181	0.685	0.436	0.081	1.597

MA0062.1 GABPA	GABPA	44,621	3.274	3.214	0.839	5.168
MA0062.2 GABPA	GABPA	67,978	8.114	8.291	0.386	8.833
MA0063.1 Nkx2-5	Nkx2-5	12	-0.538	-0.606	0.036	-0.008
MA0067.1 Pax2	Pax2	330,601	1.999	1.771	0.630	2.296
MA0070.1 PBX1	PBX1	9,673	-0.387	-0.470	0.017	0.146
MA0073.1 RREB1	RREB1	50,401	0.803	0.730	0.144	1.026
MA0075.1 Prrx2	Prrx2	0	-0.637	-0.706	0.070	-0.082
MA0076.1 ELK4	ELK4	7,016	4.282	4.478	0.670	7.818
MA0077.1 SOX9	SOX9	5,396	-0.190	-0.486	0.031	0.268
MA0079.1 SP1	SP1	291,866	3.739	3.559	1.210	4.276
MA0079.2 SP1	SP1	544,512	6.136	5.759	1.501	8.545
MA0080.1 SPI1	SPI1	278,678	3.207	3.111	0.858	4.741
MA0080.2 SPI1	SPI1	440,026	0.626	0.535	0.379	1.285
MA0082.1 squamosa	squamosa	17,229	-0.980	-1.074	0.017	-0.038
MA0084.1 SRY	SRY	14	-0.673	-0.724	0.018	-0.013
MA0086.1 sna	sna	3,299	1.133	0.845	0.638	0.281
MA0087.1 Sox5	Sox5	12	-0.528	-0.560	0.030	0.021
MA0088.1 znf143	znf143	24,528	1.475	1.538	0.793	2.248
MA0090.1 TEAD1	TEAD1	12,671	0.729	0.606	0.230	0.784
MA0093.1 USF1	USF1	117,382	1.915	1.709	0.627	2.285
MA0094.2 Ubx	Ubx	6	-0.849	-0.895	0.050	-0.197
MA0095.1 YY1	YY1	30,547	0.818	0.602	0.649	0.838
MA0096.1 bZIP910	bZIP910	7,084	1.783	1.638	0.515	2.534
MA0097.1 bZIP911	bZIP911	2,052	2.061	1.769	0.137	2.600
MA0098.1 ETS1	ETS1	342,854	2.908	2.840	1.031	4.043
MA0099.1 Fos	Fos	334,357	0.863	0.643	0.381	1.759
MA0100.1 Myb	Myb	114,608	1.740	1.484	0.665	2.206
MA0101.1 REL	REL	183,234	0.865	0.487	0.249	1.620
MA0103.1 ZEB1	ZEB1	2,106	1.132	0.844	0.641	0.281
MA0105.1 NFKB1	NFKB1	16,869	1.594	1.122	0.372	1.751
MA0109.1 Hltf	Hltf	25,898	-0.538	-0.614	0.022	0.490
MA0112.1 ESR1	ESR1	17,084	1.081	0.568	0.149	1.554
MA0112.2 ESR1	ESR1	100,738	0.878	0.486	0.059	1.275
MA0116.1 Zfp423	Zfp423	9,702	1.120	0.594	0.091	1.253
MA0117.1 Mafb	Mafb	273,348	3.431	2.914	0.807	3.458
MA0118.1 Macho-1	Macho-1	200,458	1.378	1.073	1.104	1.085
MA0119.1 TLX1::NFIC	TLX1::NFIC	15,257	1.079	0.747	0.217	1.657
MA0121.1 ARR10	ARR10	48,954	-0.256	-1.373	0.017	1.277
MA0122.1 Nkx3-2	Nkx3-2	15,350	-1.177	-1.675	0.018	0.437
MA0123.1 abi4	abi4	263,746	8.394	6.324	0.965	4.469
MA0124.1 NKX3-1	NKX3-1	4,500	-0.727	-0.824	0.018	-0.027

MA0126.1 ovo	ovo	6,180	-0.653	-0.965	0.025	0.439
MA0127.1 PEND	PEND	8,667	-0.733	-0.779	0.016	-0.060
MA0128.1 EmBP-1	EmBP-1	32,943	1.355	1.155	0.517	1.443
MA0129.1 TGA1A	TGA1A	64,570	1.534	1.518	0.641	1.930
MA0131.1 MIZF	MIZF	12,221	4.364	3.966	0.417	3.637
MA0135.1 Lhx3	Lhx3	17,231	-0.790	-0.805	0.106	-0.405
MA0138.1 REST	REST	8,569	1.659	1.318	0.205	1.209
MA0138.2 REST	REST	10,302	1.776	1.542	0.065	1.187
MA0139.1 CTCF	CTCF	61,302	2.676	3.507	0.101	3.680
MA0141.1 Esrrb	Esrrb	36,091	0.614	0.929	0.184	0.654
MA0142.1 Pou5f1	Pou5f1	22,150	0.647	1.449	0.305	0.189
MA0143.1 Sox2	Sox2	19,306	0.696	1.508	0.402	0.237
MA0145.1 Tcfcp2l1	Tcfcp2l1	121,478	1.571	1.332	0.454	1.604
MA0146.1 Zfx	Zfx	138,763	7.707	6.031	0.654	1.064
MA0147.1 Myc	Myc	90,520	2.269	1.769	0.400	2.590
MA0149.1 EWSR1-FLI1	EWSR1-FLI1	5,009	-0.869	-0.786	0.059	-0.217
MA0150.1 NFE2L2	NFE2L2	44,595	0.711	0.682	0.148	2.219
MA0151.1 ARID3A	ARID3A	12	-0.685	-0.739	0.044	-0.087
MA0153.1 HNF1B	HNF1B	9,804	-0.756	-0.839	0.019	-0.032
MA0154.1 EBF1	EBF1	74,550	1.217	0.899	0.657	0.945
MA0155.1 INSM1	INSM1	28,473	1.864	1.374	0.630	1.930
MA0159.1 RXR::RAR_DR5	RXR::RAR	39,383	0.718	0.554	0.077	1.278
MA0160.1 NR4A2	NR4A2	62,081	0.804	0.767	0.582	0.884
MA0162.1 Egr1	Egr1	37,193	5.490	4.490	0.828	4.578
MA0163.1 PLAG1	PLAG1	13,458	1.878	1.189	0.532	1.829
MA0165.1 Abd-B	Abd-B	41	-0.622	-0.738	0.020	0.114
MA0166.1 Antp	Antp	5	-0.488	-0.578	0.033	0.013
MA0167.1 Awh	Awh	16	-0.711	-0.756	0.079	-0.162
MA0168.1 B-H1	B-H1	31	-0.538	-0.606	0.037	-0.008
MA0169.1 B-H2	B-H2	13	-0.538	-0.606	0.035	-0.008
MA0170.1 C15	C15	14	-0.711	-0.756	0.082	-0.162
MA0171.1 CG11085	CG11085	116	-0.538	-0.606	0.035	-0.008
MA0172.1 CG11294	CG11294	0	-0.711	-0.756	0.079	-0.162
MA0173.1 CG11617	CG11617	26	-0.558	-0.596	0.032	-0.002
MA0174.1 CG42234	CG42234	9	-0.852	-0.905	0.037	-0.139
MA0175.1 CG13424	CG13424	5	-0.538	-0.606	0.035	-0.008
MA0177.1 CG18599	CG18599	7	-0.591	-0.628	0.073	-0.080
MA0178.1 CG32105	CG32105	22	-0.711	-0.756	0.079	-0.162
MA0182.1 CG4328	CG4328	5	-0.710	-0.772	0.052	-0.068
MA0183.1 CG7056	CG7056	28	-0.849	-0.895	0.050	-0.197
MA0185.1 Deaf1	Deaf1	113,020	2.028	1.736	0.488	2.001

MA0195.1 Lim3	Lim3	11	-0.711	-0.756	0.079	-0.162
MA0205.1 Trl	Trl	38,250	-1.344	-2.086	0.016	0.535
MA0206.1 abd-A	abd-A	10	-0.711	-0.756	0.079	-0.162
MA0213.1 brk	brk	67,555	4.622	3.730	0.875	3.989
MA0215.1 btn	btn	14	-0.488	-0.578	0.033	0.013
MA0223.1 exex	exex	3	-0.493	-0.567	0.042	0.019
MA0230.1 lab	lab	4	-0.711	-0.756	0.079	-0.162
MA0235.1 onecut	onecut	0	-0.489	-0.570	0.027	-0.037
MA0240.1 repo	repo	16	-0.711	-0.756	0.079	-0.162
MA0242.1 run::Bgb	run::Bgb	33,407	1.010	0.640	0.129	1.102
MA0248.1 tup	tup	24	-0.538	-0.606	0.035	-0.008
MA0250.1 unc-4	unc-4	10	-0.538	-0.606	0.035	-0.008
MA0251.1 unpg	unpg	10	-0.711	-0.756	0.079	-0.162
MA0259.1 HIF1A::ARNT	HIF1A::ARNT	35,611	3.061	2.410	0.429	1.127
MA0263.1 ttx-3::ceh-10	ttx-3::ceh-10	3,606	-0.513	-0.623	0.016	0.096
MA0267.1 ACE2	ACE2	57,097	0.889	0.637	0.762	0.755
MA0268.1 ADR1	ADR1	272,648	1.403	1.175	1.124	1.258
MA0270.1 AFT2	AFT2	38,632	1.625	1.455	0.547	1.751
MA0271.1 ARG80	ARG80	171,483	2.944	2.611	0.687	3.109
MA0273.1 ARO80	ARO80	31,982	1.147	0.878	0.109	1.448
MA0275.1 ASG1	ASG1	126,458	3.666	3.645	0.612	5.261
MA0276.1 ASH1	ASH1	153,877	1.916	1.221	0.334	1.972
MA0277.1 AZF1	AZF1	29,224	-0.560	-0.534	0.096	-0.040
MA0278.1 BAS1	BAS1	43,270	0.814	0.464	0.036	1.344
MA0279.1 CAD1	CAD1	4,660	-0.571	-0.715	0.020	0.178
MA0280.1 CAT8	CAT8	193,739	3.666	3.645	1.018	5.261
MA0282.1 CEP3	CEP3	9,873	1.630	1.505	0.271	2.493
MA0283.1 CHA4	CHA4	59,413	5.580	5.078	0.694	5.413
MA0285.1 CRZ1	CRZ1	200,691	-0.295	-0.658	0.021	1.107
MA0286.1 CST6	CST6	55,906	2.387	2.337	0.253	4.892
MA0289.1 DAL80	DAL80	30,934	0.986	0.814	0.104	1.573
MA0291.1 DAL82	DAL82	40,539	1.751	1.418	0.259	3.267
MA0292.1 ECM22	ECM22	40,987	3.939	3.562	0.674	3.167
MA0293.1 ECM23	ECM23	127	-0.371	-0.468	0.023	0.161
MA0295.1 FHL1	FHL1	21,462	2.249	2.035	0.347	3.067
MA0296.1 FKH1	FKH1	18,997	-1.049	-1.161	0.024	0.039
MA0299.1 GAL4	GAL4	31,298	3.239	2.638	0.339	1.142
MA0301.1 GAT3	GAT3	225	-0.596	-1.017	0.016	0.181
MA0304.1 GCR1	GCR1	58,249	1.060	0.830	0.255	1.131
MA0305.1 GCR2	GCR2	105,859	1.015	0.830	0.592	1.326

MA0308.1 GSM1	GSM1	22,708	1.477	1.206	0.161	2.222
MA0310.1 HAC1	HAC1	18,589	1.467	1.227	0.181	1.874
MA0311.1 HAL9	HAL9	70,288	2.829	2.726	0.661	3.695
MA0312.1 HAP1	HAP1	57,282	1.650	1.569	0.435	2.004
MA0314.1 HAP3	HAP3	10,847	2.316	2.750	0.117	4.108
MA0315.1 HAP4	HAP4	83,754	3.049	3.406	0.463	4.693
MA0316.1 HAP5	HAP5	66,987	3.508	3.841	0.354	5.034
MA0317.1 HCM1	HCM1	211	-0.578	-0.660	0.023	0.055
MA0318.1 HMRA2	HMRA2	49	-0.637	-0.756	0.023	0.002
MA0320.1 IME1	IME1	4,579	9.815	7.851	0.211	6.785
MA0323.1 IXR1	IXR1	2,263	0.743	0.505	0.037	0.840
MA0324.1 LEU3	LEU3	13,839	6.086	5.188	0.368	6.120
MA0325.1 LYS14	LYS14	73,319	1.932	1.902	0.536	2.200
MA0328.1 MATALPHA2	MATALPH					
	A2	13,747	-0.735	-0.814	0.021	0.073
MA0329.1 MBP1	MBP1	87,732	5.007	4.459	0.458	5.550
MA0330.1 MBP1::SWI6	MBP1::SW					
	I6	35,574	4.975	4.460	0.232	6.507
MA0333.1 MET31	MET31	103,825	2.511	2.060	0.564	2.518
MA0334.1 MET32	MET32	304,060	2.855	2.486	0.986	2.674
MA0336.1 MGA1	MGA1	9,544	-0.847	-0.980	0.015	-0.044
MA0341.1 MSN2	MSN2	330,439	1.533	1.269	1.182	1.609
MA0344.1 NHP10	NHP10	59,274	4.980	4.074	0.683	3.787
MA0345.1 NHP6A	NHP6A	62,533	-1.505	-1.559	0.026	-0.652
MA0348.1 OAF1	OAF1	70,219	1.567	1.275	0.400	2.517
MA0349.1 OPI1	OPI1	103,354	3.029	2.734	0.465	3.335
MA0350.1 TOD6	TOD6	15,087	1.379	0.883	0.084	0.897
MA0351.1 DOT6	DOT6	31,123	1.491	0.987	0.093	1.214
MA0352.1 PDR1	PDR1	89,310	9.372	7.956	0.665	7.554
MA0354.1 PDR8	PDR8	12,131	2.461	2.212	0.281	1.958
MA0356.1 PHO2	PHO2	4	-0.972	-1.040	0.066	-0.187
MA0357.1 PHO4	PHO4	29,000	1.866	1.491	0.300	0.505
MA0359.1 RAP1	RAP1	20,759	-0.625	-0.910	0.015	0.637
MA0360.1 RDR1	RDR1	4,457	2.828	2.489	0.311	3.200
MA0361.1 RDS1	RDS1	106,573	12.642	10.256	0.458	6.297
MA0362.1 RDS2	RDS2	48,595	3.825	3.128	0.393	3.401
MA0364.1 REI1	REI1	166,796	1.171	0.894	0.617	1.164
MA0365.1 RFX1	RFX1	48,595	1.013	0.839	0.290	1.075
MA0366.1 RGM1	RGM1	250,936	1.533	1.269	1.159	1.609
MA0367.1 RGT1	RGT1	85,385	1.089	1.050	0.359	1.442
MA0368.1 RIM101	RIM101	47,494	3.667	3.241	0.545	3.597
MA0369.1 RLM1	RLM1	5,543	-0.501	-0.615	0.021	0.265

MA0371.1 ROX1	ROX1	18,529	0.353	0.566	0.401	0.284
MA0373.1 RPN4	RPN4	46,283	3.856	3.307	0.858	1.640
MA0374.1 RSC3	RSC3	93,171	15.117	12.573	0.476	8.789
MA0375.1 RSC30	RSC30	122,558	5.886	5.157	0.637	8.387
MA0377.1 SFL1	SFL1	27,903	-1.058	-1.146	0.015	-0.184
MA0378.1 SFP1	SFP1	67,104	-0.616	-0.609	0.028	-0.296
MA0379.1 SIG1	SIG1	0	-0.993	-1.096	0.123	-0.237
MA0382.1 SKO1	SKO1	0	-2.167	-3.040	0.015	0.120
MA0383.1 SMP1	SMP1	7,789	-1.221	-1.345	0.017	-0.217
MA0384.1 SNT2	SNT2	1,940	3.469	2.739	0.041	2.184
MA0387.1 SPT2	SPT2	272	-1.023	-1.065	0.020	-0.116
MA0390.1 STB3	STB3	23,636	-1.121	-1.197	0.016	-0.183
MA0391.1 STB4	STB4	9,155	2.245	2.060	0.162	2.690
MA0392.1 STB5	STB5	61,477	1.927	1.674	0.452	3.399
MA0394.1 STP1	STP1	32,963	14.768	12.034	0.275	7.930
MA0395.1 STP2	STP2	55,458	8.191	6.485	0.353	6.028
MA0396.1 STP3	STP3	7,625	2.474	2.048	0.135	3.459
MA0399.1 SUT1	SUT1	161,764	12.598	10.300	0.891	6.526
MA0400.1 SUT2	SUT2	22,016	0.869	0.665	0.065	1.801
MA0401.1 SWI4	SWI4	12,711	2.203	2.118	0.148	3.241
MA0404.1 TBS1	TBS1	56,939	10.690	9.115	0.710	7.206
MA0405.1 TEA1	TEA1	92,648	2.813	2.193	0.532	3.957
MA0407.1 THI2	THI2	142	-0.452	-0.560	0.019	0.416
MA0409.1 TYE7	TYE7	51,636	2.083	1.999	0.500	2.654
MA0410.1 UGA3	UGA3	94,001	10.023	7.792	0.614	8.148
MA0412.1 UME6	UME6	1,529	0.889	0.795	0.131	1.632
MA0414.1 XBP1	XBP1	72,596	2.212	1.876	0.285	2.335
MA0415.1 YAP1	YAP1	4,541	-0.608	-0.739	0.024	0.160
MA0419.1 YAP7	YAP7	42,296	-0.573	-0.728	0.021	0.623
MA0420.1 YBR239C	YBR239C	21,870	2.263	2.187	0.328	3.907
MA0421.1 YDR026C	YDR026C	5,051	1.180	0.856	0.054	1.319
MA0422.1 YDR520C	YDR520C	15,350	1.145	0.992	0.188	1.951
MA0424.1 YER184C	YER184C	87,502	2.837	2.630	0.669	3.326
MA0428.1 YKL222C	YKL222C	58,886	1.139	0.996	0.247	1.474
MA0429.1 YLL054C	YLL054C	123,003	9.717	7.877	0.684	5.876
MA0430.1 YLR278C	YLR278C	48,080	1.939	1.571	0.482	2.213
MA0432.1 YNR063W	YNR063W	19,567	1.089	0.629	0.095	2.704
MA0435.1 YPR015C	YPR015C	4,413	-0.441	-0.586	0.017	0.291
MA0436.1 YPR022C	YPR022C	92,167	3.378	2.855	0.765	3.041
MA0437.1 YPR196W	YPR196W	147,187	1.383	1.202	0.266	2.251
MA0438.1 YRM1	YRM1	131,905	0.644	0.491	0.106	2.716

MA0439.1 YRR1	YRR1	92,916	1.429	1.421	0.334	2.449
MA0440.1 ZAP1	ZAP1	766	0.834	0.661	0.020	0.656
MA0443.1 btd	btd	135,190	8.165	7.953	1.138	8.621
MA0444.1 CG34031	CG34031	60	-0.538	-0.606	0.035	-0.008
MA0446.1 fkh	fkh	13,506	-0.495	-0.645	0.016	0.326
MA0447.1 gt	gt	1,033	-0.598	-0.717	0.031	0.106
MA0449.1 h	h	26,262	3.166	2.513	0.676	0.362
MA0450.1 hkb	hkb	17,551	3.255	2.960	0.804	2.440
MA0453.1 nub	nub	34,047	0.366	0.631	0.162	0.709
MA0454.1 odd	odd	12,741	-0.197	-0.484	0.020	0.716
MA0456.1 opa	opa	42,202	3.841	2.964	0.970	2.616
MA0457.1 PHDP	PHDP	17	-0.711	-0.756	0.081	-0.162
MA0458.1 slp1	slp1	11,715	-0.508	-0.628	0.023	0.251
MA0459.1 tll	tll	16,668	-0.690	-0.830	0.016	0.045
MA0460.1 ttk	ttk	38	-1.055	-1.300	0.016	0.071
MF0001.1 ETS class		319,872	3.487	3.644	0.812	2.017
MF0002.1 bZIP CREB/G-box-like subclass		95,268	2.002	1.892	0.350	2.829
MF0004.1 Nuclear Receptor class		14,906	0.682	0.543	0.678	0.482
MF0005.1 Forkhead class		2,596	-0.638	-0.726	0.023	0.065
MF0006.1 bZIP cEBP-like subclass		37	-0.808	-0.951	0.016	0.024
MF0007.1 bHLH(zip) class		281,689	1.526	1.460	0.834	2.028
MF0009.1 TRP(MYB) class		116,249	1.333	1.279	0.705	1.539
MF0010.1 Homeobox class		12	-1.011	-1.097	0.032	-0.178
PB0001.1 Arid3a_1	Arid3a	10,946	-0.814	-0.834	0.019	-0.266
PB0002.1 Arid5a_1	Arid5a	5,124	-1.106	-1.170	0.017	-0.222
PB0003.1 Ascl2_1	Ascl2	195,956	1.750	1.208	0.499	1.643
PB0004.1 Atf1_1	Atf1	31,490	4.213	4.189	0.246	5.109
PB0005.1 Bbx_1	Bbx	10,724	-1.006	-1.093	0.018	-0.109
PB0007.1 Bhlhb2_1	Bhlhb2	45,641	2.026	1.942	0.239	2.380
PB0008.1 E2F2_1	E2F2	42,493	9.029	7.989	0.428	6.903
PB0010.1 Egr1_1	Egr1	80,172	7.423	6.557	0.872	7.552
PB0011.1 Ehf_1	Ehf	162,455	3.037	3.168	0.632	3.817
PB0015.1 Foxa2_1	Foxa2	35,024	-1.135	-1.278	0.023	-0.061
PB0016.1 Foxj1_1	Foxj1	20,596	-0.639	-0.652	0.021	0.016
PB0017.1 Foxj3_1	Foxj3	26,952	-0.619	-0.698	0.022	0.001
PB0019.1 Foxl1_1	Foxl1	32,427	-1.122	-1.211	0.026	-0.167
PB0020.1 Gabpa_1	Gabpa	33,221	3.892	4.213	0.387	5.366
PB0021.1 Gata3_1	Gata3	99,664	-0.707	-0.858	0.018	1.002
PB0022.1 Gata5_1	Gata5	109,705	-0.516	-0.671	0.017	1.352

PB0023.1 Gata6_1	Gata6	162,738	-1.009	-1.176	0.018	0.877
PB0024.1 Gcm1_1	Gcm1	53,549	1.834	1.313	0.340	1.464
PB0026.1 Gm397_1	Gm397	10,894	-0.263	-0.571	0.018	0.206
PB0027.1 Gmeb1_1	Gmeb1	49,936	1.149	0.907	0.242	2.294
PB0028.1 Hbp1_1	Hbp1	32,970	-0.195	-0.244	0.040	0.059
PB0035.1 Irf5_1	Irf5	13,639	0.665	0.532	0.039	0.991
PB0036.1 Irf6_1	Irf6	19,774	0.765	0.581	0.047	1.017
PB0037.1 Isgf3g_1	Isgf3g	16,170	-0.387	-0.488	0.024	0.365
PB0039.1 Klf7_1	Klf7	111,313	7.654	8.028	1.036	11.853
PB0042.1 Mafk_1	Mafk	24,115	-0.612	-0.774	0.018	0.341
PB0043.1 Max_1	Max	106,476	1.632	1.323	0.301	2.446
PB0044.1 Mtf1_1	Mtf1	24,604	1.326	0.909	0.060	1.710
PB0047.1 Myf6_1	Myf6	47,678	-0.140	-0.396	0.019	0.745
PB0050.1 Osr1_1	Osr1	11,662	-0.383	-0.604	0.019	0.443
PB0052.1 Plagl1_1	Plagl1	140,346	5.911	4.487	0.929	3.110
PB0054.1 Rfx3_1	Rfx3	22,789	0.710	0.584	0.046	1.170
PB0055.1 Rfx4_1	Rfx4	22,551	2.057	1.960	0.230	2.071
PB0056.1 Rfxdc2_1	Rfxdc2	36,775	2.179	2.104	0.347	2.449
PB0058.1 Sfpi1_1	Sfpi1	259,481	0.616	0.541	0.160	2.082
PB0059.1 Six6_1	Six6	6,177	-0.476	-0.687	0.023	0.155
PB0062.1 Sox12_1	Sox12	14,452	-0.802	-0.823	0.021	-0.040
PB0063.1 Sox13_1	Sox13	18,134	-1.055	-1.092	0.021	-0.163
PB0064.1 Sox14_1	Sox14	47,973	-1.245	-1.288	0.026	-0.262
PB0065.1 Sox15_1	Sox15	8,837	-0.835	-0.804	0.020	-0.100
PB0066.1 Sox17_1	Sox17	12,396	-1.015	-1.037	0.020	-0.280
PB0068.1 Sox1_1	Sox1	6,063	-1.084	-1.135	0.018	-0.209
PB0070.1 Sox30_1	Sox30	4,031	-0.551	-0.594	0.017	-0.143
PB0073.1 Sox7_1	Sox7	16,426	-1.066	-1.088	0.020	-0.282
PB0076.1 Sp4_1	Sp4	71,466	7.959	7.727	0.879	9.524
PB0077.1 Spdef_1	Spdef	80,478	1.812	1.621	0.358	2.690
PB0078.1 Srf_1	Srf	26,011	-0.611	-0.772	0.023	0.527
PB0079.1 Sry_1	Sry	25,416	-1.330	-1.355	0.023	-0.221
PB0081.1 Tcf1_1	Tcf1	5,587	-0.430	-0.580	0.023	0.133
PB0082.1 Tcf3_1	Tcf3	15,041	-0.465	-0.610	0.023	0.126
PB0085.1 Tcfap2a_1	Tcfap2a	139,191	1.011	0.737	0.392	1.313
PB0086.1 Tcfap2b_1	Tcfap2b	119,855	1.413	0.970	0.419	1.464
PB0088.1 Tcfap2e_1	Tcfap2e	90,769	1.040	0.846	0.418	1.323
PB0093.1 Zfp105_1	Zfp105	86,745	-0.528	-0.474	0.067	-0.204
PB0094.1 Zfp128_1	Zfp128	6,456	1.047	0.754	0.053	1.100
PB0095.1 Zfp161_1	Zfp161	52,393	5.162	4.477	0.330	6.538
PB0096.1 Zfp187_1	Zfp187	5,141	-0.969	-1.101	0.016	-0.114

PB0097.1 Zfp281_1	Zfp281	326,830	1.355	1.188	0.530	2.394
PB0098.1 Zfp410_1	Zfp410	12,025	-0.372	-0.666	0.012	0.396
PB0101.1 Zic1_1	Zic1	186,823	3.577	2.704	1.020	3.562
PB0105.1 Arid3a_2	Arid3a	1	-0.665	-0.768	0.015	-0.055
PB0107.1 Ascl2_2	Ascl2	450,098	1.846	1.546	1.144	3.169
PB0110.1 Bcl6b_2	Bcl6b	339,436	4.968	4.794	1.238	5.910
PB0112.1 E2F2_2	E2F2	67,491	4.585	4.051	0.510	4.769
PB0115.1 Ehf_2	Ehf	4,541	-0.459	-0.570	0.015	0.228
PB0117.1 Eomes_2	Eomes	106,607	1.585	1.138	0.351	1.465
PB0122.1 Foxk1_2	Foxk1	28,698	-0.959	-1.198	0.017	-0.227
PB0123.1 Foxl1_2	Foxl1	75,172	-0.519	-0.477	0.044	-0.103
PB0124.1 Gabpa_2	Gabpa	499,243	1.378	1.101	0.908	2.195
PB0125.1 Gata3_2	Gata3	6,263	-0.626	-0.787	0.016	0.115
PB0126.1 Gata5_2	Gata5	16,058	-0.328	-0.523	0.015	0.348
PB0127.1 Gata6_2	Gata6	15,084	4.380	3.598	0.383	0.658
PB0129.1 Glis2_2	Glis2	3,759	-1.215	-1.291	0.016	-0.339
PB0131.1 Gmeb1_2	Gmeb1	93,068	1.803	1.450	0.365	1.521
PB0135.1 Hoxa3_2	Hoxa3	2,310	-0.851	-0.970	0.015	-0.081
PB0137.1 Irf3_2	Irf3	62,303	0.984	0.739	0.423	0.823
PB0138.1 Irf4_2	Irf4	238,625	1.491	1.199	0.450	2.389
PB0139.1 Irf5_2	Irf5	46,199	0.882	0.643	0.076	1.165
PB0140.1 Irf6_2	Irf6	284,110	2.228	1.725	0.716	2.348
PB0141.1 Isgf3g_2	Isgrf3g	428	-0.391	-0.510	0.015	0.171
PB0143.1 Klf7_2	Klf7	48,513	1.839	1.661	0.313	1.961
PB0144.1 Lef1_2	Lef1	6,592	-0.488	-0.638	0.022	0.064
PB0145.1 Mafb_2	Mafb	7,588	-0.816	-0.897	0.018	-0.018
PB0146.1 Mafk_2	Mafk	9,748	-0.651	-0.843	0.016	0.034
PB0147.1 Max_2	Max	115,472	2.809	2.384	0.599	1.510
PB0150.1 Mybl1_2	Mybl1	84,517	0.970	0.574	0.047	1.599
PB0151.1 Myf6_2	Myf6	320,348	2.620	2.135	1.019	2.655
PB0153.1 Nr2f2_2	Nr2f2	76,101	3.544	2.792	0.576	2.748
PB0157.1 Rara_2	Rara	133,689	1.666	1.192	0.491	1.731
PB0164.1 Smad3_2	Smad3	273,833	5.658	5.105	1.014	6.959
PB0165.1 Sox11_2	Sox11	4,873	-0.956	-1.043	0.024	-0.141
PB0169.1 Sox15_2	Sox15	557	-0.695	-0.794	0.017	0.070
PB0170.1 Sox17_2	Sox17	1,618	-0.630	-0.781	0.015	0.133
PB0171.1 Sox18_2	Sox18	174	-0.452	-0.618	0.015	0.140
PB0172.1 Sox1_2	Sox1	2,995	-0.816	-0.892	0.016	-0.128
PB0173.1 Sox21_2	Sox21	1,906	0.054	0.435	0.272	0.149
PB0174.1 Sox30_2	Sox30	6,888	-1.150	-1.185	0.017	-0.121
PB0176.1 Sox5_2	Sox5	15	-0.757	-0.824	0.015	-0.021

PB0178.1 Sox8_2	Sox8	3,039	-0.618	-0.872	0.016	0.133
PB0179.1 Sp100_2	Sp100	42,149	3.042	2.803	0.261	3.269
PB0180.1 Sp4_2	Sp4	160,726	3.373	3.658	0.865	5.881
PB0184.1 Tbp_2	Tbp	47,193	0.771	0.547	0.141	1.190
PB0187.1 Tcf7_2	Tcf7	134	-0.913	-0.963	0.016	-0.194
PB0189.1 Tcfap2a_2	Tcfap2a	23,378	1.225	0.788	0.614	-0.630
PB0190.1 Tcfap2b_2	Tcfap2b	165,148	1.335	1.005	0.413	1.471
PB0191.1 Tcfap2c_2	Tcfap2c	221,187	1.726	1.253	0.838	1.603
PB0193.1 Tcfe2a_2	Tcfe2a	70,719	0.836	0.493	0.070	0.957
PB0197.1 Zfp105_2	Zfp105	3,445	-0.961	-1.120	0.016	-0.010
PB0199.1 Zfp161_2	Zfp161	55,304	12.636	10.105	0.521	6.841
PB0200.1 Zfp187_2	Zfp187	52,257	1.099	0.675	0.100	0.781
PB0204.1 Zfp740_2	Zfp740	108,651	1.502	1.037	0.295	1.526
PB0205.1 Zic1_2	Zic1	104,786	1.012	0.707	0.217	1.146
PF0001.1 RCGCANGCGY (Nrf)	Nrf	371	12.151	12.697	0.074	20.376
PF0003.1 SCGGAAGY		2,694	4.993	5.213	0.061	8.240
PF0004.1 ACTAYRNNNNCCR		2,121	6.018	7.263	0.040	3.707
PF0005.1 GATTGGY		5,025	1.888	1.974	0.124	3.123
PF0006.1 GGGCGGR		10,158	8.187	7.576	0.308	8.172
PF0008.1 TMTCGCGANR (KAISO)	KAISO	56	16.966	20.024	0.031	21.728
PF0009.1 TGAYRTCA		11,092	4.360	4.430	0.108	2.263
PF0010.1 GCCATNTTG		2,894	1.162	1.117	0.041	1.959
PF0011.1 MGGAAGTG		8,807	1.897	1.205	0.093	2.545
PF0015.1 CAGCTG		19,718	1.275	0.957	0.431	1.226
PF0016.1 RYTTCTG		8,861	0.868	0.744	0.156	1.559
PF0018.1 TCANNTGAY		30,201	1.530	1.408	0.109	1.994
PF0019.1 GKCGCN>NNNNNTGAYG		308	12.279	12.115	0.040	12.094
PF0020.1 GTGACGY		3,978	2.915	2.867	0.047	4.404
PF0021.1 GGAANC GGANY		1,160	5.371	5.823	0.047	2.612
PF0022.1 TGCGCANK		2,403	4.921	4.409	0.083	8.154
PF0024.1 GGGAGGRR		20,708	2.302	2.129	0.421	2.880
PF0025.1 TGACCTY		1,601	0.553	0.570	0.224	0.603
PF0026.1 TTAYRTAA		0	-1.166	-1.282	0.033	-0.272
PF0027.1 TGGNNNNNNNKCCAR		9,350	1.741	1.054	0.066	2.234
PF0028.1 CTAWWWATA		19	-0.672	-0.774	0.019	-0.498
PF0029.1 CTTTAAR		5	-0.414	-0.440	0.030	0.187
PF0030.1 YGCGYRCGC		2,157	4.713	4.192	0.098	9.536
PF0031.1 GGGYGTGNY		19,065	5.575	5.748	0.102	5.516
PF0032.1 TGASTMAGC		3,109	1.167	1.084	0.081	3.371
PF0033.1 YTATTTNR		1	-0.777	-0.811	0.023	-0.248
PF0034.1 CYTAGCAAY		510	0.941	0.809	0.042	1.089

PF0035.1 GCANCTGNY		21,606	2.301	1.852	0.194	1.843
PF0037.1 GTTRYCATRR		2,239	1.702	1.568	0.054	1.219
PF0039.1 TCCCRNNRGTGC		5,343	1.708	1.718	0.082	1.319
PF0043.1 GTTGNYNNRGNAAC		626	1.990	1.928	0.073	2.802
PF0044.1 YATGNWAAT		1,202	0.464	0.680	0.085	0.653
PF0045.1 CCANNAGRKGCG		199	2.716	3.283	0.101	2.939
PF0046.1 WTTGKCTG		18,845	1.804	1.871	0.130	2.937
PF0048.1 GCGNNANTTCC		504	4.728	4.772	0.079	6.341
PF0050.1 RGAGGAARY		4,134	0.730	0.648	0.103	1.841
PF0053.1 RYTGCNNRGNAAC		1,120	1.420	1.440	0.069	1.947
PF0054.1 TAAWWATAG		0	-0.504	-0.566	0.018	0.044
PF0056.1 GGGTGGRR		13,806	2.110	1.969	0.427	2.345
PF0058.1 YCATTAA		0	-0.488	-0.578	0.033	0.013
PF0061.1 YTAATTAA		0	-0.690	-0.719	0.086	-0.224
PF0063.1 AAGWWRNYGGC		1,501	2.646	2.388	0.057	1.940
PF0064.1 TTANTCA		0	-0.505	-0.552	0.021	0.040
PF0066.1 RACTNNRTTNC		2,835	0.927	1.085	0.048	1.485
PF0067.1 TGANNYRGCA		14,618	0.791	0.735	0.063	2.531
PF0069.1 SGCGSSAAA		833	5.419	5.265	0.146	7.345
PF0070.1 CGTSACG		1,629	6.398	6.067	0.028	8.825
PF0074.1 GGAMTNNNNNNTCCY		2,578	2.570	2.546	0.092	2.620
PF0075.1 TNCATNTCCYR		1,828	0.941	1.060	0.054	1.393
PF0078.1 GCTNWTTGK		8,003	2.086	2.027	0.099	1.859
PF0080.1 SNACANNNSYAGA		1,784	2.099	2.251	0.065	2.594
PF0081.1 CGGAARNGGCNG		982	8.637	8.474	0.062	8.948
PF0084.1 RGTTAMWNATT		0	-0.742	-0.889	0.017	0.108
PF0086.1 GGGNNTTCC		1,431	0.745	0.511	0.057	1.530
PF0087.1 RYTGCNWTTGGR		2,360	1.927	1.701	0.091	1.457
PF0088.1 GGCNKCCATNK		2,216	2.488	2.174	0.118	2.094
PF0089.1 GTTNYNNNGGTNA		1,548	0.818	0.660	0.037	1.128
PF0090.1 YAATNRNNNNYNATT		0	-1.170	-1.244	0.029	-0.304
PF0091.1 GTGGGTGK		2,482	1.235	1.064	0.139	1.073
PF0092.1 TGCTGAY		6,191	0.881	0.629	0.165	1.174
PF0094.1 TGATTTTRY		0	-0.655	-0.755	0.020	-0.026
PF0096.1 YGCANTGCR		3,311	2.088	1.797	0.087	1.332
PF0097.1 YATTNATC		0	-0.835	-0.963	0.019	-0.031
PF0098.1 GTCNYYATGR		2,540	1.703	1.481	0.064	1.318
PF0099.1 ATCMNTCCGY		406	2.349	2.231	0.112	2.025
PF0100.1 CRGAARNNNNCGA		565	3.051	2.864	0.061	4.741
PF0101.1 CTGCAGY		9,561	1.963	1.542	0.232	1.214
PF0102.1 ATGGYGGAA		3,357	0.778	-0.141	0.019	0.901

PF0103.1 ACAWNRNSRCGG		1,073	3.542	3.227	0.107	4.368
PF0104.1 CCAATNNSNNGCG		179	9.199	9.652	0.084	15.856
PF0105.1 ACTWSNACTNY		2,434	1.323	1.385	0.075	1.542
PF0106.1 CCGNMNNTNACG		508	7.291	7.010	0.048	10.948
PF0107.1 RTTTNNNYTGGM		43	-0.541	-0.730	0.017	0.351
PF0108.1 AACWWCAANK		1,450	0.265	0.382	0.028	0.756
PF0109.1 YGTCCTGR		152	0.811	0.637	0.047	0.657
PF0110.1 MCAATNNNNNGCG		652	4.896	5.013	0.134	7.070
PF0112.1 KTGGYRSGAA		1,226	1.653	1.605	0.080	1.257
PF0113.1 AACYNNNNTCCS		1,802	1.744	1.955	0.071	1.963
PF0114.1 YTCCRNNAGGY		1,921	2.140	1.958	0.124	2.422
PF0115.1 YRTCANNRCGC		515	4.076	3.650	0.111	3.450
PF0116.1 KMCATNNWGGA		1,221	0.805	0.595	0.028	0.735
PF0117.1 TGTYNNNNNRGCARM		916	1.117	0.973	0.052	0.882
PF0118.1 GGCNRNWCTTYS		2,038	2.132	2.133	0.095	1.856
PF0119.1 GGGNRMNNYCATT		1,768	1.804	1.222	0.085	1.378
PF0120.1 KRCTCANNMANAGC		537	1.012	0.646	0.021	1.251
PF0122.1 RNTCANNRNNYNATTW		0	-0.857	-0.938	0.019	-0.055
PF0123.1 GGCNNMSMYNTTG		1,514	2.140	1.743	0.107	1.890
PF0124.1 CCAWYNNGAAR		6,638	1.670	2.009	0.126	1.792
PF0125.1 RAAGNYNNCTTY		36	-0.600	-0.809	0.019	0.361
PF0126.1 WYAAANNRNNNGCG		604	2.771	2.616	0.102	2.963
PF0128.1 RYCACNNRNRCAG		8,749	1.560	1.577	0.128	1.476
PF0130.1 CCCNNGGGAR		6,447	2.191	1.447	0.100	2.244
PF0133.1 RYTAAWNNNTGAY		0	-0.627	-0.730	0.017	0.131
PF0134.1 CATRRAGC		491	0.943	0.589	0.061	0.768
PF0136.1 TAAYNRNNNTCC		10	-0.562	-0.775	0.019	0.225
PF0138.1 MYAATNNNNNNNGGC		3,421	2.092	1.857	0.152	2.220
PF0139.1 AAAYWAACM		34	-0.423	-0.432	0.088	-0.118
PF0140.1 RNGTGGGC		15,143	2.295	1.942	0.167	2.033
PF0143.1 CAGNWMCNNNGAC		774	1.114	0.735	0.045	1.075
PF0145.1 YKACATT		0	-0.811	-0.868	0.025	-0.057
PF0146.1 RRCCGTTA		580	1.693	1.522	0.020	2.946
PF0148.1 GATGKMRGCG		186	5.135	4.636	0.080	6.066
PF0149.1 YGACNNYACAR		1,723	1.028	0.790	0.043	1.207
PF0150.1 YTTCCNNNGGAMR		563	0.664	0.485	0.022	1.122
PF0155.1 WGTTNNNNNAAA		1	-0.764	-0.772	0.018	-0.040
PF0156.1 YRCCAKNNGNCGC		1,048	6.502	6.121	0.089	5.155
PF0157.1 KCCGNSWT		901	3.129	2.960	0.093	3.083
PF0159.1 GGCKCATGS		81	1.658	1.470	0.077	-0.126
PF0161.1 TTANWNANTGGM		0	-0.486	-0.528	0.022	0.003

PF0162.1 TAANNYSGCG		758	3.794	3.710	0.068	4.243
PF0163.1 GGARNTKYCCA		342	0.796	0.594	0.023	0.966
PF0164.1 GCGSCMNTTT		558	3.654	3.434	0.129	4.673
PF0165.1 CCAWNWWNNNGGC		1,642	1.718	1.341	0.075	1.297
PF0168.1 YTAAYNGCT		1	-1.732	-2.354	0.015	0.146
PF0170.1 YNGTTNNNATT		4	-0.668	-0.739	0.019	-0.068
PF0171.1 CTCNANGTGY		2,256	1.483	1.078	0.070	1.016
PF0173.1 YWATTWNNGC		2	-0.567	-0.719	0.015	0.185
PF0174.1 WTGAAAT		2	-0.568	-0.646	0.025	0.075
PH0001.1 Alx3	Alx3	10,970	-0.969	-1.057	0.085	-0.287
PH0002.1 Alx4	Alx4	6,848	-0.399	-0.499	0.040	-0.013
PH0003.1 Arx	Arx	8,935	-0.512	-0.543	0.058	-0.191
PH0004.1 Nkx3-2	Nkx3-2	23,211	-0.622	-0.753	0.020	0.308
PH0005.1 Barhl1	Barhl1	10,363	-0.647	-0.701	0.028	0.000
PH0006.1 Barhl2	Barhl2	11,443	-0.737	-0.761	0.025	-0.147
PH0007.1 Barx1	Barx1	6,809	-0.676	-0.724	0.021	-0.072
PH0008.1 Barx2	Barx2	11,967	-0.841	-0.872	0.067	-0.314
PH0010.1 Alx1_1	Alx1	7,870	-0.669	-0.823	0.049	-0.130
PH0011.1 Alx1_2	Alx1	11,238	-0.842	-0.949	0.047	-0.279
PH0012.1 Cdx1	Cdx1	10,806	-0.773	-0.860	0.026	-0.056
PH0013.1 Cdx2	Cdx2	9,252	-0.753	-0.871	0.026	0.005
PH0017.1 Cux1_2	Cux1	5,014	-0.931	-1.069	0.016	-0.198
PH0019.1 Dbx2	Dbx2	13,443	-0.964	-1.052	0.085	-0.403
PH0020.1 Dlx1	Dlx1	6,777	-0.630	-0.741	0.029	-0.081
PH0021.1 Dlx2	Dlx2	6,307	-0.806	-0.933	0.019	0.036
PH0022.1 Dlx3	Dlx3	4,904	-0.679	-0.835	0.022	0.138
PH0029.1 En2	En2	6,454	-0.666	-0.788	0.042	-0.051
PH0030.1 Esx1	Esx1	12,324	-0.892	-0.960	0.063	-0.209
PH0033.1 Gbx1	Gbx1	5,088	-0.424	-0.503	0.033	0.144
PH0036.1 Gsx2	Gsx2	5,483	-0.550	-0.660	0.030	-0.064
PH0037.1 Hdx	Hdx	5,493	-0.508	-0.665	0.016	0.065
PH0040.1 Hmbox1	Hmbox1	6,809	-0.508	-0.647	0.016	0.124
PH0041.1 Hmx1	Hmx1	8,349	-0.571	-0.700	0.023	0.111
PH0042.1 Hmx2	Hmx2	10,386	-1.035	-1.160	0.027	-0.007
PH0044.1 Homez	Homez	6,279	-0.571	-0.643	0.015	0.214
PH0045.1 Hoxa1	Hoxa1	6,220	-0.394	-0.493	0.034	0.014
PH0046.1 Hoxa10	Hoxa10	16,004	-0.968	-1.026	0.020	-0.166
PH0047.1 Hoxa11	Hoxa11	6,687	-0.606	-0.724	0.028	0.294
PH0048.1 Hoxa13	Hoxa13	5,479	-0.763	-0.884	0.021	0.162
PH0051.1 Hoxa4	Hoxa4	9,445	-0.929	-1.025	0.038	-0.293
PH0053.1 Hoxa6	Hoxa6	8,134	-0.665	-0.730	0.032	-0.094

PH0054.1 Hoxa7_1	Hoxa7	3,631	-0.483	-0.581	0.035	-0.110
PH0055.1 Hoxa7_2	Hoxa7	5,881	-0.644	-0.803	0.030	-0.001
PH0057.1 Hoxb13	Hoxb13	14,896	-1.057	-1.111	0.019	0.009
PH0061.1 Hoxb6	Hoxb6	4,560	-0.760	-0.856	0.021	0.005
PH0062.1 Hoxb7	Hoxb7	8,028	-0.645	-0.743	0.033	-0.063
PH0063.1 Hoxb8	Hoxb8	7,505	-0.817	-0.941	0.019	-0.179
PH0064.1 Hoxb9	Hoxb9	14,863	-0.801	-0.968	0.019	-0.051
PH0065.1 Hoxc10	Hoxc10	7,475	-0.372	-0.483	0.028	0.416
PH0067.1 Hoxc12	Hoxc12	3,891	-0.415	-0.550	0.025	0.355
PH0068.1 Hoxc13	Hoxc13	8,050	-0.921	-1.045	0.022	0.027
PH0070.1 Hoxc5	Hoxc5	10,756	-0.737	-0.757	0.064	-0.267
PH0071.1 Hoxc6	Hoxc6	11,826	-0.821	-0.835	0.057	-0.345
PH0072.1 Hoxc8	Hoxc8	7,252	-0.878	-0.964	0.028	-0.136
PH0073.1 Hoxc9	Hoxc9	8,311	-0.560	-0.690	0.019	0.103
PH0074.1 Hoxd1	Hoxd1	8,339	-0.670	-0.702	0.037	-0.156
PH0075.1 Hoxd10	Hoxd10	23,949	-1.136	-1.192	0.019	-0.310
PH0076.1 Hoxd11	Hoxd11	5,136	-0.498	-0.637	0.027	0.317
PH0079.1 Hoxd3	Hoxd3	5,748	-0.700	-0.882	0.027	-0.028
PH0081.1 Pdx1	Pdx1	6,822	-0.602	-0.712	0.032	-0.017
PH0082.1 Irx2	Irx2	20,492	-1.264	-1.417	0.025	-0.204
PH0084.1 Irx3_2	Irx3	19,170	-1.269	-1.378	0.026	-0.205
PH0085.1 Irx4	Irx4	20,647	-1.186	-1.293	0.024	-0.154
PH0088.1 Isl2	Isl2	13,681	-0.811	-0.817	0.043	-0.299
PH0090.1 Lbx2	Lbx2	9,320	-0.677	-0.812	0.042	-0.034
PH0091.1 Lhx1	Lhx1	19,524	-0.983	-1.027	0.049	-0.344
PH0092.1 Lhx2	Lhx2	7,665	-0.702	-0.741	0.047	-0.162
PH0096.1 Lhx6_1	Lhx6	5,384	-0.544	-0.656	0.033	-0.084
PH0099.1 Lhx9	Lhx9	7,544	-0.808	-0.884	0.053	-0.235
PH0100.1 Lmx1a	Lmx1a	20,154	-0.884	-0.930	0.036	-0.349
PH0103.1 Meox1	Meox1	6,359	-0.388	-0.559	0.026	0.133
PH0106.1 Msx1	Msx1	6,103	-1.051	-1.128	0.051	-0.352
PH0108.1 Msx3	Msx3	10,961	-0.774	-0.774	0.031	-0.190
PH0109.1 Nkx1-1	Nkx1-1	31,789	0.604	0.480	0.065	1.126
PH0110.1 Nkx1-2	Nkx1-2	4,863	-0.576	-0.726	0.045	-0.118
PH0112.1 Nkx2-3	Nkx2-3	19,835	-0.496	-0.602	0.024	0.141
PH0113.1 Nkx2-4	Nkx2-4	15,991	-0.484	-0.688	0.026	0.267
PH0114.1 Nkx2-5	Nkx2-5	13,414	-0.363	-0.551	0.026	0.289
PH0116.1 Nkx2-9	Nkx2-9	18,741	-0.827	-0.897	0.024	0.052
PH0117.1 Nkx3-1	Nkx3-1	22,651	-0.805	-0.878	0.022	0.053
PH0118.1 Nkx6-1_1	Nkx6-1	13,194	-0.835	-0.923	0.044	-0.266
PH0124.1 Obox5_1	Obox5	8,794	-0.470	-0.638	0.025	0.159

PH0125.1 Obox5_2	Obox5	9,694	-0.622	-0.808	0.024	0.098
PH0126.1 Obox6	Obox6	4,773	-0.374	-0.504	0.018	0.119
PH0128.1 Otp	Otp	9,840	-0.698	-0.719	0.052	-0.260
PH0130.1 Otx2	Otx2	7,666	-0.323	-0.515	0.028	0.190
PH0131.1 Pax4	Pax4	9,035	-0.434	-0.554	0.031	0.018
PH0132.1 Pax6	Pax6	12,601	-0.973	-1.080	0.111	-0.341
PH0133.1 Pax7	Pax7	3,145	-0.818	-0.891	0.032	-0.150
PH0134.1 Pbx1	Pbx1	6,405	-0.451	-0.591	0.016	0.034
PH0135.1 Phox2a	Phox2a	6,960	-0.665	-0.809	0.033	-0.171
PH0136.1 Phox2b	Phox2b	10,811	-0.701	-0.732	0.055	-0.238
PH0138.1 Pitx2	Pitx2	6,815	-0.522	-0.736	0.027	0.117
PH0139.1 Pitx3	Pitx3	23,328	0.793	0.480	0.045	1.106
PH0144.1 Pou2f2	Pou2f2	36,952	0.269	0.514	0.119	0.738
PH0148.1 Pou3f3	Pou3f3	15,002	-1.065	-1.098	0.016	-0.251
PH0150.1 Pou4f3	Pou4f3	15,147	-0.891	-0.968	0.030	-0.325
PH0152.1 Pou6f1_2	Pou6f1	9,628	-0.505	-0.686	0.021	0.230
PH0154.1 Prrx1	Prrx1	9,714	-0.917	-0.994	0.108	-0.208
PH0159.1 Rhox6	Rhox6	7,534	-0.564	-0.679	0.037	-0.080
PH0161.1 Six1	Six1	5,303	-0.380	-0.607	0.023	0.147
PH0162.1 Six2	Six2	5,271	-0.352	-0.608	0.024	0.135
PH0163.1 Six3	Six3	5,256	-0.361	-0.557	0.024	0.119
PH0165.1 Six6_1	Six6	4,565	-0.417	-0.607	0.024	0.057
PH0166.1 Six6_2	Six6	5,524	-0.561	-0.752	0.023	0.056
PH0167.1 Tcf1	Tcf1	7,737	-0.396	-0.591	0.021	0.314
PH0175.1 Vax2	Vax2	3,782	-0.500	-0.678	0.025	0.065
PH0176.1 Vsx1	Vsx1	11,802	-0.716	-0.742	0.063	-0.250
PL0004.1 hlh-27		21,380	2.156	1.528	0.170	1.945
PL0005.1 hlh-30		46,539	1.042	0.987	0.165	1.877
PL0007.1 mxl-3		56,698	1.288	1.089	0.235	2.056
PL0008.1 hlh-29		21,710	1.329	0.878	0.066	1.347
PL0011.1 hlh-2::hlh-4		7,546	-0.666	-1.115	0.016	0.358
PL0013.1 hlh-2::hlh-15		172,709	1.413	0.801	0.301	1.623
PL0014.1 mxl-1::mdl-1		46,778	1.281	1.063	0.254	1.556
PL0018.1 hlh-25		13,998	2.378	1.697	0.161	2.056
POL001.1 MTE		785	3.044	2.560	0.547	3.786
POL003.1 GC-box		276,599	10.002	10.035	1.142	10.184
POL004.1 CCAAT-box		225,430	2.340	2.734	0.615	3.594
POL006.1 BREu		222,059	11.431	9.649	0.919	2.054
POL008.1 DCE_S_I		250,859	1.299	1.082	0.936	1.501
POL009.1 DCE_S_II		97,252	1.114	0.839	0.993	1.071
POL011.1 XCPE1		10,919	7.520	6.832	0.906	6.385

POL013.1 MED-1		35,735	5.658	4.919	1.118	4.567
SA0001.1 at_AC_acceptor		47,404	-0.465	-0.453	0.031	0.038
SA0003.1 at_AC_acceptor		14,293	-0.610	-0.735	0.015	0.152
SD0003.1 at_AC_acceptor		8,463	-0.785	-0.974	0.015	0.043
YL_ES_Brg_3_0_c74		174	-0.592	-0.807	0.016	-0.762
YL_ES_Med12_3_0_c1651		270,750	2.110	1.969	1.033	2.345
YL_ES_Med15_3_0_c356		22,004	5.053	4.888	0.268	8.034

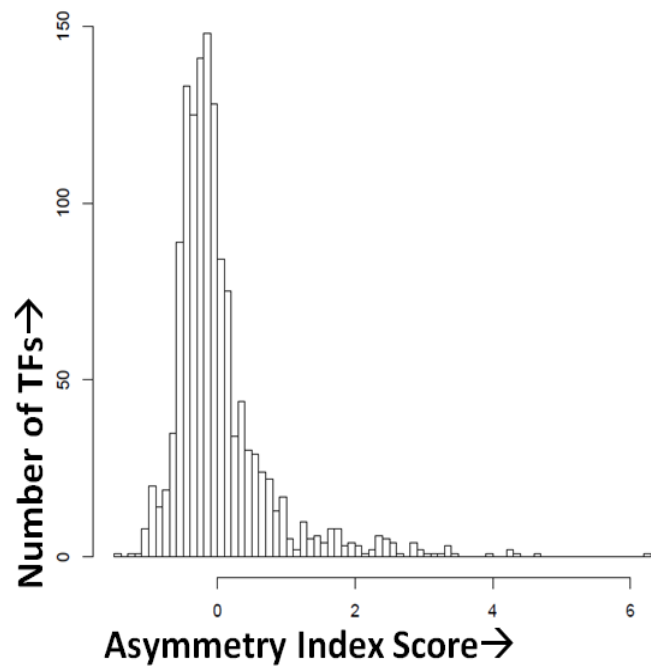
Supplementary Table 3: Directional pioneer TF classification

A. Asymmetry index values and directional pioneer classification for pioneer TF motifs. Pioneer TFs are classified as directional if over 75% of their chromatin opening occurs in a single direction. Motifs for directional and non-directional pioneer TFs are grouped into ten motif families that represent the most robust pioneer TFs found in this dataset: Klf/Sp, NFYA, Nrf, ETS, Creb/ATF, Zfp161, KAISO, Zinc Finger, E2F, and CTCF.

Motif	TF name	Asymmetry Index	Fraction of Pioneer Activity in Dominant Direction	Directional or non-directional?	Pioneer TF family
PF0006.1 GGGCGGR		5.502	0.785	Directional	Klf/Sp
ES_Suz12_3_0_c598		5.406	0.781	Directional	
PF0070.1 CGTSACG		5.016	0.848	Directional	
PB0039.1 Klf7_1	Klf7	4.861	0.831	Directional	Klf/Sp
MA0060.1 NFYA	NFYA	3.934	0.808	Directional	NFYA
PB0180.1 Sp4_2	Sp4	3.252	0.858	Directional	Klf/Sp
PF0104.1 CCAATNNNSNNNGCG		3.206	0.839	Directional	NFYA
PF0001.1 RCGCANGCGY (Nrf)	Nrf	3.147	0.872	Directional	Nrf
PB0076.1 Sp4_1	Sp4	2.797	0.818	Directional	Klf/Sp
PF0110.1 MCAATNNNNNGCG		2.282	0.827	Directional	NFYA
PB0164.1 Smad3_2	Smad3	2.242	0.825	Directional	
MA0098.1 ETS1	ETS1	2.065	0.646	Non-directional	ETS
PF0081.1 CGGAARNGGCNG		2.006	0.880	Directional	
PF0019.1 GKCGCNNNNNNNTGAYG		1.982	0.838	Directional	
PF0030.1 YGCGYRCGC		1.947	0.714	Non-directional	
PF0031.1 GGGYGTGNY		1.881	0.924	Directional	
PF0020.1 GTGACGY		1.743	0.750	Directional	
MA0028.1 ELK1	ELK1	1.725	0.694	Non-directional	ETS
MA0080.1 SPI1	SPI1	1.686	0.811	Directional	ETS
MA0018.1 CREB1	CREB1	1.684	0.889	Directional	Creb/ATF
PB0095.1 Zfp161_1	Zfp161	1.598	0.756	Directional	Zfp161
PF0008.1 TMTCGCGANR (KAISO)	KAISO	1.424	0.642	Non-directional	KAISO
PB0127.1 Gata6_2	Gata6	1.409	0.860	Directional	GATA
MA0014.1 Pax5	Pax5	1.355	0.954	Directional	
PF0022.1 TGCGCANK		1.318	1.016	Directional	
PF0115.1 YRTCANNRCGC		1.265	0.776	Directional	

PF0106.1 CCGNMNNTNACG		1.248	0.814	Directional	
MA0062.2 GABPA	GABPA	1.133	0.709	Non-directional	ETS
PF0003.1 SCGGAAGY		1.120	0.736	Non-directional	ETS
PB0110.1 Bcl6b_2	Bcl6b	1.117	0.899	Directional	
PF0069.1 SGCGSSAAA		1.113	0.683	Non-directional	
MA0131.1 MIZF	MIZF	1.098	0.740	Non-directional	Zinc finger
PB0179.1 Sp100_2	Sp100	1.064	0.669	Non-directional	
MA0024.1 E2F1	E2F1	1.024	0.708	Non-directional	E2F
MA0076.1 ELK4	ELK4	0.968	0.728	Non-directional	ETS
PF0162.1 TAANNYSGCG		0.821	0.601	Non-directional	
MA0139.1 CTCF	CTCF	0.789	0.632	Non-directional	CTCF
PB0112.1 E2F2_2	E2F2	0.653	0.733	Non-directional	E2F
PB0020.1 Gabpa_1	Gabpa	0.650	0.748	Non-directional	ETS
PB0011.1 Ehf_1	Ehf	0.576	0.718	Non-directional	ETS
PF0157.1 KCCGNSWTTT		0.557	0.577	Non-directional	
PF0045.1 CCANNAGRKGCG		0.502	0.647	Non-directional	

B. Histogram of Asymmetry Index scores for all PIQ motifs



Supplementary Table 4: Motif and chromatin dependence values

For each motif used in PIQ, the values for the chromatin dependence, motif dependence, and motif information content are shown as well as classification of the TF as a pioneer, settler or migrant TF. Indices and classifications are based on the mESC lineage.

Motif	TF names	Chromatin-Dependence	Motif-Dependence	Information Content	Classification
CN0001.1 LM1		0.745	0.113	12.974	Migrant
CN0002.1 LM2		0.555	0.328	13.144	Migrant
CN0003.1 LM3		0.774	0.089	14.587	Settler
CN0004.1 LM4		0.808	0.22	15.843	Pioneer
CN0005.1 LM5		-0.498	0.024	15.947	Migrant
CN0006.1 LM6		0.71	0.344	22.616	Migrant
CN0007.1 LM7		0.586	0.327	12.708	Pioneer
CN0008.1 LM8		-0.352	0.025	14.24	Migrant
CN0009.1 LM9		0.736	0.105	15.194	Migrant
CN0010.1 LM10		0.595	0.088	12.286	Migrant
CN0011.1 LM11		-0.366	0.023	17.415	Migrant
CN0017.1 LM17		-0.33	0.02	14.667	Migrant
CN0018.1 LM18		-0.068	0.033	15.994	Migrant
CN0019.1 LM19		0.663	0.088	13.019	Migrant
CN0021.1 LM21		-0.036	0.037	16.998	Migrant
CN0022.1 LM22		0.72	0.016	14.144	Migrant
CN0023.1 LM23		0.599	0.38	13.05	Pioneer
CN0025.1 LM25		-0.507	0.024	14.061	Migrant
CN0030.1 LM30		-0.566	0.143	15.006	Migrant
CN0031.1 LM31		-0.438	0.019	15.918	Migrant
CN0034.1 LM34		-0.569	0.037	14.704	Migrant
CN0036.1 LM36		-0.012	0.051	15.451	Migrant
CN0039.1 LM39		0.778	0.07	14.244	Settler
CN0041.1 LM41		-0.038	0.047	14.647	Migrant
CN0047.1 LM47		0.642	0.256	15.712	Migrant
CN0048.1 LM48		-0.483	0.026	13.21	Migrant
CN0051.1 LM51		0.174	0.027	14.628	Migrant
CN0052.1 LM52		-0.486	0.046	17.292	Migrant
CN0053.1 LM53		-0.547	0.031	14.688	Migrant
CN0056.1 LM56		-0.367	0.031	13.752	Migrant
CN0059.1 LM59		-0.501	0.026	13.745	Migrant
CN0061.1 LM61		-0.284	0.026	16.738	Migrant
CN0065.1 LM65		-0.474	0.012	14.756	Migrant

CN0067.1 LM67		-0.342	0.038	13.852	Migrant
CN0076.1 LM76		0.141	0.062	15.252	Migrant
CN0077.1 LM77		-0.275	0.043	16.24	Migrant
CN0080.1 LM80		-0.372	0.025	13.823	Migrant
CN0081.1 LM81		-0.212	0.06	15.391	Migrant
CN0085.1 LM85		-0.352	0.044	13.895	Migrant
CN0087.1 LM87		-0.532	0.042	14.184	Migrant
CN0088.1 LM88		-0.145	0.09	13.193	Migrant
CN0090.1 LM90		0.762	0.025	14.404	Settler
CN0092.1 LM92		-0.472	0.035	14.017	Migrant
CN0094.1 LM94		-0.324	0.045	14.153	Migrant
CN0096.1 LM96		-0.44	0.037	12.901	Migrant
CN0098.1 LM98		-0.126	0.021	16.558	Migrant
CN0100.1 LM100		0.846	0.072	14.983	Settler
CN0102.1 LM102		-0.081	0.033	14.963	Migrant
CN0108.1 LM108		-0.413	0.035	16.022	Migrant
CN0110.1 LM110		-0.453	0.042	15.991	Migrant
CN0114.1 LM114		-0.443	0.058	13.022	Migrant
CN0116.1 LM116		-0.49	0.042	13.692	Migrant
CN0117.1 LM117		0.009	0.055	14.986	Migrant
CN0118.1 LM118		-0.444	0.039	13.671	Migrant
CN0122.1 LM122		-0.441	0.045	13.154	Migrant
CN0123.1 LM123		-0.461	0.064	14.052	Migrant
CN0125.1 LM125		-0.567	0.053	14.394	Migrant
CN0130.1 LM130		0.876	0.11	14.007	Pioneer
CN0131.1 LM131		-0.469	0.039	15.533	Migrant
CN0132.1 LM132		-0.296	0.098	12.91	Migrant
CN0138.1 LM138		0.208	0.046	14.441	Migrant
CN0142.1 LM142		0.179	0.085	14.657	Migrant
CN0143.1 LM143		-0.446	0.072	13.178	Migrant
CN0146.1 LM146		0.541	0.196	16.361	Migrant
CN0147.1 LM147		-0.4	0.041	13.119	Migrant
CN0150.1 LM150		-0.531	0.046	12.658	Migrant
CN0151.1 LM151		-0.47	0.056	17.217	Migrant
CN0153.1 LM153		0.217	0.067	13.117	Migrant
CN0158.1 LM158		-0.347	0.038	13.676	Migrant
CN0160.1 LM160		-0.423	0.024	13.603	Migrant
CN0161.1 LM161		-0.386	0.046	13.224	Migrant
CN0162.1 LM162		-0.118	0.034	14.048	Migrant
CN0163.1 LM163		-0.377	0.029	14.051	Migrant
CN0164.1 LM164		-0.349	0.034	13.632	Migrant

CN0169.1 LM169		0.811	0.013	13.021	Settler
CN0170.1 LM170		-0.22	0.066	13.069	Migrant
CN0171.1 LM171		-0.515	0.042	12.742	Migrant
CN0172.1 LM172		-0.474	0.056	14.072	Migrant
CN0173.1 LM173		-0.168	0.048	13.522	Migrant
CN0176.1 LM176		0.831	-0.009	12.783	Settler
CN0178.1 LM178		-0.374	0.015	13.766	Migrant
CN0180.1 LM180		-0.393	0.008	13.497	Migrant
CN0182.1 LM182		-0.588	0.015	13.947	Migrant
CN0185.1 LM185		-0.197	0.025	13.504	Migrant
CN0187.1 LM187		-0.384	0.055	13.891	Migrant
CN0188.1 LM188		-0.432	0.043	13.639	Migrant
CN0189.1 LM189		-0.334	0.036	14.001	Migrant
CN0190.1 LM190		-0.433	0.029	13.966	Migrant
CN0192.1 LM192		-0.508	0.043	14.886	Migrant
CN0193.1 LM193		-0.445	0.023	13.451	Migrant
CN0194.1 LM194		0.589	0.171	15.632	Migrant
CN0196.1 LM196		-0.411	0.035	14.027	Migrant
CN0197.1 LM197		-0.313	0.026	15.064	Migrant
CN0200.1 LM200		-0.452	0.033	17.045	Migrant
CN0201.1 LM201		-0.279	0.016	13.233	Migrant
CN0203.1 LM203		-0.47	0.028	13.127	Migrant
CN0204.1 LM204		0.127	0.04	15.981	Migrant
CN0205.1 LM205		-0.482	0.03	14.029	Migrant
CN0206.1 LM206		-0.231	0.024	14.577	Migrant
CN0209.1 LM209		-0.335	0.023	13.597	Migrant
CN0210.1 LM210		-0.501	0.023	14.551	Migrant
CN0215.1 LM215		-0.402	0.048	13.985	Migrant
CN0216.1 LM216		-0.153	0.033	13.851	Migrant
CN0217.1 LM217		-0.376	0.022	13.499	Migrant
CN0223.1 LM223		-0.469	0.028	15.654	Migrant
CN0224.1 LM224		-0.491	0.059	13.113	Migrant
CN0226.1 LM226		-0.327	0.035	13.083	Migrant
CN0227.1 LM227		-0.276	0.053	14.437	Migrant
CN0228.1 LM228		-0.283	0.064	13.401	Migrant
CN0229.1 LM229		-0.411	0.055	13.385	Migrant
CN0230.1 LM230		-0.483	0.006	14.403	Migrant
CN0232.1 LM232		-0.255	0.026	13.789	Migrant
CN0233.1 LM233		-0.304	0.025	13.776	Migrant
ES_Nr5a2_3_0_c3657		0.671	0.04	8.044	Migrant
ES_Suz12_3_0_c598		0.898	-0.168	8.486	Pioneer

ES_Tbx3_R1D3_3_0_c387		0.555	0.019	6.959	Migrant
MA0003.1 TFAP2A	TFAP2A	0.825	0.063	5.062	Pioneer
MA0004.1 Arnt	Arnt	0.644	-0.138	4.802	Migrant
MA0006.1 Arnt::Ahr	Arnt::Ahr	0.787	-0.039	4.48	Settler
MA0008.1 HAT5	HAT5	-0.414	0.026	5.656	Migrant
MA0010.1 br_Z1	br	-0.296	0.031	3.718	Migrant
MA0011.1 br_Z2	br	-0.436	0.024	2.788	Migrant
MA0012.1 br_Z3	br	-0.269	0.017	3.279	Migrant
MA0014.1 Pax5	Pax5	0.757	0.036	4.343	Settler
MA0015.1 Cf2_II	Cf2	-0.466	0.087	6.725	Migrant
MA0016.1 usp	usp	0.75	0.014	7.374	Settler
MA0018.1 CREB1	CREB1	0.874	0.097	5.024	Pioneer
MA0018.2 CREB1	CREB1	0.551	0.057	3.422	Pioneer
MA0021.1 Dof3	Dof3	0.572	-0.008	3.964	Migrant
MA0022.1 dl_1	dl	0.483	0.024	4.741	Migrant
MA0024.1 E2F1	E2F1	0.865	0.077	4.338	Pioneer
MA0025.1 NFIL3	NFIL3	-0.457	0.013	6.511	Migrant
MA0026.1 Eip74EF	Eip74EF	0.549	0.083	4.27	Pioneer
MA0028.1 ELK1	ELK1	0.531	0.095	4.398	Pioneer
MA0029.1 Evi1	Evi1	-0.503	0.031	8.753	Migrant
MA0030.1 FOXF2	FOXF2	-0.201	0.002	7.159	Migrant
MA0033.1 FOXL1	FOXL1	-0.398	0.041	2.857	Migrant
MA0034.1 Gamyb	Gamyb	0.757	0.036	4.428	Pioneer
MA0035.1 Gata1	Gata1	0.705	0.023	3.285	Migrant
MA0039.2 Klf4	Klf4	0.819	0.111	8.723	Settler
MA0040.1 Foxq1	Foxq1	-0.508	0.03	5.933	Migrant
MA0042.1 FOXI1	FOXI1	-0.073	0.099	6.592	Migrant
MA0044.1 HMG-1	HMG-1	0.282	0.02	3.02	Migrant
MA00445.1 D	D	0.417	0.032	6.344	Migrant
MA0045.1 HMG-I/Y	HMG-I/Y	-0.127	0.111	3.911	Migrant
MA0046.1 HNF1A	HNF1A	-0.26	0.002	7.05	Migrant
MA0047.1 Foxa2	Foxa2	-0.357	0.073	5.087	Migrant
MA0048.1 NHLH1	NHLH1	0.808	0.037	8.118	Pioneer
MA0052.1 MEF2A	MEF2A	-0.188	0.012	9.043	Migrant
MA0055.1 Myf	Myf	0.81	-0.007	6.228	Settler
MA0056.1 MZF1_1-4	MZF1	0.749	-0.011	3.797	Migrant
MA0057.1 MZF1_5-13	MZF1	0.782	0.01	3.779	Settler
MA0058.1 MAX	MAX	0.805	0.075	5.233	Settler
MA0059.1 MYC::MAX	MYC::MAX	0.781	0.026	6.467	Settler
MA0060.1 NFYA	NFYA	0.862	0.125	8.136	Pioneer
MA0061.1 NF-kappaB	NF-kappaB	0.752	0.008	7.12	Settler

MA0062.1 GABPA	GABPA	0.825	0.08	3.482	Pioneer
MA0062.2 GABPA	GABPA	0.848	0.15	9.113	Pioneer
MA0063.1 Nkx2-5	Nkx2-5	-0.386	0	3.36	Migrant
MA0067.1 Pax2	Pax2	0.504	0.05	3.233	Migrant
MA0070.1 PBX1	PBX1	-0.565	0.038	6.292	Migrant
MA0073.1 RREB1	RREB1	0.592	0.051	7.261	Migrant
MA0075.1 Prrx2	Prrx2	-0.505	-0.001	5.238	Migrant
MA0076.1 ELK4	ELK4	0.796	0.062	6.202	Pioneer
MA0077.1 SOX9	SOX9	0.444	0.027	5.551	Migrant
MA0079.1 SP1	SP1	0.808	0.051	2.64	Pioneer
MA0079.2 SP1	SP1	0.791	0.057	5.894	Pioneer
MA0080.1 SPI1	SPI1	0.785	0.037	4.207	Pioneer
MA0080.2 SPI1	SPI1	0.662	0.024	5.302	Migrant
MA0082.1 squamosa	squamosa	-0.395	0.016	6.207	Migrant
MA0084.1 SRY	SRY	-0.344	0.017	4.537	Migrant
MA0086.1 sna	sna	0.515	0.054	5.755	Migrant
MA0087.1 Sox5	Sox5	-0.305	0.001	5.04	Migrant
MA0088.1 znf143	znf143	0.74	0.018	5.503	Migrant
MA0090.1 TEAD1	TEAD1	0.698	0.053	5.439	Migrant
MA0093.1 USF1	USF1	0.771	0.113	5.662	Settler
MA0094.2 Ubx	Ubx	-0.473	0.021	5.11	Migrant
MA0095.1 YY1	YY1	0.501	0.034	3.347	Migrant
MA0096.1 bZIP910	bZIP910	0.89	-0.062	6.457	Settler
MA0097.1 bZIP911	bZIP911	0.879	0.017	10.148	Settler
MA0098.1 ETS1	ETS1	0.558	0.048	3.8	Pioneer
MA0099.1 Fos	Fos	0.621	0.05	4.626	Migrant
MA0100.1 Myb	Myb	0.77	0.016	5.629	Settler
MA0101.1 REL	REL	0.499	0.025	4.421	Migrant
MA0103.1 ZEB1	ZEB1	0.562	0.03	4.54	Migrant
MA0105.1 NFKB1	NFKB1	0.747	0.033	6.585	Migrant
MA0109.1 Hltf	Hltf	-0.311	0.028	4.224	Migrant
MA0112.1 ESR1	ESR1	0.796	0.008	5.28	Settler
MA0112.2 ESR1	ESR1	0.694	0.008	9.225	Migrant
MA0116.1 Zfp423	Zfp423	0.807	-0.008	8.919	Settler
MA0117.1 Mafb	Mafb	0.798	-0.018	2.739	Pioneer
MA0118.1 Macho-1	Macho-1	0.738	0.014	4.058	Migrant
MA0119.1 TLX1::NFIC	TLX1::NFIC	0.724	0.06	7.946	Migrant
MA0121.1 ARR10	ARR10	0.674	0.015	3.698	Migrant
MA0122.1 Nkx3-2	Nkx3-2	0.389	0.011	3.998	Migrant
MA0123.1 abi4	abi4	0.839	0.13	5.446	Pioneer
MA0124.1 NKX3-1	NKX3-1	-0.387	-0.013	4.952	Migrant

MA0126.1 ovo	ovo	0.205	0.014	4.321	Migrant
MA0127.1 PEND	PEND	-0.416	0.016	5.633	Migrant
MA0128.1 EmBP-1	EmBP-1	0.785	0.092	4.516	Settler
MA0129.1 TGA1A	TGA1A	0.539	0.013	3.871	Migrant
MA0131.1 MIZF	MIZF	0.851	0.089	5.875	Pioneer
MA0135.1 Lhx3	Lhx3	-0.262	0.028	7.205	Migrant
MA0138.1 REST	REST	0.754	0.136	10.672	Settler
MA0138.2 REST	REST	0.709	0.183	15.931	Migrant
MA0139.1 CTCF	CTCF	0.606	0.374	11.781	Pioneer
MA0141.1 Esrrb	Esrrb	0.65	0.063	8.85	Migrant
MA0142.1 Pou5f1	Pou5f1	0.486	0.077	10.19	Migrant
MA0143.1 Sox2	Sox2	0.43	0.064	8.846	Migrant
MA0145.1 Tcfcp2l1	Tcfcp2l1	0.799	0.017	8.054	Settler
MA0146.1 Zfx	Zfx	0.854	0.072	8.826	Pioneer
MA0147.1 Myc	Myc	0.821	0.036	7.362	Settler
MA0149.1 EWSR1-FLI1	EWSR1-FLI1	-0.624	0.24	20.432	Migrant
MA0150.1 NFE2L2	NFE2L2	0.689	0.039	6.387	Migrant
MA0151.1 ARID3A	ARID3A	-0.347	0.019	4.765	Migrant
MA0153.1 HNF1B	HNF1B	-0.5	0.004	4.929	Migrant
MA0154.1 EBF1	EBF1	0.762	0.009	5.506	Settler
MA0155.1 INSM1	INSM1	0.813	0.016	6.888	Settler
MA0159.1 RXR::RAR_DR5	RXR::RAR	0.756	0.003	7.516	Settler
MA0160.1 NR4A2	NR4A2	0.703	0.035	3.859	Migrant
MA0162.1 Egr1	Egr1	0.802	0.093	5.63	Pioneer
MA0163.1 PLAG1	PLAG1	0.838	0.023	8.169	Settler
MA0165.1 Abd-B	Abd-B	-0.458	0.013	4.251	Migrant
MA0166.1 Antp	Antp	-0.512	0.02	4.807	Migrant
MA0167.1 Awh	Awh	-0.516	0.015	5.472	Migrant
MA0168.1 B-H1	B-H1	-0.452	-0.003	4.534	Migrant
MA0169.1 B-H2	B-H2	-0.404	0.04	4.658	Migrant
MA0170.1 C15	C15	-0.505	0.014	3.914	Migrant
MA0171.1 CG11085	CG11085	-0.531	0.026	3.988	Migrant
MA0172.1 CG11294	CG11294	-0.528	0.053	4.932	Migrant
MA0173.1 CG11617	CG11617	-0.375	0.01	4.277	Migrant
MA0174.1 CG42234	CG42234	-0.383	0.018	3.736	Migrant
MA0175.1 CG13424	CG13424	-0.514	0.013	4.535	Migrant
MA0177.1 CG18599	CG18599	-0.502	0.044	5.096	Migrant
MA0178.1 CG32105	CG32105	-0.481	0.019	4.535	Migrant
MA0182.1 CG4328	CG4328	-0.376	0.033	4.254	Migrant
MA0183.1 CG7056	CG7056	-0.41	0.037	4.042	Migrant
MA0185.1 Deaf1	Deaf1	0.613	-0.067	2.561	Migrant

MA0195.1 Lim3	Lim3	-0.492	0.006	3.816	Migrant
MA0205.1 Trl	Trl	-0.169	0.138	4.645	Migrant
MA0206.1 abd-A	abd-A	-0.49	0.019	4.445	Migrant
MA0213.1 brk	brk	0.826	0.206	3.416	Pioneer
MA0215.1 btn	btn	-0.527	0.037	4.695	Migrant
MA0223.1 exex	exex	-0.444	0.005	5.225	Migrant
MA0230.1 lab	lab	-0.486	0.004	4.668	Migrant
MA0235.1 onecut	onecut	-0.435	0.027	4.475	Migrant
MA0240.1 repo	repo	-0.483	-0.018	5.58	Migrant
MA0242.1 run::Bgb	run::Bgb	0.725	0.011	6.876	Migrant
MA0248.1 tup	tup	-0.5	-0.007	3.793	Migrant
MA0250.1 unc-4	unc-4	-0.514	0.005	4.986	Migrant
MA0251.1 unpg	unpg	-0.501	0.006	4.741	Migrant
MA0259.1 HIF1A::ARNT	HIF1A::ARNT	0.579	-0.006	6.009	Migrant
MA0263.1 ttx-3::ceh-10	ttx-3::ceh-10	-0.511	0.039	8.934	Migrant
MA0267.1 ACE2	ACE2	0.77	-0.043	5.869	Settler
MA0268.1 ADR1	ADR1	0.778	-0.017	5.214	Settler
MA0270.1 AFT2	AFT2	0.764	0.057	7.044	Settler
MA0271.1 ARG80	ARG80	0.746	0.067	5.911	Pioneer
MA0273.1 ARO80	ARO80	0.848	-0.025	7.603	Settler
MA0275.1 ASG1	ASG1	0.639	-0.02	5.553	Pioneer
MA0276.1 ASH1	ASH1	0.782	0.028	7.06	Settler
MA0277.1 AZF1	AZF1	-0.117	0.083	7.128	Migrant
MA0278.1 BAS1	BAS1	0.725	0.018	10.871	Migrant
MA0279.1 CAD1	CAD1	-0.506	0.025	10.77	Migrant
MA0280.1 CAT8	CAT8	0.716	-0.069	5.377	Pioneer
MA0282.1 CEP3	CEP3	0.51	-0.036	7.195	Migrant
MA0283.1 CHA4	CHA4	0.862	0.04	6.906	Pioneer
MA0285.1 CRZ1	CRZ1	0.815	-0.009	5.134	Settler
MA0286.1 CST6	CST6	0.82	0.134	7.174	Settler
MA0289.1 DAL80	DAL80	0.638	0.017	6.784	Migrant
MA0291.1 DAL82	DAL82	0.869	-0.017	5.762	Settler
MA0292.1 ECM22	ECM22	0.756	-0.033	5.758	Pioneer
MA0293.1 ECM23	ECM23	-0.2	-0.001	4.686	Migrant
MA0295.1 FHL1	FHL1	0.805	-0.006	7.127	Settler
MA0296.1 FKH1	FKH1	-0.482	0.01	11.099	Migrant
MA0299.1 GAL4	GAL4	0.623	-0.036	7.943	Pioneer
MA0301.1 GAT3	GAT3	0.293	0.016	4.688	Migrant
MA0304.1 GCR1	GCR1	0.705	0.002	7.941	Migrant
MA0305.1 GCR2	GCR2	0.739	0.022	6.636	Migrant
MA0308.1 GSM1	GSM1	0.573	0.007	9.163	Migrant

MA0310.1 HAC1	HAC1	0.545	-0.002	7.103	Migrant
MA0311.1 HAL9	HAL9	0.656	-0.069	5.518	Pioneer
MA0312.1 HAP1	HAP1	0.749	-0.029	6.26	Migrant
MA0314.1 HAP3	HAP3	0.887	0.082	10.686	Pioneer
MA0315.1 HAP4	HAP4	0.833	0.068	8.087	Pioneer
MA0316.1 HAP5	HAP5	0.768	0.084	9.246	Pioneer
MA0317.1 HCM1	HCM1	-0.331	0.047	5.498	Migrant
MA0318.1 HMRA2	HMRA2	-0.408	-0.004	6.612	Migrant
MA0320.1 IME1	IME1	0.888	0.218	9.085	Pioneer
MA0323.1 IXR1	IXR1	0.737	0.024	13.434	Migrant
MA0324.1 LEU3	LEU3	0.87	-0.103	7.46	Pioneer
MA0325.1 LYS14	LYS14	0.521	0.056	7.124	Migrant
MA0328.1 MATALPHA2	MATALPHA2	-0.453	0.014	4.878	Migrant
MA0329.1 MBP1	MBP1	0.774	0.043	4.487	Pioneer
MA0330.1 MBP1::SWI6	MBP1::SWI6	0.77	-0.065	6.802	Pioneer
MA0333.1 MET31	MET31	0.778	0.075	6.964	Settler
MA0334.1 MET32	MET32	0.625	0.025	5.7	Migrant
MA0336.1 MGA1	MGA1	-0.498	0.019	8.375	Migrant
MA0341.1 MSN2	MSN2	0.782	-0.032	5.363	Settler
MA0344.1 NHP10	NHP10	0.796	-0.018	7.313	Pioneer
MA0345.1 NHP6A	NHP6A	-0.327	0.035	7.038	Migrant
MA0348.1 OAF1	OAF1	0.768	-0.045	6.388	Settler
MA0349.1 OPI1	OPI1	0.793	0.057	6.737	Pioneer
MA0350.1 TOD6	TOD6	0.791	0.02	9.553	Settler
MA0351.1 DOT6	DOT6	0.79	0.016	9.144	Settler
MA0352.1 PDR1	PDR1	0.846	0.272	6.235	Pioneer
MA0354.1 PDR8	PDR8	0.56	-0.001	7.549	Migrant
MA0356.1 PHO2	PHO2	-0.377	0.01	4.526	Migrant
MA0357.1 PHO4	PHO4	0.797	0.046	7.522	Settler
MA0359.1 RAP1	RAP1	0.434	0.041	7.871	Migrant
MA0360.1 RDR1	RDR1	0.856	0.004	7.335	Settler
MA0361.1 RDS1	RDS1	0.803	0.107	6.024	Pioneer
MA0362.1 RDS2	RDS2	0.778	0.009	6.275	Pioneer
MA0364.1 REI1	REI1	0.764	0.02	7.084	Settler
MA0365.1 RFX1	RFX1	0.763	-0.006	6.942	Settler
MA0366.1 RGM1	RGM1	0.777	0.001	5.512	Settler
MA0367.1 RGT1	RGT1	0.472	0.063	6.027	Migrant
MA0368.1 RIM101	RIM101	0.77	0.001	7.548	Pioneer
MA0369.1 RLM1	RLM1	-0.269	0.047	11.027	Migrant
MA0371.1 ROX1	ROX1	0.655	0.021	4.321	Migrant
MA0373.1 RPN4	RPN4	0.823	0.108	7.186	Pioneer

MA0374.1 RSC3	RSC3	0.828	0.034	4.912	Pioneer
MA0375.1 RSC30	RSC30	0.779	-0.031	6.168	Pioneer
MA0377.1 SFL1	SFL1	-0.38	0.004	7.519	Migrant
MA0378.1 SFP1	SFP1	0.252	0.034	8.605	Migrant
MA0379.1 SIG1	SIG1	-0.384	-0.001	5.874	Migrant
MA0382.1 SKO1	SKO1	-0.576	-0.039	9.921	Migrant
MA0383.1 SMP1	SMP1	-0.333	0.01	6.417	Migrant
MA0384.1 SNT2	SNT2	0.89	0.009	12.221	Pioneer
MA0387.1 SPT2	SPT2	-0.438	0.014	7.172	Migrant
MA0390.1 STB3	STB3	-0.609	0.022	10.948	Migrant
MA0391.1 STB4	STB4	0.461	0.024	6.991	Migrant
MA0392.1 STB5	STB5	0.782	-0.043	5.573	Settler
MA0394.1 STP1	STP1	0.853	0.179	6.935	Pioneer
MA0395.1 STP2	STP2	0.797	0.052	7.89	Pioneer
MA0396.1 STP3	STP3	0.867	0.045	6.845	Settler
MA0399.1 SUT1	SUT1	0.841	0.154	4.939	Pioneer
MA0400.1 SUT2	SUT2	0.402	0.038	9.934	Migrant
MA0401.1 SWI4	SWI4	0.801	0.018	7.36	Settler
MA0404.1 TBS1	TBS1	0.854	0.109	6.161	Pioneer
MA0405.1 TEA1	TEA1	0.87	-0.053	5.71	Settler
MA0407.1 THI2	THI2	-0.127	0.006	14.786	Migrant
MA0409.1 TYE7	TYE7	0.537	0.047	7.286	Migrant
MA0410.1 UGA3	UGA3	0.875	0.018	6.804	Pioneer
MA0412.1 UME6	UME6	0.764	0.066	8.142	Settler
MA0414.1 XBP1	XBP1	0.723	0.003	5.486	Migrant
MA0415.1 YAP1	YAP1	-0.246	0.028	10.862	Migrant
MA0419.1 YAP7	YAP7	-0.491	0.005	9.517	Migrant
MA0420.1 YBR239C	YBR239C	0.865	0.012	7.03	Settler
MA0421.1 YDR026C	YDR026C	0.825	0.048	11.205	Settler
MA0422.1 YDR520C	YDR520C	0.83	-0.034	6.994	Settler
MA0424.1 YER184C	YER184C	0.787	-0.028	5.686	Pioneer
MA0428.1 YKL222C	YKL222C	0.572	-0.068	6.519	Migrant
MA0429.1 YLL054C	YLL054C	0.827	0.129	5.289	Pioneer
MA0430.1 YLR278C	YLR278C	0.725	-0.021	6.536	Migrant
MA0432.1 YNR063W	YNR063W	0.524	-0.019	7.359	Migrant
MA0435.1 YPR015C	YPR015C	0.2	0.034	11.449	Migrant
MA0436.1 YPR022C	YPR022C	0.721	0.089	6.59	Pioneer
MA0437.1 YPR196W	YPR196W	0.489	0.077	5.94	Migrant
MA0438.1 YRM1	YRM1	0.52	0.035	6.615	Migrant
MA0439.1 YRR1	YRR1	0.831	0.018	6.217	Settler
MA0440.1 ZAP1	ZAP1	0.656	0.041	14.289	Migrant

MA0443.1 btd	btd	0.871	0.222	6.312	Pioneer
MA0444.1 CG34031	CG34031	-0.508	0.022	5.216	Migrant
MA0446.1 fkh	fkh	-0.058	0.025	5.945	Migrant
MA0447.1 gt	gt	-0.608	0.013	8.117	Migrant
MA0449.1 h	h	0.831	-0.069	5.498	Pioneer
MA0450.1 hkb	hkb	0.882	-0.024	7.109	Pioneer
MA0453.1 nub	nub	0.637	0.032	7.294	Migrant
MA0454.1 odd	odd	0.431	0.033	6.12	Migrant
MA0456.1 opa	opa	0.814	0.04	6.398	Pioneer
MA0457.1 PHDP	PHDP	-0.476	0.014	4.027	Migrant
MA0458.1 slp1	slp1	-0.247	0.01	6.323	Migrant
MA0459.1 tll	tll	-0.475	0.055	7.801	Migrant
MA0460.1 ttk	ttk	-0.593	0.031	6.248	Migrant
MF0001.1 ETS class		0.788	0.053	5.649	Pioneer
MF0002.1 bZIP CREB/G-box-like subclass		0.814	0.131	6.655	Settler
MF0004.1 Nuclear Receptor class		0.697	-0.007	3.413	Migrant
MF0005.1 Forkhead class		-0.26	0.039	6.421	Migrant
MF0006.1 bZIP cEBP-like subclass		-0.403	0.009	4.971	Migrant
MF0007.1 bHLH(zip) class		0.752	0.037	4.87	Settler
MF0009.1 TRP(MYB) class		0.468	0.018	4.03	Migrant
MF0010.1 Homeobox class		-0.395	0.017	3.868	Migrant
PB0001.1 Arid3a_1	Arid3a	-0.228	0.015	5.783	Migrant
PB0002.1 Arid5a_1	Arid5a	-0.366	0.016	6.529	Migrant
PB0003.1 Ascl2_1	Ascl2	0.785	0.017	7.077	Settler
PB0004.1 Atf1_1	Atf1	0.546	0.107	9.166	Pioneer
PB0005.1 Bbx_1	Bbx	-0.443	0.011	6.748	Migrant
PB0007.1 Bhlhb2_1	Bhlhb2	0.74	0.062	8.572	Migrant
PB0008.1 E2F2_1	E2F2	0.866	0.042	7.247	Pioneer
PB0010.1 Egr1_1	Egr1	0.806	0.069	8.925	Pioneer
PB0011.1 Ehf_1	Ehf	0.572	0.052	7.101	Pioneer
PB0015.1 Foxa2_1	Foxa2	-0.351	0.045	8.439	Migrant
PB0016.1 Foxj1_1	Foxj1	-0.168	0.037	6.791	Migrant
PB0017.1 Foxj3_1	Foxj3	-0.214	0.048	8.267	Migrant
PB0019.1 Foxl1_1	Foxl1	-0.306	0.007	9.619	Migrant
PB0020.1 Gabpa_1	Gabpa	0.852	0.095	9.029	Pioneer
PB0021.1 Gata3_1	Gata3	-0.363	0.018	9.09	Migrant
PB0022.1 Gata5_1	Gata5	-0.348	0.019	8.061	Migrant
PB0023.1 Gata6_1	Gata6	-0.379	0.007	7.212	Migrant
PB0024.1 Gcm1_1	Gcm1	0.787	0.026	7.642	Settler
PB0026.1 Gm397_1	Gm397	-0.358	0.03	9.172	Migrant
PB0027.1 Gmeb1_1	Gmeb1	0.594	-0.033	5.193	Migrant

PB0028.1 Hbp1_1	Hbp1	-0.226	0.012	8.357	Migrant
PB0035.1 Irf5_1	Irf5	0.446	0.022	8.532	Migrant
PB0036.1 Irf6_1	Irf6	0.475	0.014	7.705	Migrant
PB0037.1 Isgf3g_1	Isgf3g	0.055	0.026	8.783	Migrant
PB0039.1 Klf7_1	Klf7	0.856	0.134	8.49	Pioneer
PB0042.1 Mafk_1	Mafk	-0.36	0.015	7.88	Migrant
PB0043.1 Max_1	Max	0.784	0.039	7.646	Settler
PB0044.1 Mtf1_1	Mtf1	0.688	0.02	8.929	Migrant
PB0047.1 Myf6_1	Myf6	0.63	0.009	6.863	Migrant
PB0050.1 Osr1_1	Osr1	-0.045	0.025	8.423	Migrant
PB0052.1 Plagl1_1	Plagl1	0.822	0.057	7.119	Pioneer
PB0054.1 Rfx3_1	Rfx3	0.745	0.041	9.687	Migrant
PB0055.1 Rfx4_1	Rfx4	0.793	0.06	9.221	Settler
PB0056.1 Rfxdc2_1	Rfxdc2	0.772	0.037	8.392	Settler
PB0058.1 Sfpi1_1	Sfpi1	0.711	0.019	6.743	Migrant
PB0059.1 Six6_1	Six6	-0.33	0.022	8.73	Migrant
PB0062.1 Sox12_1	Sox12	-0.352	0.005	7.148	Migrant
PB0063.1 Sox13_1	Sox13	-0.334	0.014	7.283	Migrant
PB0064.1 Sox14_1	Sox14	-0.265	0.028	6.854	Migrant
PB0065.1 Sox15_1	Sox15	-0.357	0.003	6.71	Migrant
PB0066.1 Sox17_1	Sox17	-0.296	0.01	6.789	Migrant
PB0068.1 Sox1_1	Sox1	-0.479	0.013	5.652	Migrant
PB0070.1 Sox30_1	Sox30	-0.268	0.004	6.703	Migrant
PB0073.1 Sox7_1	Sox7	-0.387	0.01	7.797	Migrant
PB0076.1 Sp4_1	Sp4	0.853	0.135	8.899	Pioneer
PB0077.1 Spdef_1	Spdef	0.82	0.036	7.485	Settler
PB0078.1 Srf_1	Srf	-0.078	0.013	7.002	Migrant
PB0079.1 Sry_1	Sry	-0.468	0.022	8.344	Migrant
PB0081.1 Tcf1_1	Tcf1	-0.251	0.016	6.812	Migrant
PB0082.1 Tcf3_1	Tcf3	-0.159	0.016	7.673	Migrant
PB0085.1 Tcfap2a_1	Tcfap2a	0.833	-0.004	6.692	Settler
PB0086.1 Tcfap2b_1	Tcfap2b	0.841	0.006	7.525	Settler
PB0088.1 Tcfap2e_1	Tcfap2e	0.811	0.014	7.251	Settler
PB0093.1 Zfp105_1	Zfp105	0.015	0.107	5.738	Migrant
PB0094.1 Zfp128_1	Zfp128	0.74	0.06	8.44	Migrant
PB0095.1 Zfp161_1	Zfp161	0.866	0.046	7.467	Pioneer
PB0096.1 Zfp187_1	Zfp187	-0.534	0.022	10.485	Migrant
PB0097.1 Zfp281_1	Zfp281	0.737	0.039	8.415	Migrant
PB0098.1 Zfp410_1	Zfp410	-0.53	0.03	9.314	Migrant
PB0101.1 Zic1_1	Zic1	0.852	0.05	6.652	Pioneer
PB0105.1 Arid3a_2	Arid3a	-0.391	0.019	2.658	Migrant

PB0107.1 Ascl2_2	Ascl2	0.709	0.036	3.117	Migrant
PB0110.1 Bcl6b_2	Bcl6b	0.819	0.052	4.832	Pioneer
PB0112.1 E2F2_2	E2F2	0.876	0.063	6.674	Pioneer
PB0115.1 Ehf_2	Ehf	-0.077	0.011	6.549	Migrant
PB0117.1 Eomes_2	Eomes	0.754	0.019	7.19	Settler
PB0122.1 Foxk1_2	Foxk1	-0.095	0.045	6.298	Migrant
PB0123.1 Foxl1_2	Foxl1	-0.019	0.039	6.002	Migrant
PB0124.1 Gabpa_2	Gabpa	0.799	0.015	2.592	Settler
PB0125.1 Gata3_2	Gata3	-0.373	0.011	6.178	Migrant
PB0126.1 Gata5_2	Gata5	-0.494	0.013	6.327	Migrant
PB0127.1 Gata6_2	Gata6	0.861	0.057	6.305	Pioneer
PB0129.1 Glis2_2	Glis2	-0.351	0.019	4.124	Migrant
PB0131.1 Gmeb1_2	Gmeb1	0.829	0.018	4.991	Settler
PB0135.1 Hoxa3_2	Hoxa3	-0.437	0.011	5.368	Migrant
PB0137.1 Irf3_2	Irf3	0.49	0.013	3.967	Migrant
PB0138.1 Irf4_2	Irf4	0.505	0.014	5.042	Migrant
PB0139.1 Irf5_2	Irf5	0.495	0.016	6.435	Migrant
PB0140.1 Irf6_2	Irf6	0.769	0.03	4.639	Settler
PB0141.1 Isgf3g_2	Isgf3g	-0.3	0.015	3.279	Migrant
PB0143.1 Klf7_2	Klf7	0.841	0.049	7.849	Settler
PB0144.1 Lef1_2	Lef1	-0.363	0.008	7.226	Migrant
PB0145.1 Mafb_2	Mafb	-0.271	0.02	5.317	Migrant
PB0146.1 Mafk_2	Mafk	-0.319	0.021	6.709	Migrant
PB0147.1 Max_2	Max	0.832	0.027	5.844	Settler
PB0150.1 Mybl1_2	Mybl1	0.76	0.006	7.742	Settler
PB0151.1 Myf6_2	Myf6	0.822	0.03	3.65	Settler
PB0153.1 Nr2f2_2	Nr2f2	0.731	0.038	7.936	Pioneer
PB0157.1 Rara_2	Rara	0.733	0.016	6.312	Migrant
PB0164.1 Smad3_2	Smad3	0.72	0.116	6.19	Pioneer
PB0165.1 Sox11_2	Sox11	-0.446	0.023	6.103	Migrant
PB0169.1 Sox15_2	Sox15	-0.448	0.021	3.575	Migrant
PB0170.1 Sox17_2	Sox17	-0.378	0.021	4.178	Migrant
PB0171.1 Sox18_2	Sox18	-0.225	0.013	3.625	Migrant
PB0172.1 Sox1_2	Sox1	-0.356	0.026	5.446	Migrant
PB0173.1 Sox21_2	Sox21	0.635	0.011	5.666	Migrant
PB0174.1 Sox30_2	Sox30	-0.453	0.015	6.372	Migrant
PB0176.1 Sox5_2	Sox5	-0.414	0.02	3.228	Migrant
PB0178.1 Sox8_2	Sox8	-0.48	0.011	5.394	Migrant
PB0179.1 Sp100_2	Sp100	0.689	0.021	4.84	Pioneer
PB0180.1 Sp4_2	Sp4	0.856	0.061	7.119	Pioneer
PB0184.1 Tbp_2	Tbp	0.743	0.024	3.382	Migrant

PB0187.1 Tcf7_2	Tcf7	-0.373	0.019	3.195	Migrant
PB0189.1 Tcfap2a_2	Tcfap2a	0.569	0.006	4.502	Migrant
PB0190.1 Tcfap2b_2	Tcfap2b	0.825	0.017	6.157	Settler
PB0191.1 Tcfap2c_2	Tcfap2c	0.813	0.024	5.057	Settler
PB0193.1 Tcfe2a_2	Tcfe2a	0.653	0.004	7.339	Migrant
PB0197.1 Zfp105_2	Zfp105	-0.4	0.025	5.548	Migrant
PB0199.1 Zfp161_2	Zfp161	0.887	0.145	7.221	Pioneer
PB0200.1 Zfp187_2	Zfp187	0.746	0.007	7.168	Migrant
PB0204.1 Zfp740_2	Zfp740	0.726	-0.001	6.862	Migrant
PB0205.1 Zic1_2	Zic1	0.767	0.025	7.634	Settler
PF0001.1 RCGCANGCGY		0.908	0.251	11.769	Pioneer
PF0003.1 SCGGAAGY		0.896	0.049	9.821	Pioneer
PF0004.1 ACTAYRNNNNCCR		0.892	0.43	14.191	Pioneer
PF0005.1 GATTGGY		0.876	0.056	9.065	Settler
PF0006.1 GGGCGGR		0.873	-0.002	9.161	Pioneer
PF0008.1 TMTCGCGANR		0.87	0.571	12.377	Pioneer
PF0009.1 TGAYRTCA		0.829	0.188	9.903	Pioneer
PF0010.1 GCCATNTTG		0.861	0.06	11.168	Settler
PF0011.1 MGGAAGTG		0.658	0.254	10.366	Migrant
PF0015.1 CAGCTG		0.774	0.002	8.29	Settler
PF0016.1 RYTTCCCTG		0.732	0.051	9.684	Migrant
PF0018.1 TCANNTGAY		0.751	0.128	9.559	Settler
PF0019.1 GKCGCNNNNNNNTGAYG		0.907	0.276	13.558	Pioneer
PF0020.1 GTGACGY		0.908	-0.068	8.972	Pioneer
PF0021.1 GGAANCDDAANY		0.922	0.235	13.667	Pioneer
PF0022.1 TGCGCANK		0.905	0.079	9.152	Pioneer
PF0024.1 GGGAGGRR		0.828	0.101	9.899	Settler
PF0025.1 TGACCTY		0.692	0.021	8.978	Migrant
PF0026.1 TTAYRTAA		-0.648	0.075	9.484	Migrant
PF0027.1 TGGNNNNNNKCCAR		0.767	0.087	9.887	Settler
PF0028.1 CTAWWWATA		-0.529	0.036	10.359	Migrant
PF0029.1 CTTTAAR		-0.034	0.071	8.966	Migrant
PF0030.1 YGCGYRCGC		0.906	-0.071	10.499	Pioneer
PF0031.1 GGGYGTGNY		0.814	0.157	10.004	Pioneer
PF0032.1 TGASTMAGC		0.676	0.116	11.2	Migrant
PF0033.1 YTATTTTNR		-0.216	0.067	9.825	Migrant
PF0034.1 CYTAGCAAY		0.773	0.115	11.349	Settler
PF0035.1 GCANCTGNY		0.788	0.087	9.315	Settler
PF0037.1 GTTRYCATRR		0.786	0.164	11.593	Settler
PF0039.1 TCCCRNNRTGC		0.853	0.043	11.515	Settler
PF0043.1 GTTGNYNNRGNAAC		0.855	0.002	13.336	Settler

PF0044.1 YATGNWAAT		0.661	0.09	10.16	Migrant
PF0045.1 CCANNAGRKGCG		0.668	0.232	12.48	Pioneer
PF0046.1 WTTGKCTG		0.815	0.086	9.883	Settler
PF0048.1 GCGNNANTTCC		0.907	0.205	11.716	Pioneer
PF0050.1 RGAGGAARY		0.752	0.072	10.39	Settler
PF0053.1 RYTGCNNRGNAAC		0.799	0.164	12.672	Settler
PF0054.1 TAAWWATAG		-0.407	0.032	11.076	Migrant
PF0056.1 GGGTGGRR		0.809	0.066	9.962	Settler
PF0058.1 YCATCAA		-0.503	0.046	8.91	Migrant
PF0061.1 YTAATTAA		-0.426	0.065	10.13	Migrant
PF0063.1 AAGWWRNYGGC		0.855	0.224	12.158	Settler
PF0064.1 TTANTCA		-0.52	0.049	8.275	Migrant
PF0066.1 RACTNNRTTNC		0.738	0.11	12.564	Migrant
PF0067.1 TGANNYRGCA		0.649	0.094	9.792	Migrant
PF0069.1 SGCGSSAAA		0.876	-0.105	10.464	Pioneer
PF0070.1 CGTSACG		0.922	-0.002	8.802	Pioneer
PF0074.1 GGAMTNNNNNNTCCY		0.803	0.112	13.076	Pioneer
PF0075.1 TNCATNTCCYR		0.562	0.061	11.859	Migrant
PF0078.1 GCTNWTTGK		0.801	0.095	9.892	Settler
PF0080.1 SNACANNNNSYAGA		0.861	0.085	14.127	Settler
PF0081.1 CGGAARNGGCNG		0.884	0.34	12.968	Pioneer
PF0084.1 RGTTAMWNATT		-0.37	0.024	11.055	Migrant
PF0086.1 GGGNNNTTCC		0.795	0.014	10.748	Settler
PF0087.1 RYTGCNWTGGNR		0.792	0.112	11.901	Settler
PF0088.1 GGCNKCCATNK		0.837	0.137	11.365	Settler
PF0089.1 GTTNYYNNGGTNA		0.776	0.096	11.486	Settler
PF0090.1 YAATNRNNNNYNATT		-0.551	0.086	10.371	Migrant
PF0091.1 GTGGGTGK		0.646	0.021	10.257	Migrant
PF0092.1 TGCTGAY		0.657	0.035	8.929	Migrant
PF0094.1 TGATTTRY		-0.639	0.08	9.575	Migrant
PF0096.1 YGCANTGCR		0.828	0.061	9.472	Settler
PF0097.1 YATTNATC		-0.416	0.038	8.896	Migrant
PF0098.1 GTCNYYATGR		0.776	0.102	10.965	Settler
PF0099.1 ATCMINTCCGY		0.628	0.28	11.7	Migrant
PF0100.1 CRGAARNNNNNCGA		0.839	0.208	11.798	Pioneer
PF0101.1 CTGCAGY		0.757	0.075	9.021	Settler
PF0102.1 ATGGYGGAA		0.816	0.229	10.311	Settler
PF0103.1 ACAWRNRNSRCGG		0.878	0.228	12.096	Pioneer
PF0104.1 CCAATNNNSNNNGCG		0.907	0.335	12.213	Pioneer
PF0105.1 ACTWSNACTNY		0.779	0.122	12.444	Settler
PF0106.1 CCGNMNNTNACG		0.921	0.283	12.332	Pioneer

PF0107.1 RTTTNNNYTGGM		-0.147	0.07	10.257	Migrant
PF0108.1 AACWWCAANK		0.748	0.055	10.7	Migrant
PF0109.1 YGTCCTTGR		0.698	-0.048	10.8	Migrant
PF0110.1 MCAATNNNNNGCG		0.889	0.228	10.933	Pioneer
PF0112.1 KTGGYRSGAA		0.778	0.135	11.135	Settler
PF0113.1 AACYNNNNTCCS		0.849	0.095	13.13	Settler
PF0114.1 YTCCCRNAGGY		0.846	0.084	12.593	Settler
PF0115.1 YRTCANNRCGC		0.906	0.253	10.555	Pioneer
PF0116.1 KMCATNNWGGA		0.739	0.077	10.741	Migrant
PF0117.1 TGTYN>NNNRGCARM		0.73	0.05	11.112	Migrant
PF0118.1 GGCNRNWCTTYS		0.799	0.151	11.947	Settler
PF0119.1 GGGNRMNNYCAT		0.784	0.127	11.096	Settler
PF0120.1 KRCTCBBBBBMANAGC		0.748	0.045	16.385	Migrant
PF0122.1 RNTCANNRNNYNATTW		-0.521	0.06	10.657	Migrant
PF0123.1 GGCNNMSMYNTTG		0.855	0.102	11.642	Settler
PF0124.1 CCAWYNNGAAR		0.81	0.027	10.699	Settler
PF0125.1 RAAGNYNNCTTY		0.586	0.016	10.152	Migrant
PF0126.1 WYAAANNRNNNGCG		0.831	0.176	10.899	Pioneer
PF0128.1 RYCACNNRNNRNAGC		0.649	0.247	10.941	Migrant
PF0130.1 CCCNNGGGAR		0.84	0.054	10.384	Settler
PF0133.1 RYTAAWNNNTGAY		-0.32	0.046	10.626	Migrant
PF0134.1 CATRRAGC		0.676	0.053	9.451	Migrant
PF0136.1 TAAYNRNNNTCC		-0.335	0.066	9.615	Migrant
PF0138.1 MYAATNNNNNNNGC		0.83	0.14	10.35	Settler
PF0139.1 AAAYWAACM		-0.041	0.11	10.556	Migrant
PF0140.1 RNGTGGGC		0.836	0.084	9.004	Settler
PF0143.1 CAGNWMCBBBBBAC		0.733	0.115	12.798	Migrant
PF0145.1 YKACATT		-0.555	0.065	9.53	Migrant
PF0146.1 RRCCGTTA		0.843	0.107	9.409	Settler
PF0148.1 GATGKMRGCG		0.861	0.377	11.99	Pioneer
PF0149.1 YGACNNYACAR		0.724	0.018	11.318	Migrant
PF0150.1 YTTCCNNNGGAMR		0.831	0.047	11.931	Settler
PF0155.1 WGTNNNNNNAAA		-0.228	0.059	9.085	Migrant
PF0156.1 YRCCAQNNGNCGC		0.814	0.371	12.612	Pioneer
PF0157.1 KCCGNSWTTT		0.708	0.098	10.668	Pioneer
PF0159.1 GGCKCATGS		0.831	0.173	11.108	Settler
PF0161.1 TTANWNANTGGM		-0.579	0.069	10.689	Migrant
PF0162.1 TAANNYSGCG		0.878	-0.086	9.817	Pioneer
PF0163.1 GGARNTKYCCA		0.724	-0.012	11.179	Migrant
PF0164.1 GCGSCMNTTT		0.886	-0.088	11.039	Pioneer
PF0165.1 CCAWNWWNNNGGC		0.787	0.159	10.585	Settler

PF0168.1 YTAAYNGCT		-0.087	0.009	9.507	Migrant
PF0170.1 YNGTTNNNATT		-0.416	0.051	9.192	Migrant
PF0171.1 CTCNANGTGNY		0.74	0.096	10.626	Migrant
PF0173.1 YWATTWNNRGCT		-0.412	0.092	10.581	Migrant
PF0174.1 WTGAAAT		-0.416	-0.008	8.916	Migrant
PH0001.1 Alx3	Alx3	-0.296	0.032	9.006	Migrant
PH0002.1 Alx4	Alx4	-0.353	0.021	8.419	Migrant
PH0003.1 Arx	Arx	-0.462	0.022	8.888	Migrant
PH0004.1 Nkx3-2	Nkx3-2	-0.197	0.033	8.22	Migrant
PH0005.1 Barhl1	Barhl1	-0.4	0.01	8.515	Migrant
PH0006.1 Barhl2	Barhl2	-0.453	0.021	9.647	Migrant
PH0007.1 Barx1	Barx1	-0.615	0.018	7.3	Migrant
PH0008.1 Barx2	Barx2	-0.294	0.016	7.499	Migrant
PH0010.1 Alx1_1	Alx1	-0.405	0.015	8.474	Migrant
PH0011.1 Alx1_2	Alx1	-0.421	0.018	8.483	Migrant
PH0012.1 Cdx1	Cdx1	-0.472	0.011	7.981	Migrant
PH0013.1 Cdx2	Cdx2	-0.472	0.01	8.274	Migrant
PH0017.1 Cux1_2	Cux1	-0.453	0.023	6.501	Migrant
PH0019.1 Dbx2	Dbx2	-0.241	0.013	6.454	Migrant
PH0020.1 Dlx1	Dlx1	-0.522	0.011	7.552	Migrant
PH0021.1 Dlx2	Dlx2	-0.59	0.007	7.157	Migrant
PH0022.1 Dlx3	Dlx3	-0.533	0.015	7.981	Migrant
PH0029.1 En2	En2	-0.473	0.012	8.083	Migrant
PH0030.1 Esx1	Esx1	-0.435	0.019	8.682	Migrant
PH0033.1 Gbx1	Gbx1	-0.44	0.005	8.038	Migrant
PH0036.1 Gsx2	Gsx2	-0.322	0.012	7.725	Migrant
PH0037.1 Hdx	Hdx	-0.145	0.017	6.106	Migrant
PH0040.1 Hmbox1	Hmbox1	-0.24	0.024	8.031	Migrant
PH0041.1 Hmx1	Hmx1	-0.473	0.013	8.501	Migrant
PH0042.1 Hmx2	Hmx2	-0.515	0.015	9.013	Migrant
PH0044.1 Homez	Homez	-0.155	0.03	8.034	Migrant
PH0045.1 Hoxa1	Hoxa1	-0.336	0.017	8.768	Migrant
PH0046.1 Hoxa10	Hoxa10	-0.356	0.017	7.326	Migrant
PH0047.1 Hoxa11	Hoxa11	-0.444	0.021	9.074	Migrant
PH0048.1 Hoxa13	Hoxa13	-0.521	0.029	9.104	Migrant
PH0051.1 Hoxa4	Hoxa4	-0.395	0.021	8.591	Migrant
PH0053.1 Hoxa6	Hoxa6	-0.468	0.007	8.286	Migrant
PH0054.1 Hoxa7_1	Hoxa7	-0.299	0.002	6.431	Migrant
PH0055.1 Hoxa7_2	Hoxa7	-0.489	0.009	7.469	Migrant
PH0057.1 Hoxb13	Hoxb13	-0.413	0.018	7.99	Migrant
PH0061.1 Hoxb6	Hoxb6	-0.418	0.009	6.748	Migrant

PH0062.1 Hoxb7	Hoxb7	-0.517	0.007	7.47	Migrant
PH0063.1 Hoxb8	Hoxb8	-0.452	0.013	7.736	Migrant
PH0064.1 Hoxb9	Hoxb9	-0.369	0.007	8.333	Migrant
PH0065.1 Hoxc10	Hoxc10	-0.407	0.027	8.655	Migrant
PH0067.1 Hoxc12	Hoxc12	-0.084	0.037	9.297	Migrant
PH0068.1 Hoxc13	Hoxc13	-0.551	0.025	8.722	Migrant
PH0070.1 Hoxc5	Hoxc5	-0.342	0.018	7.998	Migrant
PH0071.1 Hoxc6	Hoxc6	-0.184	0.013	7.039	Migrant
PH0072.1 Hoxc8	Hoxc8	-0.469	0.004	7.182	Migrant
PH0073.1 Hoxc9	Hoxc9	-0.285	0.009	7.458	Migrant
PH0074.1 Hoxd1	Hoxd1	-0.319	0.014	7.764	Migrant
PH0075.1 Hoxd10	Hoxd10	-0.333	0.024	7.325	Migrant
PH0076.1 Hoxd11	Hoxd11	-0.257	0.034	9.241	Migrant
PH0079.1 Hoxd3	Hoxd3	-0.424	0.013	7.22	Migrant
PH0081.1 Pdx1	Pdx1	-0.413	0.012	7.628	Migrant
PH0082.1 Irx2	Irx2	-0.405	0.03	8.639	Migrant
PH0084.1 Irx3_2	Irx3	-0.398	0.025	8.383	Migrant
PH0085.1 Irx4	Irx4	-0.432	0.021	7.495	Migrant
PH0088.1 Isl2	Isl2	-0.385	0.021	7.162	Migrant
PH0090.1 Lbx2	Lbx2	-0.49	0.03	7.699	Migrant
PH0091.1 Lhx1	Lhx1	-0.329	0.019	9.082	Migrant
PH0092.1 Lhx2	Lhx2	-0.379	0.023	7.893	Migrant
PH0096.1 Lhx6_1	Lhx6	-0.585	0.027	7.826	Migrant
PH0099.1 Lhx9	Lhx9	-0.401	0.024	8.119	Migrant
PH0100.1 Lmx1a	Lmx1a	-0.259	0.001	8.579	Migrant
PH0103.1 Meox1	Meox1	-0.452	0.01	7.436	Migrant
PH0106.1 Msx1	Msx1	-0.376	0.019	7.406	Migrant
PH0108.1 Msx3	Msx3	-0.356	0.006	8.998	Migrant
PH0109.1 Nkx1-1	Nkx1-1	0.762	0.021	7.775	Settler
PH0110.1 Nkx1-2	Nkx1-2	-0.44	0.013	7.344	Migrant
PH0112.1 Nkx2-3	Nkx2-3	0.048	0.021	8.257	Migrant
PH0113.1 Nkx2-4	Nkx2-4	0.106	0.027	7.956	Migrant
PH0114.1 Nkx2-5	Nkx2-5	0.186	0.022	9.155	Migrant
PH0116.1 Nkx2-9	Nkx2-9	-0.126	0.032	8.239	Migrant
PH0117.1 Nkx3-1	Nkx3-1	-0.18	0.033	8.101	Migrant
PH0118.1 Nkx6-1_1	Nkx6-1	-0.319	0.015	8.625	Migrant
PH0124.1 Obox5_1	Obox5	-0.195	0.024	9.663	Migrant
PH0125.1 Obox5_2	Obox5	-0.358	0.02	9.399	Migrant
PH0126.1 Obox6	Obox6	-0.065	0.014	8.879	Migrant
PH0128.1 Otp	Otp	-0.406	0.029	9.634	Migrant
PH0130.1 Otx2	Otx2	-0.055	0.02	8.471	Migrant

PH0131.1 Pax4	Pax4	-0.391	0.013	8.498	Migrant
PH0132.1 Pax6	Pax6	-0.332	-0.002	7.664	Migrant
PH0133.1 Pax7	Pax7	-0.529	0.011	6.212	Migrant
PH0134.1 Pbx1	Pbx1	-0.344	0.012	6.456	Migrant
PH0135.1 Phox2a	Phox2a	-0.555	0.014	8.129	Migrant
PH0136.1 Phox2b	Phox2b	-0.395	0.025	8.988	Migrant
PH0138.1 Pitx2	Pitx2	-0.22	0.019	8.079	Migrant
PH0139.1 Pitx3	Pitx3	0.744	0.035	9.455	Migrant
PH0144.1 Pou2f2	Pou2f2	0.642	0.04	9.064	Migrant
PH0148.1 Pou3f3	Pou3f3	-0.513	0.019	8.877	Migrant
PH0150.1 Pou4f3	Pou4f3	-0.448	0.011	9.381	Migrant
PH0152.1 Pou6f1_2	Pou6f1	-0.432	0.013	9.706	Migrant
PH0154.1 Prrx1	Prrx1	-0.405	0.017	9.336	Migrant
PH0159.1 Rhox6	Rhox6	-0.373	0.017	7.418	Migrant
PH0161.1 Six1	Six1	-0.392	0.021	8.44	Migrant
PH0162.1 Six2	Six2	-0.305	0.024	9.41	Migrant
PH0163.1 Six3	Six3	-0.407	0.03	9.429	Migrant
PH0165.1 Six6_1	Six6	-0.415	0.024	9.47	Migrant
PH0166.1 Six6_2	Six6	-0.412	0.022	8.574	Migrant
PH0167.1 Tcf1	Tcf1	0.298	0.023	7.225	Migrant
PH0175.1 Vax2	Vax2	-0.496	0.006	7.549	Migrant
PH0176.1 Vsx1	Vsx1	-0.397	0.018	8.66	Migrant
PL0004.1 hh-27		0.802	0.044	9.691	Settler
PL0005.1 hh-30		0.751	0.057	9.022	Settler
PL0007.1 mxl-3		0.775	0.048	8.343	Settler
PL0008.1 hh-29		0.785	0.03	8.09	Settler
PL0011.1 hh-2::hh-4		-0.097	0.064	9.366	Migrant
PL0013.1 hh-2::hh-15		0.782	0.023	7.546	Settler
PL0014.1 mxl-1::mdl-1		0.804	0.086	8.088	Settler
PL0018.1 hh-25		0.805	0.068	9.894	Settler
POL001.1 MTE		0.863	0.01	6.04	Pioneer
POL003.1 GC-box		0.844	0.157	7.638	Pioneer
POL004.1 CCAAT-box		0.775	0.039	6.97	Pioneer
POL006.1 BREu		0.821	0.118	3.54	Pioneer
POL008.1 DCE_S_I		0.754	0.039	2.654	Settler
POL009.1 DCE_S_II		0.755	0.018	2.645	Settler
POL011.1 XCPE1		0.845	-0.052	7.401	Pioneer
POL013.1 MED-1		0.806	0.194	4.136	Pioneer
SA0001.1 at_AC_acceptor		0.018	0.044	6.225	Migrant
SA0003.1 at_AC_acceptor		-0.141	0.027	5.264	Migrant
SD0003.1 at_AC_acceptor		-0.446	0.015	7.133	Migrant

YL_ES_Brg_3_0_c74		-0.007	0.202	22.302	Migrant
YL_ES_Med12_3_0_c1651		0.784	0.07	7.653	Settler
YL_ES_Med15_3_0_c356		0.873	0.002	8.236	Pioneer

Supplementary Table 5: Table of Oligonucleotides

Oligonucleotide name	Oligonucleotide sequence
DNase-Seq primers	
DNase_PosCtl_1_fw	TTGGAAACAACCACAGTGC
DNase_PosCtl_1_rv	CAATACGCGAGCTTGACAG
DNase_PosCtl_2_fw	GGGCTGACTCCTTCATTCAC
DNase_PosCtl_2_rv	CTAAAATGTGCCCCCAAGAA
DNase_PosCtl_3_fw	GTTAAACCCAGCCTCAGTGG
DNase_PosCtl_3_rv	CTTCCAGGGCCTTCTTGAT
DNase_NegCtl_1_fw	TTGACTGCTCCCAGGTAGAGA
DNase_NegCtl_1_rv	TCTTGGTATTTCATTCATAGGC
DNase_NegCtl_2_fw	TCCATAATGATTGGGAAAG
DNase_NegCtl_2_rv	GAAAGTTCTGGAAGACAGTGCAT
DNase_NegCtl_3_fw	CCAACTGCCTCATTAGAGC
DNase_NegCtl_3_rv	TGCATGCTGTGAATGTCAA
RT qPCR primers	
Gapdh_RTqPCR fw	TTGATGGCAACAATCTCCAC
Gapdh_RTqPCR rv	CGTCCCGTAGACAAAATGGT
Actb_RTqPCR fw	ATGGAGGGAAATACAGCCC
Actb_RTqPCR rv	TTCTTGCAAGCTCCTCGTT
Tol2GFP_RTqPCR fw	TACAAGACGCGTGTGAAGT
Tol2GFP_RTqPCR rv	CAATGTTGTGGCGAATTTG
Tol2Promoter_RTqPCR fw	GAGCTCAGGAACATCCAAA
Tol2Promoter_RTqPCR rv	TAGAGGCTCTGCCAGCAC
Tol2Enhancer_RTqPCR fw	CGAAAGGAGTTCACTGAGATG
Tol2Enhancer_RTqPCR rv	ATTAATGACCCGCCTGTGAC
Tol2 Reporter primers	
BIA_2xRXRRAR_Pacl_rv	GAUTGACTTTAATTATGACCCGCCTGTGACCCCTGCAGGCCGGACCGT GACATCTCAGTGAACCTTTCGTTA
Ascl_neg_BIA_fw	GTCCGTGCGGCGGCCACTGTTCCGTAAACGAAAGG
Ascl_Gata6_1_BIA_fw	GTCCGTGCGGCGGCCAGATAAGTAACGAAAGG
Ascl_Oct4_BIA_fw	GTCCGTGCGGCGGCCAGCCACCGTATGCAAATAGTAACGAAAGG
Ascl_Sox2_BIA_fw	GTCCGTGCGGCGGCCAGCCATTGTGCCGCAACTAGTAACGAAAGG
Ascl_Gata6_2rc_BIA_fw	GTCCGTGCGGCGGCCAGCTGCATATGCCGCTAACGAAAGG
Ascl_Klf7rc_BIA_fw	GTCCGTGCGGCGGCCATAGGGCGGGTCGATAACGAAAGG
Ascl_Creb1fw_BIA_fw	GTCCGTGCGGCGGCCCTGGTACGTCTAACGAAAGG
Ascl_T_BIA_fw	GTCCGTGCGGCGGCCCTAGGTGTGAATAACGAAAGG
Ascl_NFYAfw_BIA_fw	GTCCGTGCGGCGGCCCTCAGCCAATCAGCGCTAACGAAAGG
Ascl_Creb1rc_BIA_fw	GTCCGTGCGGCGGCCAGTCACCAGGTAAACGAAAGG

Ascl_Ets1rc_BIA_fw	GTCCGTGCGGCGCGCCGAGCCGGAAGTAACGAAAGG
Ascl_Nrfrc_BIA_fw	GTCCGTGCGGCGCGCCGCGCTGCGCTAACGAAAGG
Ascl_NFYArc_BIA_fw	GTCCGTGCGGCGCGCCGCGCTGATTGGCTGAGTAACGAAAGG
Ascl_Gata6_2fw_BIA_fw	GTCCGTGCGGCGCGCCGCGCTGATTCAGCTAACGAAAGG
Ascl_Hnf1b_BIA_fw	GTCCGTGCGGCGCGCCTAGTTAATGATTAACGAAAGG
Ascl_Bhlhb2_BIA_fw	GTCCGTGCGGCGCGCCACGTGATAACGAAAGG
Ascl_Zfp161rc_BIA_fw	GTCCGTGCGGCGCGCCCTCAGGCAGCGCGCCATAACGAAAGG
Ascl_Klf7fw_BIA_fw	GTCCGTGCGGCGCGCCCTGACCCGCCCTATTAAACGAAAGG
Ascl_KAISO_BIA_fw	GTCCGTGCGGCGCGCCCTCGCGAGATAACGAAAGG
Ascl_Zfp161fw_BIA_fw	GTCCGTGCGGCGCGCCCTGGCGCGCGCCGATAACGAAAGG
Ascl_Foxa2_BIA_fw	GTCCGTGCGGCGCGCCCTGTTACTTTAACGAAAGG
Ascl_E2f1_BIA_fw	GTCCGTGCGGCGCGCCCTTGGCGCCGATAACGAAAGG
Ascl_Cdx2_BIA_fw	GTCCGTGCGGCGCGCCCTTATTGCTAACGAAAGG
Ascl_Nrf1rc_BIA_fw	GTCCGTGCGGCGCGCCGCGCCGCTGCGCTAACGAAAGG
Ascl_KAISO_BIA_fw	GTCCGTGCGGCGCGCCCTCGCGAGATAACGAAAGG
2kb spacer DNA PacI fw	GCGTTAATTAAAGAAGCCCCAATTCAAGATTCA
2 kb spacer DNA PvulFsel fw	CATCGATCGGCCGGCCACTCCCCATCCATTC
Dominant negative DNase-qPCR primers	
Nrf1_DN_Exp1_FW	GGAGCCCGAGACTATGTG
Nrf1_DN_Exp1_RV	GCAATGCCGCTTCCAC
Nrf1_DN_Exp2_FW	CTGCGCACAGCAGTGGAC
Nrf1_DN_Exp2_RV	GCGGGACTTCTGTCTCAG
Nrf1_DN_Exp3_FW	CATGTCCGTTGAGGTGTG
Nrf1_DN_Exp3_RV	TGCGCACAGGTTTCTACTG
Nrf1_DN_Exp4_FW	CTTGGGTTCCCATCCAGGTA
Nrf1_DN_Exp4_RV	CGCAAGAGTCCTGTCCTTT
Nrf1_DN_Exp5_FW	TGATATGGAAGCACCCAAAT
Nrf1_DN_Exp5_RV	GGCGGCGTCATCTTTG
Nrf1_DN_Exp6_FW	TACACCGTTGCCGTAAACAA
Nrf1_DN_Exp6_RV	GTTGGCGCCAGATTAG
NFYA_DN_Exp1_FW	ACCCGCTCCAATCAGGA
NFYA_DN_Exp1_RV	TGTCTCCCGCAGCTAGA
NFYA_DN_Exp2_FW	GGGGAAAGGGATGTAGAAGG
NFYA_DN_Exp2_RV	GAGTGAGCTGTCAGTCAGTGC
NFYA_DN_Exp3_FW	GGAGGGATGCCAGTGTCTAC
NFYA_DN_Exp3_RV	CCGGAGGGAGAGCTAACTTGT
NFYA_DN_Exp4_FW	CATGGGTCAGATCACAGCAG
NFYA_DN_Exp4_RV	GCTCACTGGGTTGCACT
NFYA_DN_Exp5_FW	CTGGCTCCACCTTCTTCTAGG
NFYA_DN_Exp5_RV	AACCTAGCCAATGAGCAAGC

Dominant negative ChIP-qPCR primers	
cmyc_PosCtl_1_FW	GATCTCCTCCTGCCTCAGTG
cmyc_PosCtl_1_RV	GGTGCTGTGCTCAGTCTC
cmyc_PosCtl_2_FW	AGAACCATATGGCTGGGATG
cmyc_PosCtl_2_RV	GCACTCTCGCCTTGAGTTT
cmyc_PosCtl_3_FW	CATGAGCAGCCATACAAGGA
cmyc_PosCtl_3_RV	CCGCTGTTCCGGTTATGAAT
DNase_NegCtl_1_fw	TTGACTGCTCCCAGGTAGAGA
DNase_NegCtl_1_rv	TCTTGGTGATTTCATTCATAGGC
DNase_NegCtl_2_fw	TCCATAATGATTGGGGAAAG
DNase_NegCtl_2_rv	GAAAGTTCTGGAAGACAGTCAT
DNase_NegCtl_3_fw	CCAACTGCCTCCATTAGAGC
DNase_NegCtl_3_rv	TGCATGCTGTGAATGTCAA
Nrf1_DN_ChIP_CmycExp1_FW	AGTCACGTGTCCGCCACT
Nrf1_DN_ChIP_CmycExp1_RV	AACGTTATTCTCGCGAGGTC
Nrf1_DN_ChIP_CmycExp2_FW	GAGATCTCGCGGCAACTTAC
Nrf1_DN_ChIP_CmycExp2_RV	GCCGCAAAAGGAAAGAGAAC
Nrf1_DN_ChIP_CmycExp3_FW	ACAACCTCCACCTTGCTTG
Nrf1_DN_ChIP_CmycExp3_RV	CGTGCTAGCGTAGGACTGTG
Nrf1_DN_ChIP_CmycExp4_FW	CTGTAACCCGCCTTCATTGG
Nrf1_DN_ChIP_CmycExp4_RV	GCGATAGTTACCTCCGTGAC
NFYA_DN_ChIP_CmycExp1_FW	CAGGTGATTAGCGGCTATGG
NFYA_DN_ChIP_CmycExp1_RV	CCGAGTCACGTGCTGCTC
NFYA_DN_ChIP_CmycExp2_FW	GTGCTGTGAGAGCGACATT
NFYA_DN_ChIP_CmycExp2_RV	GCGGCTCTCCTAGCCAAT
NFYA_DN_ChIP_CmycExp3_FW	ACGTGATGGCAAGCAAGAAC
NFYA_DN_ChIP_CmycExp3_RV	GAGGCCAGAGAACAACTTGC
NFYA_DN_ChIP_CmycExp4_FW	GGAACGTCCACTTGATTG
NFYA_DN_ChIP_CmycExp4_RV	CGTCTGACCCAGGTAAAGC